INHIBITION OF CORROSION BY GLYCEROL STEARATE ON SELECTED METALS

by

THABO PESHA

THESIS

Submitted in fulfilment of the requirements for the degree of

DOCTOR OF PHILOSOPHY

in

CHEMISTRY

in the

FACULTY OF SCIENCE AND AGRICULTURE

(School of Physical and Mineral Sciences)

at the

UNIVERSITY OF LIMPOPO

SUPERVISOR: PROF V. L. MULAUDZI

CO-SUPERVISOR: PROF L. M. CELE

2023

DEDICATION

To my family

Success Pesha, David Pesha, Cathrine Pesha, Eric Pesha, Phineas Kgang and Caroline Kgang.

DECLARATION BY CANDIDATE

I declare that the thesis hereby submitted to the University of Limpopo, for the degree of Doctor of Philosophy in Chemistry has not previously been submitted by me for a degree at this or any other University; that it is my work in design and in execution, and that all material contained herein has been duly acknowledged.

Pesha T (Mr)

05/04//2023

Full Names Date

ACKNOWLEDGEMENTS

To Jesus Christ, my Lord and Savior, I want to convey the depth of my appreciation for all that you have done for me. I think that it is a once-in-a-lifetime opportunity to carry out research under the direction of my supervisor, Professor Vusimuzi L. Mulaudzi, because of his congenial guidance, extensive and vast source of inspiration, and consistent support throughout the entirety of the duration of the study. I consider this to be a very rare opportunity. His ability to maintain his humanity in the face of challenging circumstances was a significant factor in my success in achieving the goal. I am thankful to having you as my mentor and supervisor since I have learnt a great deal from you, and I expect to learn even more in the future. The guidance and assistance that I received from my co-supervisor, Professor L. M. Cele, who motivated me to perform to the best of my abilities, is also very much appreciated.

My deepest appreciation goes to Mintek and Prof. M.E. Makhatha in the Doorfontein Campus University of Johannesburg for granting me permission to use the laboratory to carry out electrochemical studies. It is important to me. In addition, my sincere appreciation goes to Thabang Tshoenyane of the University of Johannesburg for the help he provided with the electrochemical characterisations. Furthermore, I would love to thank Dr. P. Mkhonto for assisting with the computational studies from the physics department in the University of Limpopo. In closing, I would like to offer my appreciation to the members of the analytical chemistry group that work in the Chemistry Department. In conclusion, my appreciation is extended to the Chemistry department in Turfloop Campus University of Limpopo for accepting my application and giving me the opportunity to successfully complete my research project with their assistance.

ABSTRACT

Using gravimetric analysis, potentiodynamic polarisation (PDP), and electrochemical impedance spectroscopy (EIS), an investigation into the corrosion prevention properties of the metals aluminium (Al), mild steel (MS), and zinc (Zn) was carried out in a solution of hydrochloric acid (HCl) with a concentration of 1. 0 M. Inhibition was shown to be more effective as the concentration of the inhibitor increased, according to the measurements from the gravimetric analysis. Glycerol stearate (GS), was investigated for its possible use as a corrosion inhibitor on aluminium, mild steel and zinc metal in 1.0 M HCl solution. Techniques such as gravimetric analysis, potentiodynamic polarisation (PDP), and impedance spectroscopy (EIS) were utilised in order to ascertain the rate of corrosion. At a concentration of 50 mol. L^{-1}, electrochemical tests (PDP and EIS) have indicated that there is the highest percentage of inhibitory efficiency of glycerol stearate such as 81.06 % (PDP), 86.18 % (EIS) for aluminium, 82.69 % (PDP), 75.44 % (EIS) for mild steel and 71.05 % (PDP), 89.50 % (EIS) for zinc metal. It was discovered using gravimetric analysis and electrochemical techniques that the rate of corrosion decreased as the inhibitor concentration increased. The findings that glycerol stearate operated as a mixed type of corrosion inhibitor were demonstrated by the disparities that existed between the corrosion potential (E_{corr}) values of the blank (1. 0 M) and inhibitor (GS) concentrations for all metals. Studies on potentiodynamic polarisation demonstrated that the addition of GS reduced the corrosion current densities on aluminium metal, mild steel, and zinc metal, which resulted in the metals being more resistant to corrosion. Using electrochemical impedance spectroscopy, the researchers found that the charge transfer resistance increased as GS concentration increased. The values of the free Gibbs energy showed that a spontaneous corrosion process was occurring at the surface of the aluminium, mild steel, and zinc metal. The Langmuir adsorption

isotherm was followed by the data collected from adsorption isotherm research for each element. The presence of the adsorption coating was validated by Fourier transform infrared spectroscopy (FTIR), which was performed on the surfaces of aluminium, mild steel, and zinc. The adsorption mechanism has been further explained by using thermodynamics and quantum chemistry parameters, both of which have been calculated and interpreted. Images obtained using scanning electron microscopy (SEM) revealed that the presence of glycerol stearate significantly reduced the amount of inhomogeneity in aluminium, mild steel, and zinc.

RESEARCH OUTPUT

PUBLICATIONS

Thabo Pesha, Vusimuzi L. Mulaudzi, Mduduzi L. Cele, Mmaphefo P. Mothapo, Nkhabelane P. Makina, Collen Mochaisa, Thapelo Mojapelo. Evaluation of corrosion inhibition effect of glycerol stearate on aluminium metal by electrochemical techniques. Manuscript accepted for publication in the Arabian Journal of Chemistry.*

Thabo Pesha, Vusimuzi L. Mulaudzi, Mduduzi L. Cele, Mmaphefo P. Mothapo, Nkhabelane P. Makina, Collen Mochaisa, Thapelo Mojapelo. Inhibition of zinc corrosion by glycerol stearate in 1.0 M hydrochloric acid medium with: Experimental, theoretical and electrochemical techniques. Manuscript in preparation.

Thabo Pesha, Vusimuzi L. Mulaudzi, Mduduzi L. Cele, Mmaphefo P. Mothapo, Nkhabelane P. Makina, Collen Mochaisa, Thapelo Mojapelo. Mitigation of mild steel degradation using glycerol stearate in acidic environment. Manuscript in preparation.

Thabo Pesha, Vusimuzi L. Mulaudzi, Mduduzi L. Cele, Mmaphefo P. Mothapo, Nkhabelane P. Makina, Collen Mochaisa, Thapelo Mojapelo. Review on nontoxic corrosion inhibitors for selected metals in acidic and basic mediums. Manuscript in preparation.

PRESENTATIONS

Thabo Pesha, Vusimuzi Lodwick Mulaudzi, Mmaphefo Patricia Mothapo, Mduduzi Leskey Cele. Inhibition of aluminium corrosion in 1. 0 M HCl by glycerol stearate. Twelveth Research Day Faculty of Science and Agriculture Postgraduate Research Day Conference Bolivia Lodge, Polokwane, Limpopo, South Africa on the 21-23rd September 2022.

TABLE OF CONTENTS

LIST OF FIGURES

LIST OF TABLES

LIST OF ABBREVIATIONS

Al	:	Aluminium
MS	:	Mild steel
Zn	:	Zinc
GS	:	Glycerol stearate
KI	:	Potassium iodide
US	:	United states of America
DFT	:	Density functional theory
CE	:	Counter electrode
PLE	:	Pressurised liquid extraction
MAE	:	Microwave-assisted extraction
SPM	:	Solid-phase microextraction
SFE	:	Supercritical fluid extraction
DSC	:	Differential scanning calorimetry
O	:	Oxygen
EIS	:	Electrochemical impedance spectroscopy
N	:	Nitrogen
S	:	Sulfur
WL / ΔW	:	Weight loss
FTIR / IR	:	Fourier transform infrared spectroscopy
HCl	:	Hydrochloric acid
HOMO	:	Highest occupied molecular orbital
IE	:	Inhibition efficiency
HE	:	Hydrogen evolution
KCl	:	Potassium chloride
LUMO	:	Lowest unoccupied molecular orbital
KBr	:	Potassium bromide
MIC	:	Microbial influence corrosion
FMO	:	Frontier Molecular orbital

PDP	:	Potentiodynamic polarisation
EIS	:	Electrochemical impedance spectroscopy
H1	:	Oak honey
H2	:	Coniferous honey dew honey
H3	:	Winter savoury honey
H4	:	Alder buck thorn honey
H5	:	Carob tree honey
WGK	:	Water hazard classes
VwVwS	:	Verwatungsvorschrift wassergefahrdende
LC	:	Lethal concentration
EC	:	Effective concentration
HPLC-MS	:	High-performance liquid chromatography mass spectrometry
PFZ	:	Precipitates free zone
RE	:	Reference electrode
SCC	:	Stress corrosion cracking
SCE	:	Saturated calomel electrode
SEM	:	Scanning electron microscopy
CO_2	:	Carbon dioxide
TGA	:	Thermogravimetric analysis
STA	:	Simulteneous thermal analysis
H_2SO_4	:	Sulfuric acid
GCMS	:	Gas chromatography-mass spectrometry
UV-vis	:	Ultraviolet-visible spectroscopy
WE	:	Working electrode
XRD	:	X-ray diffraction
SC-CO_2	:	Supercritical carbon dioxide
HNO_3	:	Nitric acid
H_3PO_4	:	Orthophosphoric acid
$CHCl_3$	:	Chloroform
Na_2CO_3	:	Sodium carbonate

NaOH	:	Sodium hydroxide
GGA	:	Generalised gradient approximation
PW91	:	Perdew-Wang 91
TS	:	Tkatchenko and Scheffler
DNP	:	Double numerical plus polarisation
C	:	Carbon
Cl^-	:	Chloride ion
CH_2	:	Alkyl carbon chain
C=O	:	Carbonyl group
EDS	:	Energy dispersive spectroscopy
Fe	:	Iron
CPS	:	Counts per second
M	:	Metal surface atom
P_{H2}	:	Partial pressure of hydrogen gas
M^{n+}	:	Ion in solution
A	:	Arrhenius pre exponential factor
ne^-	:	Electrons in a metal
n	:	Number of electrons transferred
pH	:	Measure of acidity and basicity
A/EA	:	Electron affinity
I/IP	:	Ionisation potential
Vs	:	Versus
Mol	:	Mole
L	:	Litre
R^2	:	Coefficient of determination

LIST OF SYMBOLS

Ag/AgCl	:	Silver/silver chloride
b_a	:	Anodic Tafel slope
b_c	:	Cathodic Tafel slope
C_R/ρ	:	Corrosion rate
C_{inh}	:	Inhibitor corrosion
C_{dl}	:	Double layer capacitance
E_a	:	Activation energy
E_r	:	Reversible potential
E^o	:	Standard reversible potential
E_{corr}	:	Corrosion potential
I_{corr}	:	Corrosion current density
K_{ads}	:	Equilibrium adsorption constant
M	:	Molar
R	:	Gas constant
R_s	:	Resistor
R_{ct}	:	Resistance of charge transfer
S	:	Surface area
T	:	Temperature
ΔS^o/ ΔS^o_{ads}	:	Entropy
ΔH^o/ ΔH^o_{ads}	:	Enthalpy
ΔG	:	Gibbs free energy
ΔG°_{ads}	:	Standard Gibbs energy of adsorption
ΔW	:	Weight loss
T	:	Time
Θ	:	Theta
F	:	Faraday constant
^oC	:	Degrees celcius
R_p	:	Polarisation resistance

$P_{o/w}$	:	Partition between 1-Octanol and water
CPE	:	Constant phase element
A	:	Angstrom
Ha	:	Hartree atomic units
X	:	Electronegativity
η	:	Global hardness
ω	:	Global electrophilicity index
σ	:	Global softness
E_{HOMO}	:	HOMO energy
E_{LUMO}	:	LUMO energy
ΔE	:	Energy gap
cm	:	Centimeter
h/h_r	:	Hour
g	:	Gram
K	:	Kelvin
J	:	Joule
k_B	:	Boltzmann's constant
h	:	Planck's constant
mV	:	Millivolt
A	:	Ampere
V	:	Volt
X	:	Multiplication
Ω	:	Ohm

CHAPTER ONE

INTRODUCTION

1.1. BACKGROUND

In structural and decorative applications, metals are the preeminent essential materials used. Corrosion, a degradation of metals is inevitable but a preventable process. In comparison to other types of natural disasters, like as earthquakes, floods, or even the Covid-19 epidemic, metal corrosion has a much more significant impact on the development of a nation. Corrosion is a natural phenomenon which follows different pathways. If corrosion is left unabated it has the potential to cripple the economy of both developed and developing countries. It has emerged as a scourge throughout all seasons although it is much elevated during rainy seasons. This is a silent destroyer that may be left undetected until it is quite late. It is a very costly occurrence that attack the core of development and maintainance. It is safe to mention that the negative effect of corrosion causes ripples throughout the economy of any country.

The effects of corrosion cannot be underestimated, for example, corrosion metals cost in the US estimation was about $276 billion on annual basis, which is ample times more than the normalised loss acquired due to natural disasters ($17 billion per annum). However, in the South African context the cost of corrosion to its economy is approximately 5% of GDP, as researched by University of Witwatersrand and Mintek in 2005 (Corrosion Awareness Day highlights the tragedy of rust 2015).

This offsets the economic value made by the mining sector as they cancel each other. It shows how serious this is if one considers the economics that mining in the country contributes. The scourge of corrosion costs the world economy in excess of 3% per annum, equivalent to $2.3 trillion in 2014. It was deemed necessary to declare Corrosion Awareness Day on 22 April 2010 and to point out the effect corrosion caused in the entire world. Corrosion is the reason why bridges collapses, piers

deteriorate, roads, transportation equipment, cars and aircrafts deteriorate serving as a world's critical infrastructure limiting factor. In many countries around the world, potable water loss due to corrosion of infrastructure and environmental damage by corroded sewer lines contributes significantly. The negative impact of corrosion may be summed up significantly as materials, resources and manpower losses, which results in a pronounced impact on the ecosystem.

By means of optimum corrosion management practices [1], it was also suggested that about 25 to 30% of the annual corrosion costs could be preserved [1]. For example, in variety of electronic applications [2], aluminium (Al) which is a light metal with good electric conductivity was used. The need to protect Al metal from corrosion has been one of the major challenges. Corrosion can be mitigated by applying several methods such as blending of production fluids, upgrading materials, process control and chemical inhibition [2–4]. Amongst these methods, the corrosion chemical inhibition due to its economic and practical usage [5–7], is reported to be the best method to combat destruction or degradation of metal surfaces in corrosive media. Therefore, the quest for an efficient corrosion inhibitor is paramount important and as a fundamental progressive step in this search, it has been found that the use of non-toxic organic compounds is one of the most practicable and feasible ways for providing protection of metals [8–10].

1.2. PROBLEM STATEMENT

Metal, metal derivatives and products have become an integral part of our daily lives in homes, industries, transport entities and infrastructure. Due to their malleability and durability, metals satisfy a wide variety of design requirements. High stiffness and strength and the fact that they can be alloyed for high rigidity, strength, and hardness make metals very important for industrial applications. Their summed-up benefits are the high capacity to absorb energy, good electrical and thermal conductivity. However, they are prone to degradation, resulting in very negative economic effects and safety aspects. In natural environment, particularly acids and bases corrode metals into their respective weak metal oxides, which compromise their structural stability [11]. Corrosion knows no national boundaries. Toxic materials, released from corroded equipment in one area, pollute the air and water farther afield. Acid rain generated in one country not only pollutes the local environment but can cause corrosion damage far beyond that country's borders and even beyond the borders of its neighbours. And toxic material ends up in the world's waterways and can poison sea life, killing many species and making others toxic to humans.

There have been many studies geared to protect and prolong metals efficiency in performing optimally and prevent an inevitable process of corrosion like painting and plating methods for the reduction of corrosion on mild steel. However, a drawback associated with the plating technique is the coating component adsorption efficiency. Due to this drawback of the plating technique, it is advisable to plate with zinc or cadmium because of their activeness. Furthermore, in painting methods, drying times have been a drawback because they are temperature and humidity dependant [12–15]. To avoid these drying times problems, corrosion based chemical inhibitors are most preferred as an inhibitive method in different mediums such as acidic, alkaline, and saline media. Chemical corrosion inhibitors are mostly preferred because they are available, simple in adsorption model and they are affordable [7]. A quest is to design or discover a material that is environmentally friendly and able to operate in both acidic and basic media. Several research groups have studied a wide spectrum of corrosion

inhibitors with competing efficiency such as metallic phthalocyanines. However, in most organic solvents, metallic phthalocyanines have low solubility, and they aggregate resulting in a poor performance as corrosion inhibitors, hence there is a need for metallic phthalocyanines to be functionalised with electron donating functional groups.

1.3. RATIONALE

The exportation and local trade of industrial products control macroeconomics. All these are in one way or the other proportional to industrial equipment, transport, and infrastructure. However, corrosion has a serious negative effect on all of these since industrial equipment, transport and infrastructure are metallic derivatives. Corrosion mitigation strategies need to be implemented to circumvent poor gross domestic product (GDP) and gross national product (GNP). Corrosion extends beyond national boundaries. Toxic material ends up in the world's waterways and can poison sea life, killing many species and making others toxic to humans. The method of corrosion inhibition of choice would be synergism that can be employed to enhance the inhibitor's potential to prevent corrosion. This method addresses poor or moderate inhibition activity and reduce the quantity of an expensive inhibitor [16]. It plays an essential role in both theoretical and practical work on corrosion inhibitors since it diversifies the activity of the inhibitor in corrosive media [17]. It is generally regarded as a nontoxic and non-irritant material. All these chemical characteristics make it ideal for use as a corrosion inhibitor.

Extensive studies have been made on cations and anions to investigate their synergistic effects when incorporated to metal corrosion inhibitors [18–20]. Also, considerable attention and wide-ranging review on the effect of synergism for halide ions have been done [21]. In this present study, the synergistic effect of glycerol stearate (GS) as a corrosion inhibitor is evaluated. GS is the synthetic product resulting from the esterification of glycerol with stearic acid. Glycerol and stearic acid are from both natural and synthetic sources hence they fit a criterion for suitable metal corrosion inhibitors because of their non-toxicity thus making them eco-friendly. The presence of the oxygen atoms makes GS a suitable inhibitor [22].

Extensive studies on glycerol and stearic acid separately as corrosion inhibitors have been conducted [23]. However, in this study, synergistic effects of glycerol and stearic acid will be examined. Synergism is the sum effect of two or more chemical

compounds combined to mitigate corrosion [24]. GS is studied as a corrosion inhibitor since it possesses an oxygen atom, which qualifies it as a suitable metal corrosion inhibitor. In addition, GS has a large molecular weight, which will result in greater surface coverage, hence blocking the active sites of the metal, protecting the metal from attack by ions from a corrosive media. GS is biodegradable and undergoes facile production as the synthetic reagent and is readily available [25].

1.4. RESEARCH AIM AND OBJECTIVES OF THE STUDY

1.4.1. AIM

The aim of this study was to investigate the corrosion inhibition potential of glycerol stearate on selected metals (mild steel, aluminium, and zinc) in both acidic and basic media. This is in line with protecting the environment and promoting green chemistry technology.

1.4.2. OBJECTIVES

The objectives were to:

i. Study glycerol stearate concentration effect on the rate of corrosion.
ii. implement adsorption principles, kinetics, and thermodynamics in investigating the inhibitive efficiency of glycerol stearate on selected metals,
iii. Evaluate metals morphological, optical and structural properties of the selected metals after inhibitor treatment, using Scanning Electron Microscopy (SEM), Fourier Transform Infrared spectrometry (FTIR).
iv. Apply computational studies such as density functional theory (DFT) to evaluate the interaction between the chemical inhibitor and the metal surface.
v. Identify the inhibition mechanism, adsorption type and adsorption isotherm.
vi. Evaluate corrosion potential, corrosion current density, charge transfer resistance using potentiodynamic polarisation (PDP) and electrochemical impedance spectroscopy (EIS).

1.5. DISSERTATION OUTLINE

This thesis explores the effect of corrosion on aluminium, mild steel and zinc metal using weight loss measurements and electrochemical techniques. The thesis consists of five chapters and a short description of each chapter, and their outline is provided below.

Chapter one: Provision of the background, problem statement, rational, aims and objectives of the study.

Chapter two: Literature review on corrosion, it includes corrosion definition and corrosion classifications, corrosion rate, corrosion affecting factors, corrosion of metals, corrosion theory, corrosion inhibitors, corrosion testing, analytical techniques.
Chapter three: This chapter provides an experimental section of the study.
Chapter four: The chapter provides results and discussions.
Chapter five: The chapter provides general discussions, conclusions of the study and recommendations for future work.

CHAPTER TWO

LITERATURE REVIEW

2.1. CORROSION

2.1.1. Definition and classifications of corrosion

Corrosion is a spontaneous chemical reaction whereby metals and metal derivatives decay. This is an oxidation-reduction reaction in which metals are oxidised by their surroundings and the oxygen in the air. This reaction can be either spontaneous or electrochemical. The formation of rust (corrosion of steel) requires iron, water, and oxygen. Although it is a complex process, the chemical equation is simply $4Fe + 3O_2 + 6H_2O \rightarrow 4Fe(OH)_3$. In addition, aluminium due to its highly negative redox potential; reacts with water to produce hydrogen gas according to $2Al + 3H_2O \rightarrow 3H_2 + Al_2O_3$. This chemical reaction may be of particular importance when it occurs between the strands of an aluminium conductor. Furthermore, the corrosion of zinc in an oxygenated hydrochloric acid electrolyte illustrates the effect of multiple cathodic reactions with the oxidation reaction occurring at the anode according to $Zn \rightarrow Zn^{2+} + 2e^-$ [26,27].

(a) (b)

Figure 2. 1: Before (a) and after (b) corrosion of microwave [26, 27].

The above Figure illustrates how corrosion degrades metal with time.

2.1.1.1. Pitting corrosion

Pitting corrosion takes place during the access of aggressive anions at the passivated metal surfaces. Thin oxide layers are attacked very effectively by halides, which is the experience that leads to the metal surface localised dissolution. In chemical industries, most serious problems are caused by chlorides due to their excess presence in many surroundings such as seawater, salt on roads, and in food. Several metals such as iron, nickel, copper, aluminium, and steels are subjected to this type of corrosion except chromium, which is one of the few exceptions. The occurance of pits within a large, passivated metal surface leads to high metal perforation, which in turn weakens the material and causes major losses of economy and safety problems. However, this process occurs with a sequence of steps [28].

In addition, It occurs in four distinct stages [3-6]: (i) the metal passive film attack external processess, at both the passive film boundary/solution interface; (ii) Whenever there are no overt changes to the microscopic structure of a film (ii), the metal passive film will launch an attack from within; (iii) this is the step between the initial development of metastable pits and their subsequent growth under pitting potential, after which a passivation film is formed; and (iv) the final step is above a specific potential and it is known as the stable pit growth.

Figure 2. 2: Pitting corrosion [28].

Above Figure depicting pitting corrosion.

2.1.1.2. Crevice corrosion

Crevice corrosion normally takes place at the crevices and shielded areas on metal-corrosive media interface. This type of corrosion occurs in small solution volumes trapped within the metal surface crevices. Metal and nonmetal interfaces can also lead to crevice corrosion. Metals that are most susceptible to crevice corrosion are stainless

steels. Metal oxidation and oxidation-reduction are mechanisms associated with crevice corrosion yielding hydroxyl ion. This type of corrosion can be mitigated using several inhibition techniques such as flushing of the equipment with an inhibitor solution, use of welded butt joints in place of bolted joints, continuous welding, soldering, vessel design with complete drainage, removal of solid deposits, use of non absorbents such as Teflon [29].

Furthermore, crevices accelerate corrosion since it makes chemical environment to store moisture, this type of corrosion is also known for trapping pollutants and concentrates the corrosion products with the exclusion of oxygen [30]. It mostly occurs in the near neutral solutions with dissolved oxygen acting a cathode reactant. Three main factors contributing to crevice corrosion [31], i.e.

i. The structure geometry, e.g., welded fabrications, riveted plates, and threaded joints.
ii. Metal/non-metallic solids contact, e.g., rubber, plastics, and glass.
iii. Deposit attacks due to corrodants on the metal surface.

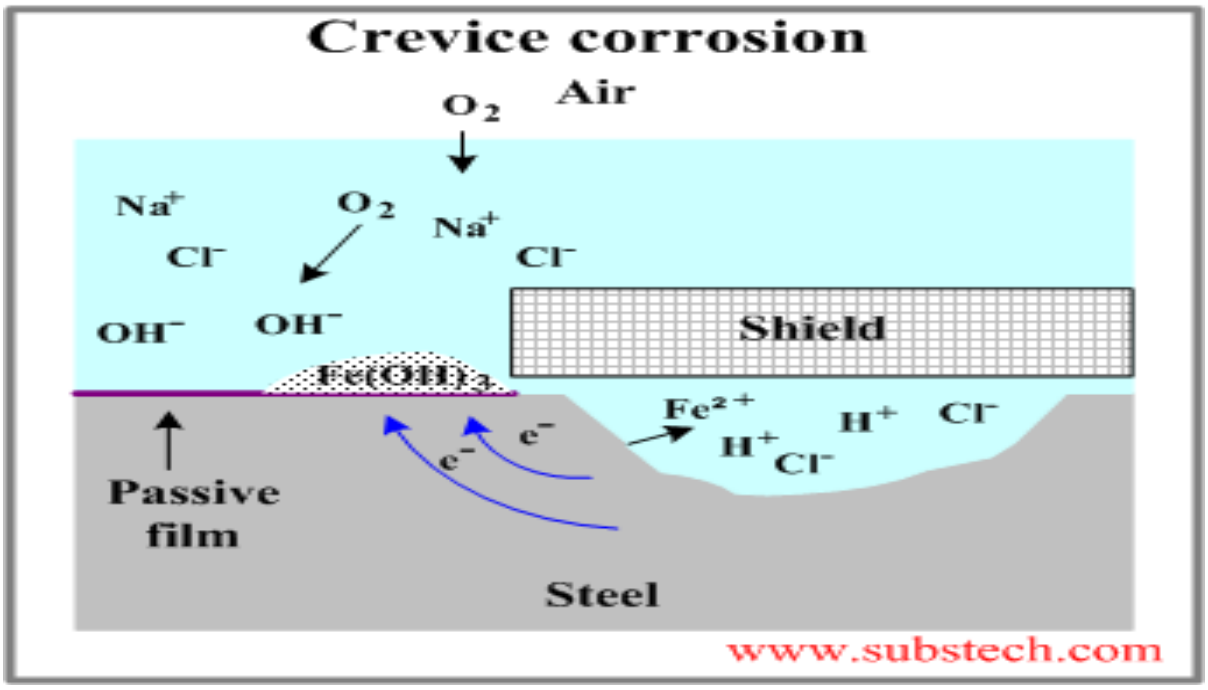

Figure 2. 3: Crevice corrosion-an overview [29].

Crevice corrosion is depicted in the above Figure.

2.1.1.3. Microbiological corrosion

Microbiological corrosion is an essential factor in the engineering alloys corrosion, and it affects the perfomances of metals and the economy of many countries. This corrosion type is due to the chemical interaction between the metal and the environment that is prone to microorganisms. The release of corrosive metabolites, including bacterial exopolymers to the environment, causes this corrosion type to occur between the metal-environment interactions. The microorganism's interactions on metals causes other corrosion forms such as stress corrosion cracking and hydrogen embrittlement [5].

Furthermore, bacterias produced products are aggressive and lead to this form of corrosion known as a microbial influenced corrosion (MIC) [32,33]. Microorganisms

are precursors for the MIC to occur and their effect lead to following additional requirements such as [34]:

i. Energy source
ii. Carbon source
iii. Electron donator species
iv. Electron acceptor species
v. Water

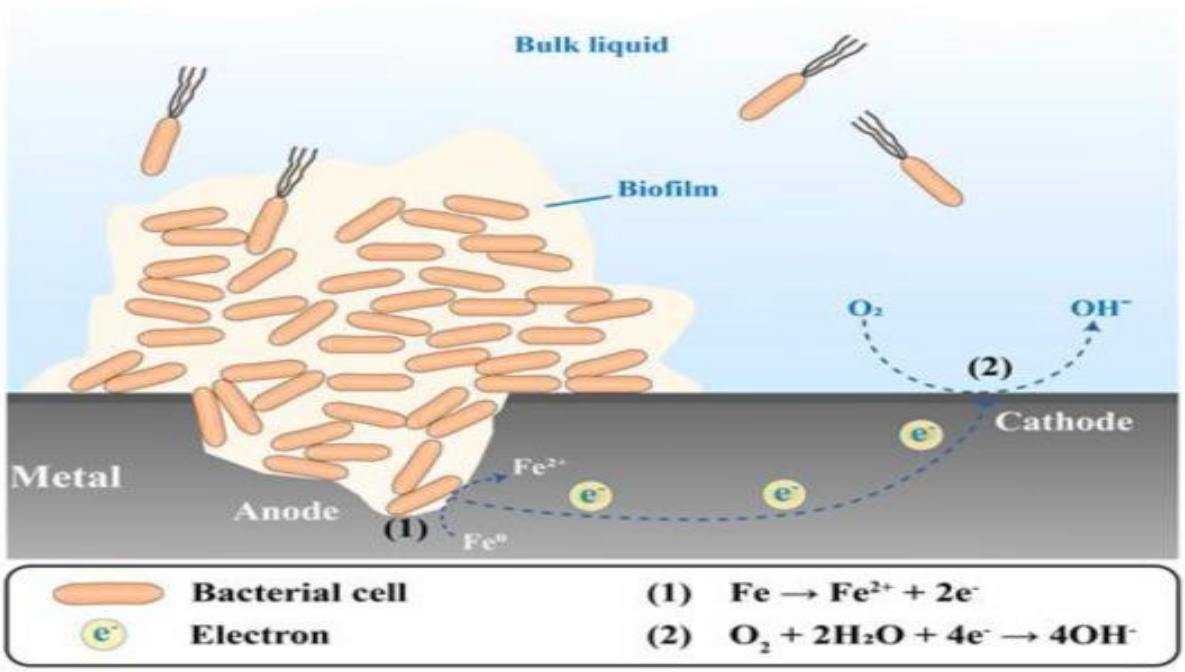

Figure 2. 4: Microbiologically influenced corrosion [32, 33].

Figure 2.4. clearly showing the influence of microorganisms to the corrosion process.

2.1.1.4. Intergranular corrosion

Intergranular corrosion also takes upon the name intracrystalline corrosion or interdendritic corrosion. The above-mentioned type of corrosion is frequently intergranular stress corrosion cracking (IGSCC) due to the tensile stress and the occurrence of cracks along the boundaries. Intergranular implies between crystals or grains. The identification of intergranular corrosion normally requires the examination

of a microstructure under a microscopy although in most cases it is recognised visually. In such as the process of coring is usually encountered in alloy castings, this type of corrosion takes place from local differences in composition. A well-recognised and accepted mechanism of intergranular corrosion is grain boundary precipitation, notably chromium carbides in stainless steels [35].

In addition, it takes place along the grain boundaries due to the micro galvanic coupling amid the precipitates free zone (PFZ) and the grain boundary precipitates [36,37]. The PFZ acts as a solute-depleted layer adjacent to the grain boundary. For the propagation of the intergranular corrosion, it is necessary that the corrosion potential amid the PFZ and the grain boundary be higher than 100 mV and also the continuity of the grain boundary precipitates contributing to the intergranular corrosion along the boundary is required [38,39].

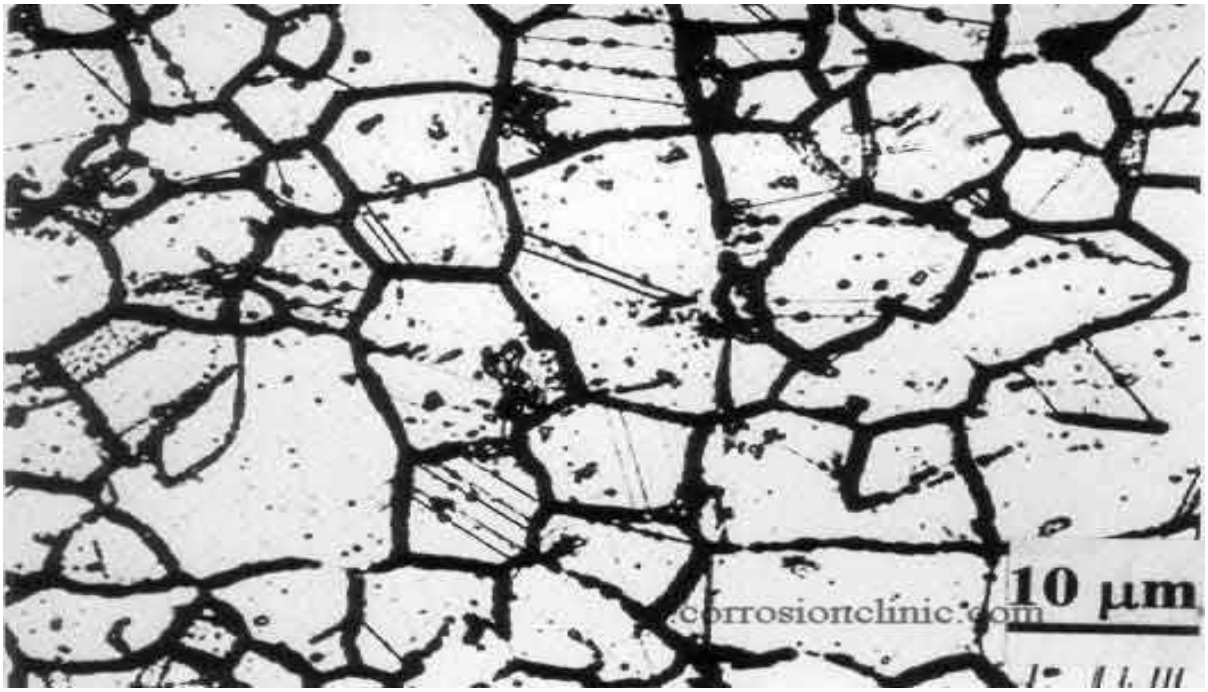

Figure 2. 5: Intergranular Corrosion [35].

This is another form of chemical reaction clearly indicating the intergranular corrosion.

2.1.1.5. Atmospheric corrosion

Atmospheric corrosion is an electrochemical process that takes place in the presence of an electrolyte such as air, rain, humidity, and dew. When a certain critical humidity is reached, invisible thin film electrolyte tends to form on metallic surfaces under atmospheric corrosion conditions. In unpolluted atmospheres, for iron metal this humidity level is around 60%. This humidity level depends on the material corroding, it is not a constant. This humidity level depends on the corrosion products hygroscopic in nature, the presence of atmospheric pollutants and surface deposits. Atmospheric corrosion proceeds by balancing anodic and cathodic reactions in the presence of thin film electrolytes. The metal dissolution in the electrolyte occurs at the anode, while the reduction of oxygen occurs at the cathode. Under thin film corrosion conditions, oxygen from the atmosphere is readily supplied to the electrolyte. Depending on relative humidity, the surface contaminants nature, and other factors such as sunlight exposure and temperature, the thickness and electrical conductivity of the film is evaluated [40]. In addition, the rate of atmospheric corrosion is totally dependant upon the period moisture is in contact with the surface, pollution degree of the atmosphere, temperature, and substrate chemical composition, e.g., carbon or stainless steel.

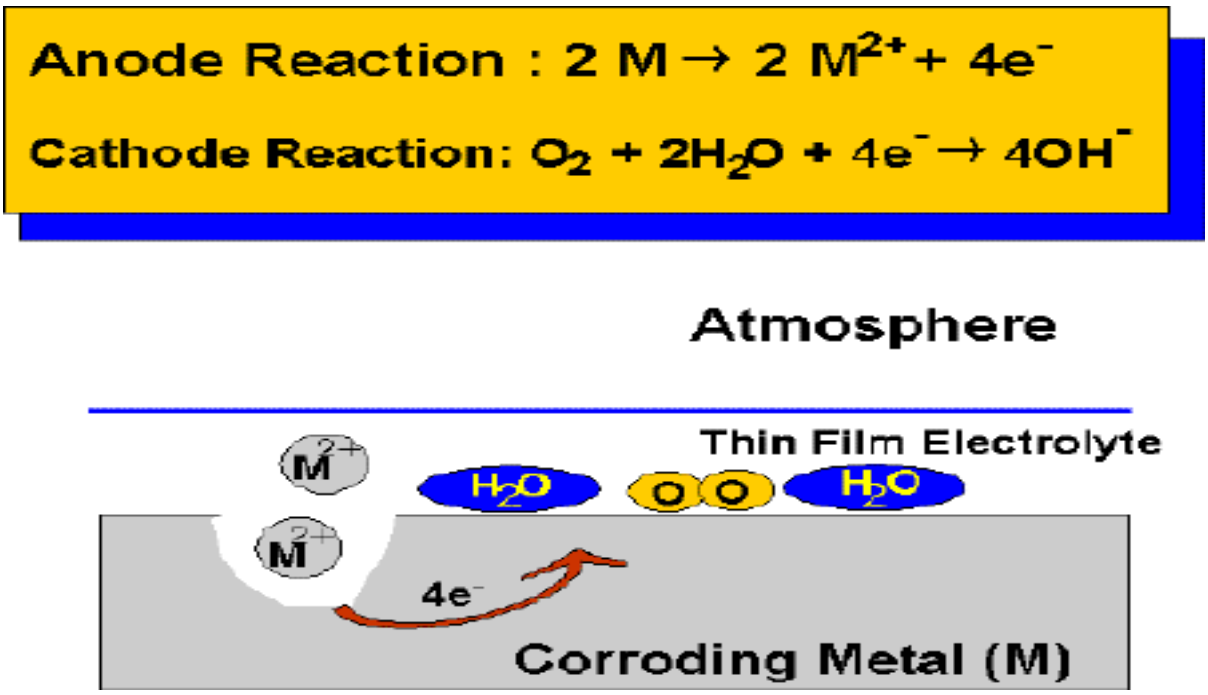

Figure 2. 6: Atmospheric corrosion [40].

The Figure above shows how corrosion is in the atmosphere.

2.1.1.6. Galvanic corrosion

Galvanic corrosion takes place in the presence of a common electrolyte in which two different metals that are physically or electrically connected to each other are immersed. The more noble metal (the cathode) corrodes at a slow rate; meanwhile the more active metal (anode) corrodes at an accelerated rate in a galvanic couple. Galvanic corrosion is affected by factors such as anode relative size, metal type, and conditions of operation such as salinity, humidity, etc. The corrosion rates of the material are directly affected by the surface area ratio of the anode and cathode [41].

Corrosion of this type can also be observed in microelectronic devices where semiconductors and metals of varying types are linked, as well as at water main junctions such as copper/steel pipe junctions. Corrosion of this kind can also be found in ships with components made of different metal alloys that are submerged in water, or in metal matrix composite materials in which graphite materials are disseminated in

a metal as strengthening substances [42]. Galvanic corrosion can result in rapid metal deterioration in many situations, but it can also provide cathodic protection when used in conjunction with sacrificial anodes [43]. Although galvanic corrosion is a widely studied phenomenon, its complexity makes it difficult to apply quantitatively [44].

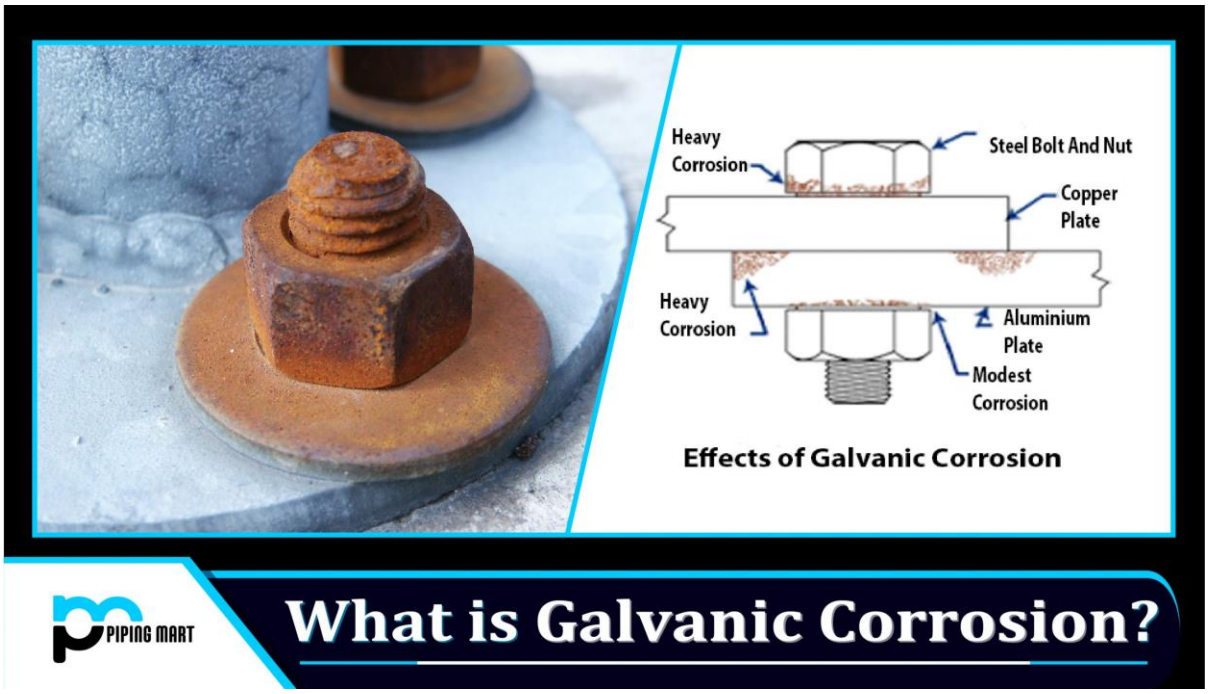

Figure 2. 7: Galvanic Corrosion [41-44].

Galvanic corrosion is shown in the above Figure.

2.1.1.7. General corrosion

General corrosion takes place because of rust. When a metallic material such as steel is exposed to water, the metal surface is oxidised and the appearance of a thin layer of rust occurs. To inhibit a metal dissolution (oxidation), an inhibitive coating must interfere with the reaction [45]. Furthermore, corrosion media permeates the entire metal surface, and it is not harzadous. It is a metal weight loss without any localised attack, it is not penetrating deeply, and the common example is the rusting of steel in air [46].

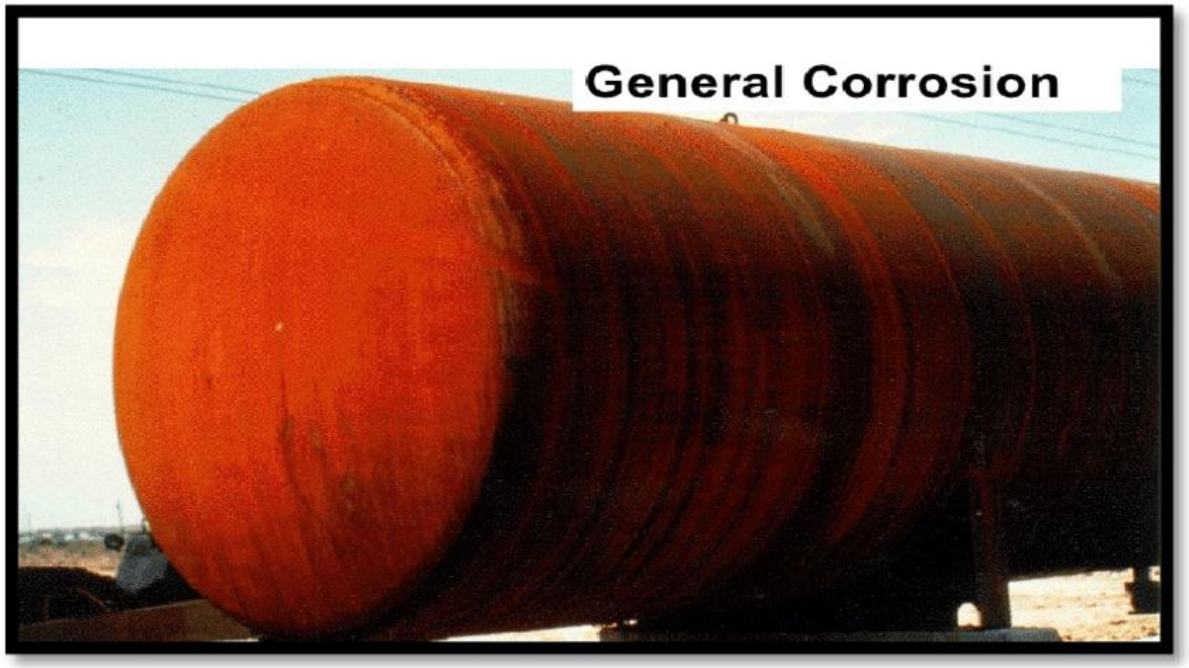

Figure 2. 8: General Corrosion [45, 46].

This Figure shows the overall effect of the general corrosion.

2.1.1.8. Stress corrosion cracking

Stress corrosion cracking (SCC) can result in a negative effect on a material beyond the repair point. A metallic material can encounter SCC along the grain boundary cracks when subjected to extreme tensile stress, and this can further lead to further corrosion. Cold work, welding, and thermal treatment are causes of SCC included. This type of corrosion is intensified when a metallic material is exposed to an environment that increases stress cracking resulting in a transition from a minor stress-corrosion to an irreparable damage. The failure due to stress corrosion is entitled ‘’season cracking’’ in consideration of brass. However, it is entitled ‘’caustic embrittlement’’ in consideration of steel. Steel hydrogen embrittlement is also regarded to be a corrosion phenomenon [47]. While a metal is exposed to a corrosive medium and under tension, SCC tends to be a slow crack growth (typically less than 10^{-6} m/s)

and occurring at the temperature above 60 ^{o}C [48]. As an engineering concern, for the material that is nominally ductile, when SCC results in brittle failure when applied at low stresses. In addition, below the bulk material's yield strength, SCC failure happens at tensile load [49].

Figure 2. 9: Accelerated Stress Corrosion Cracking [47-49].

Figure 2.9. shows the effect of accelerated stress corrosion cracking.

2.1.1.9. Selective leaching

Selective leaching occurs via corrosion processes resulting in a removal of one element from a solid alloy. The most common example is dezincification, which is the selective removal of zinc in brass alloys. Leaching also occurs in other alloy systems resulting in the removal of aluminium, iron, cobalt, chromium, and other elements. However, selective leaching is a general description of these dealloying processes such as dealuminumification and decobaltification, etc. There is also a metallurgical term ‘’parting’’ which is sometimes applied, but the most preferred term is selective

leaching [50]. In some alloys, this type of corrosion occurs by either mechanism, depending on temperature, concentration, and corrodent flow rate.

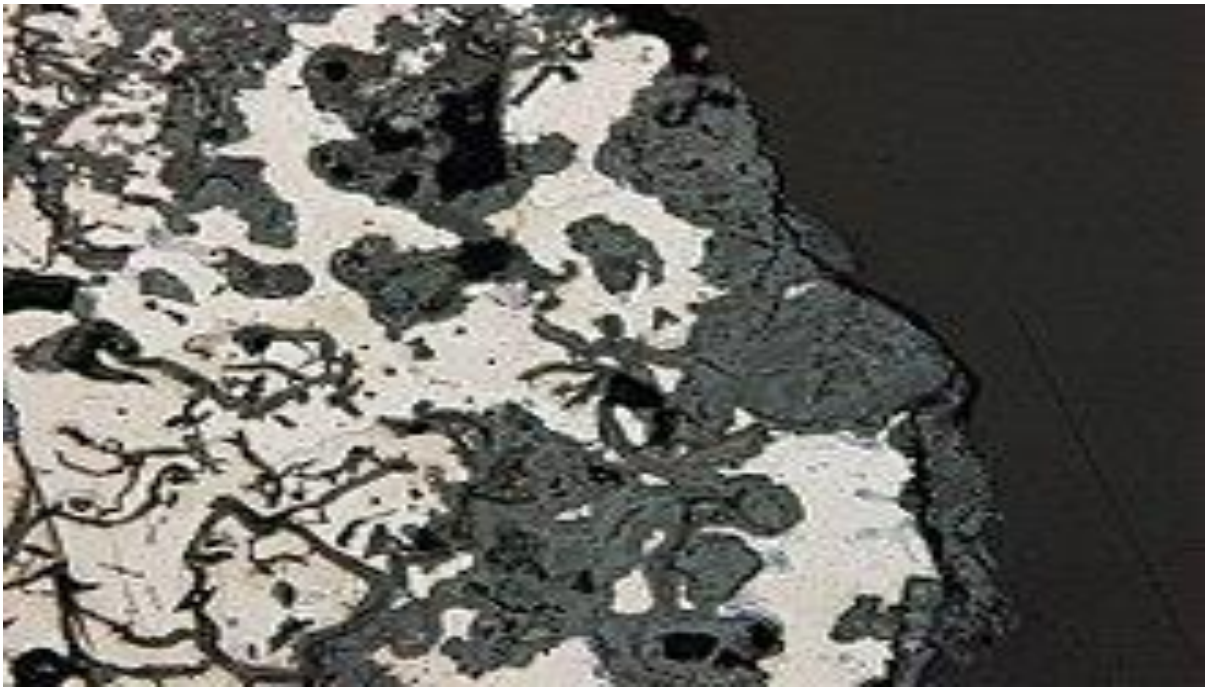

Figure 2. 10: Selective leaching [50].

Above is the Figure that shows the result of selective leaching.

2.1.1.10. Localised corrosion

Localised corrosion occurs when a small area of a metallic material encounters corrosion or when the material is in contact with a corrosion causing stresses. The rate of corrosion is faster at the small local that corrodes than at the rest of the component. This type of corrosion works hand in hand with stress and fatigue, and the combined resut is much worse as compared to the stress and fatigue result respectively [51]. It is known for an extreme attack at limited areas on surface components, while the remaining surface area deteriorates at a lower rate.

Figure 2. 11: Localised Corrosion - an overview [51].

This Figure depicts the results of how localised corrosion will look like.

2.1.1.11. Caustic agent corrosion

Caustic agent corrosion is the result of the degradation of a metallic material by the presence of impure gas, liquids, or solids. When a metal is in a dry form, it is not susceptible to degradation by most impure gases except when the metal be exposed to moiusture resulting in dissolution forming harmful corrosive droplets. An example of such caustic agent is hydrogen sulfide [52]. In addition, this corrosion type is present in many common household products. The severity of the damage is dependant on the corrosive properties and concentration of agents ingested. Furthermore, strong alkaline cleaning products, such as drain cleaners and lye soaps are often responsible for serious injuries.

Figure 2. 12: Caustic agent corrosion [52].

Figure 2.12. shows the results of caustic seeping through the cracks resulting in corrosion.

2.1.2. Consequences of corrosion

Lives of humanity are affected by corrosion on daily basis. Kitchen sinks, car bodies, charcoal grills, and any other metal tools used in homes are all subject to the deterioration process caused by corrosion, which is taking place on them. The corrosion of household appliances can present a potential health risk (e.g., corrosion product inside water pipes or tanks can mix with drinking water putting lives at risk). In the human body, metals can also be used as implants, but metals have the potential to deteriorate, which would lower the structural quality of the implant and could also provoke a biological response in the body of the host. Corrosion products were found in the tissue surrounding the metal implant, which is evidence of the implant's deterioration and could potentially lead to bone loss [53].

The process of corrosion has a negative impact on the global economy; Mazeika and Linas said, Industries that are energy intensive, such as cement, often experience severe corrosion damage caused by hot combustion gases. Metals are used by petroleum companies to carry or transport fuels, and several other metals, including fans and chimneys, are experiencing a high rate of corrosion. In addition, corrosion can result in product contamination, which can ultimately lead to the closure of a plant or an entire company. The repair or replacement of corroded metals is an expensive endeavour that has the potential to put the economy at risk [54].

Corrosion consequencies have the potential to endanger livelihood as shown in Figure 2.13. Metal that has been corroded loses its strength, which can lead to catastrophic events such as the collapse of buildings and bridges, the crushing of aircraft, the failure of gas and water pipes, and so on. These things can result in severe injuries or even the loss of livelihood.

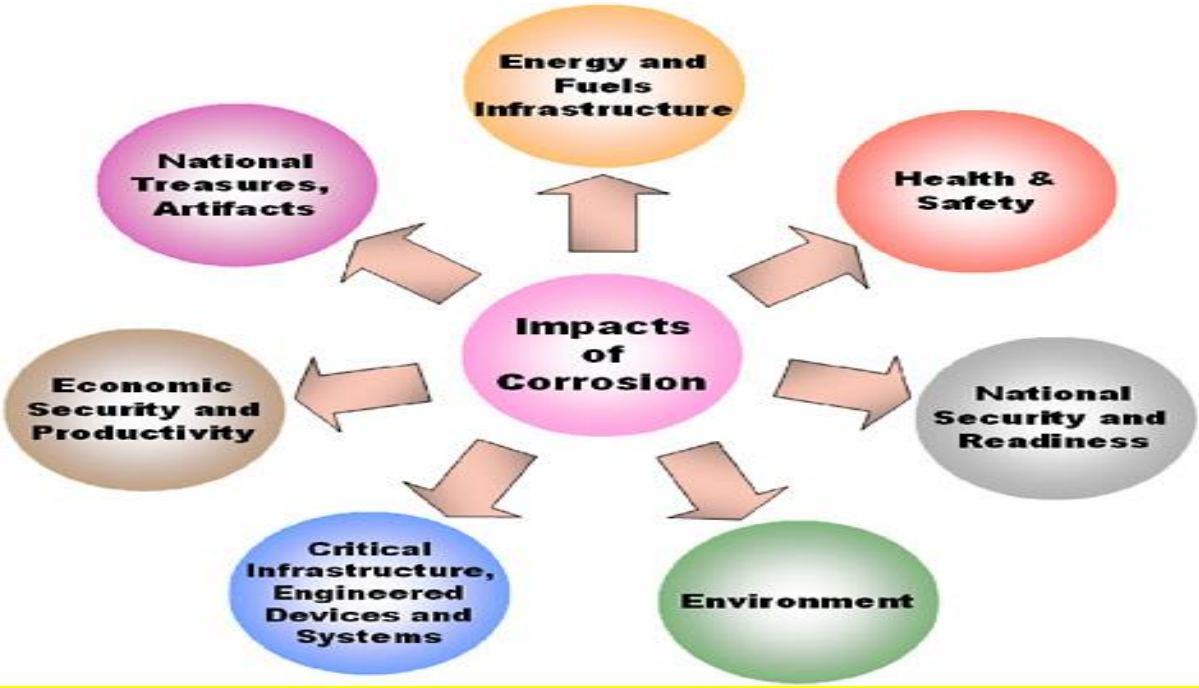

Figure 2. 13: Impacts of corrosion [53-55].

Corrosion affects nearly every aspect of modern society. In many of these areas, however, its impact is difficult to quantify [55]

2.1.3. Corrosion prevention methods

Studies have shown that corrosion or corrosion rate can be inhibited or reduced using various prevention methods as depicted in Figure 2.14.

Figure 2. 14: Methods of corrosion prevention [56].

Below is the outline of some corrosion prevention methods.

i. Barrier protection

This is the first protection method which was used to reduce the rate of corrosion rate during olden days. In this method the barrier amid the surface of the metal and corrosive environment is formed, hence the name barrier

protection. Examples of this method is coating by paint and galvanizing. When barrier (e.g., paint) is removed from metal surface, corrosion occurs.

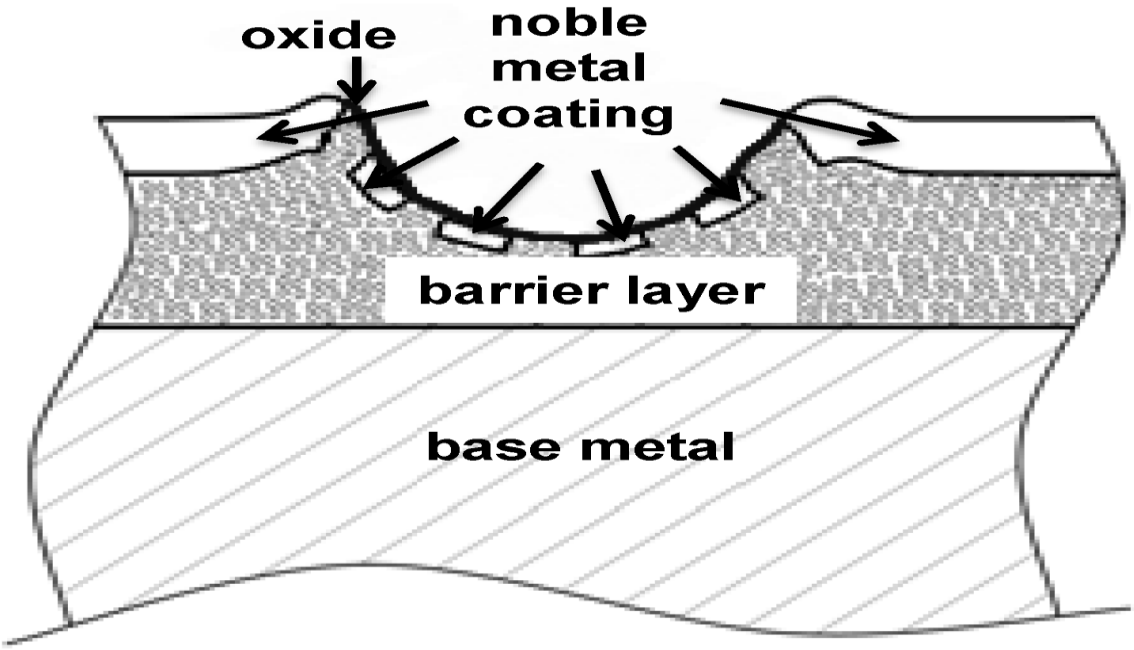

Figure 2. 15: Barrier protection [57].

Barrier protection Figure 2.15 detailed [57]:

ii. Cathodic protection

This was studied, proven and become widely used corrosion prevention method with example shown in Figure 2.16. It is mostly used to protect pipeline which are buried or submerged, buried tanks, offshore gas and oil platform, steel in concrete and plenty of other structures.

Figure 2. 16: Cathodic protection [57].

iii. Electroplating [58]

This is a process in which electrochemical reaction is applied to coat metallic surface by metal as shown in Figure 2.17. It consists of anode, cathode, electrolyte, and power supply source. Cheap metals such as zinc and steel are used for coating.

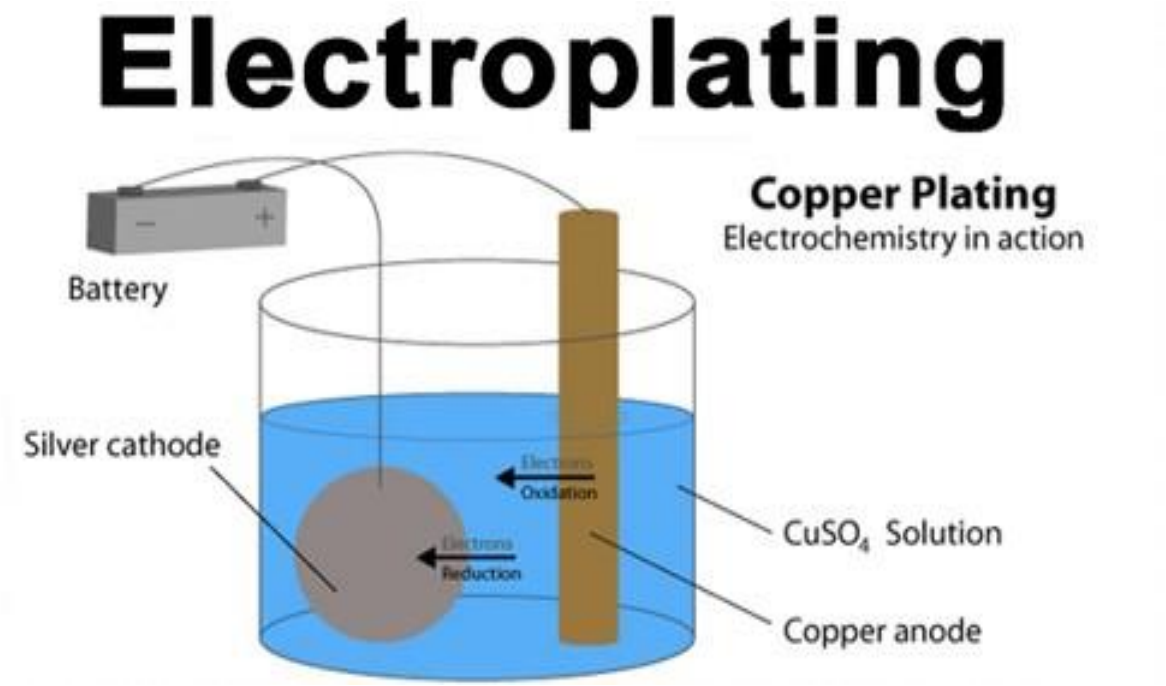

Figure 2. 17: Electroplating [58].

iv. Corrosion inhibitors

Inhibitors are applied at low concentrations to reduce the rate of corrosion. The usage of inhibitors is mainly in water treatment facilities, chemical production companies, oil and gas exploration etc. corrosion inhibitor method is the most widely used corrosion prevention presently. Corrosion inhibitors are broad and slow the rate of corrosion in various ways. Inhibitors can be classified as mixed and adsorption inhibitors. Mixed inhibitors slow down both cathodic and anodic reactions, while in adsorption the inhibitor adsorb to the metal surface forming a thin film to protect metal from corrosion. Different inhibitors are used for different metals in different environment. Corrosion inhibitors are effective, and most of them are eco-friendly, especially organic compounds such as Ionic liquids. Ionic liquids can reduce corrosion rate on metals such as aluminium, mild steel, and zinc.

2.1.4. Rate of corrosion

Corrosion rate is defined as to how fast the degradation of a metal takes place. The rate of corrosion is depended on factors such as the environment, material type and the exposure time [59]. Corrosion rate (C_R) is calculated as given in Equation 2.1 [60]:

$$C_R = \frac{\Delta W}{St} \quad (2.\ 1)$$

where, ΔW is the weight loss of the metal in immersion per time (*t*), and *S* is the surface area of the metal exposed.

2.1.4.1. Factors affecting the rate of corrosion [61,62]:

2.1.4.1.1. Nature of metal [61]

i. Metal purity: High corrosion rate is associated with the metal's impurity.
ii. Metal physical state: The more stressed the metal is, the higher the corrosion rate.
iii. Oxide layer nature: Depending on the porosity, stability and instability of the metal, corrosion rate is determined.
iv. Corrosive products' nature: The more soluble the products are, the higher the rate of corrosion.

2.1.4.1.2. Nature of corrosive environment:

i. Temperature: The higher the temperature, the higher the rate of corrosion.
ii. Moisture: The presence of moisture causes a high rate of corrosion.
iii. pH value: The rate of corrosion in pH levels less than 7 is high (e.g., acidic conditions).
iv. Electrolyte nature: The presence of salts in the electrolyte tends to increase the rate of corrosion.

2.1.5. Corrosion of metals

2.1.5.1. Mild steel

Mild steel is an alloy which has a large iron content with other metals such as carbon, manganese, copper, and silicon in small amounts. Due to a low carbon content, mild steel is also called low carbon steel. Mild steel's strength depends on the carbon present. Due to its accesseability and cost effectiveness, mild steel is mainly used for construction [63]. Metals or alloys tend to degrade when exposed to corrosive environment which is saline. In a mild steel, the most well known corrodent is iron which later results in iron oxide commonly known as rust. The corrosion of iron is because of high humidity of more than 60% [4]. Other factors such as rain, dew, radiation, and wind can accelerate corrosion rate. Metals are of a high economic significance, hence the need for their protection. Depending on environmental conditions and ecosystem, the higher rate of corrosion can be prevented. The commonly used prevention methods are painting, water absorption products and dehumidification. Because of high operational labour, and application cost, these methods are not favoured and considered not to be eco-friendly [64]. As depicted in Figure 2.18., redox reaction is taking place upon the corrosion of mild steel. For this reaction (corrosion) to take place, oxygen and moisture are involved. In a solution, iron is oxidised to form rust.

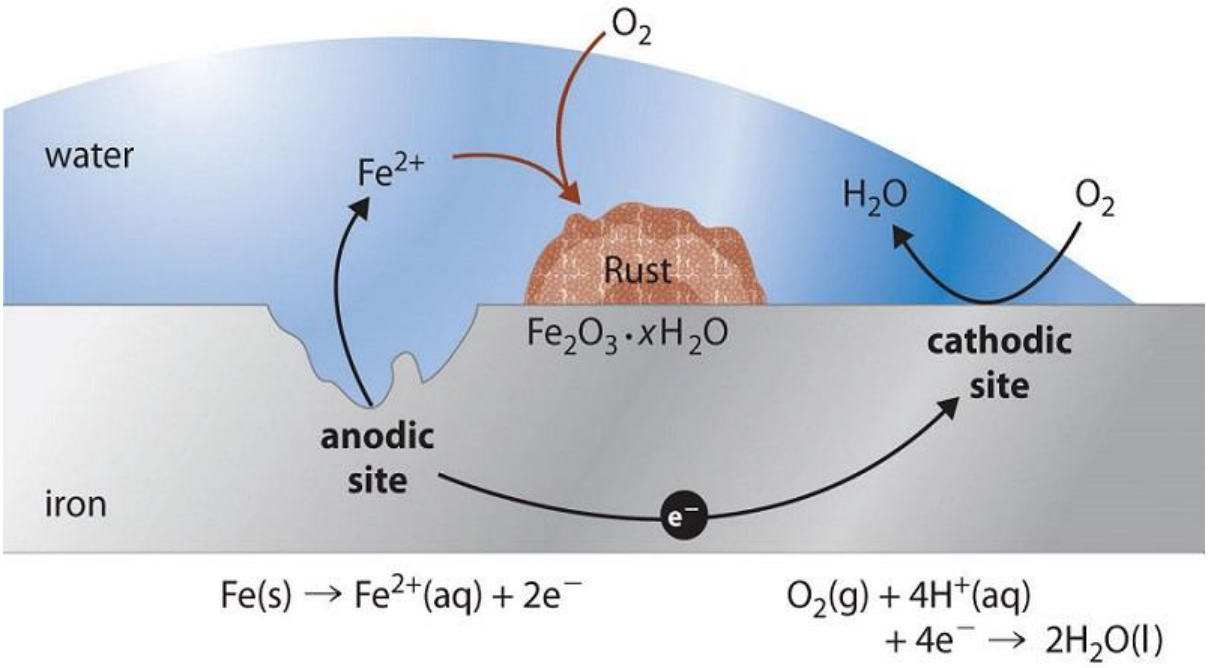

Figure 2. 18: Corrosion process for mild steel [65].

2.1.5.2. Zinc metal

In majority of natural environments, zinc is reckoned to resist corrosion [66]. The most cost-effective way of protecting zinc against corrosion is by metallic coating method. The formation of an oxide layer on a zinc metal is due to the gradual attack by the atmospheric oxygen. The interior layer located on a zinc metal serves as an inhibitor for the furtherance of zinc corrosion process [67].

Zinc metal can progressively corrode in certain tropical temperatures, resulting in zinc oxide being produced in the product. It has been stated that corrosion can take place in a variety of different open and enclosed settings since the air temperature can range anywhere from -18 ^oC to 70 ^oC. The process of corrosion is an electrochemical phenomenon because it involves the passage of electrons between the surface of a metal and an electrolyte [68]. The process of corrosion can also be characterised as the tendency of a metal to interact with water, oxygen, and other substances in an aqueous medium. This is another definition of the corrosion process.

Corrosion of the metal takes place at the anode, while reduction of oxygen and hydrogen takes place at the cathode [69]. Figure 2.19 displays how corrosion takes place on a zinc metal. Firstly, the metal undergoes a loss of electrons leading to the metal's degradation process. The outlined reactions below show in depth how the zinc corrosion process occurs.

Anodic reaction: $Zn_{(s)} \rightarrow Zn^{2+} + 2e^-$ (2.2)

Cathodic reaction: $2H^+ + 2e^- \rightarrow H_{2\,(g)}$ (2.3)

Overall corrosion reaction: $Zn + 2H^+ \rightarrow Zn^{2+} + H_{2\,(g)}$ (2.4)

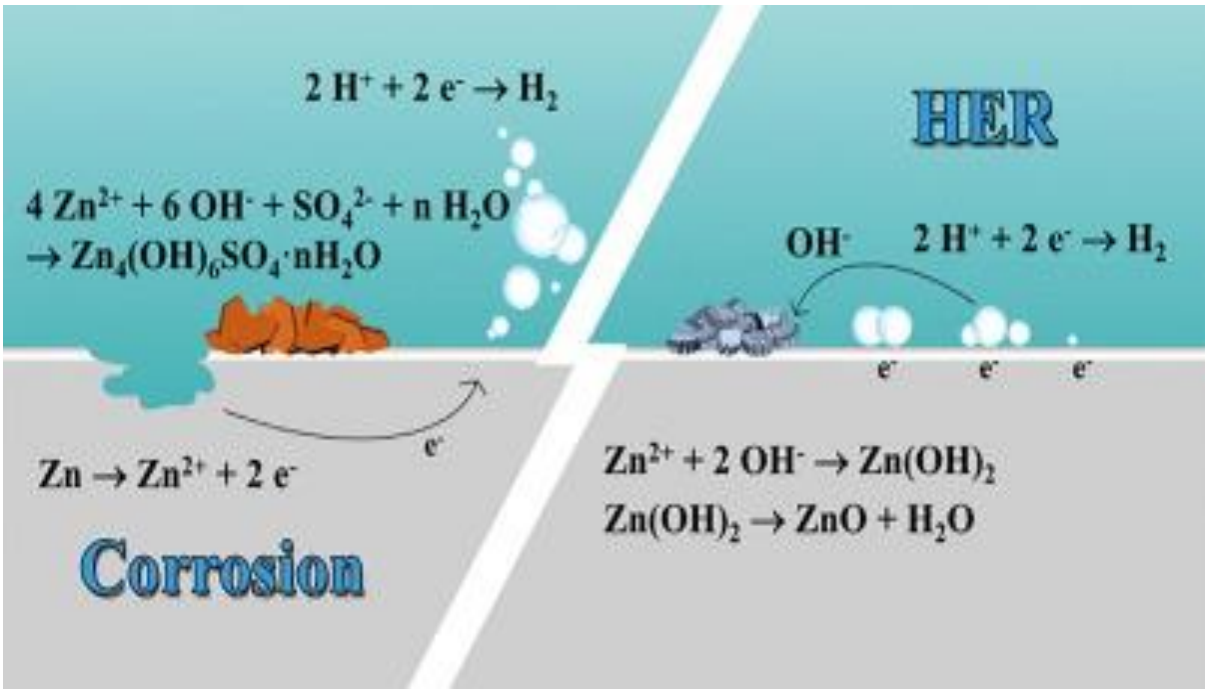

Figure 2. 19: Zinc metal corrosion process [67-69].

2.1.5.3. Aluminium metal

Many industrial companies have employed the use of aluminium to make pipes, batteries, and machines due to aluminium's unique features such as light weight [70]. Due to this light weight, aluminium is one of the most produced metal and it is easy to transport [71]. Other advantages aluminium posseses are electrical conductivity, thermal conductivity, ease of use, corrosion resistance, surface treatment, suitability, and aluminium alloys diversity [72].

The rate of corrosion on aluminium is slow as compared to mild steel, zinc, and other metals. Due to the thin protective surface layer, aluminium remains the most corrosion resistance metal [73]. In addition, the thin film is non-labile and serves as blockade of electron transfer between the metal surface and the corrosive environment. Corrosion on the aluminium metal surface occurs if the pH of an electrolyte is below and above 4-9 range [74]. In addition, this makes the investigation for suitable corrosion inhibitors on aluminium in both acidic and basic condition to be conducted.

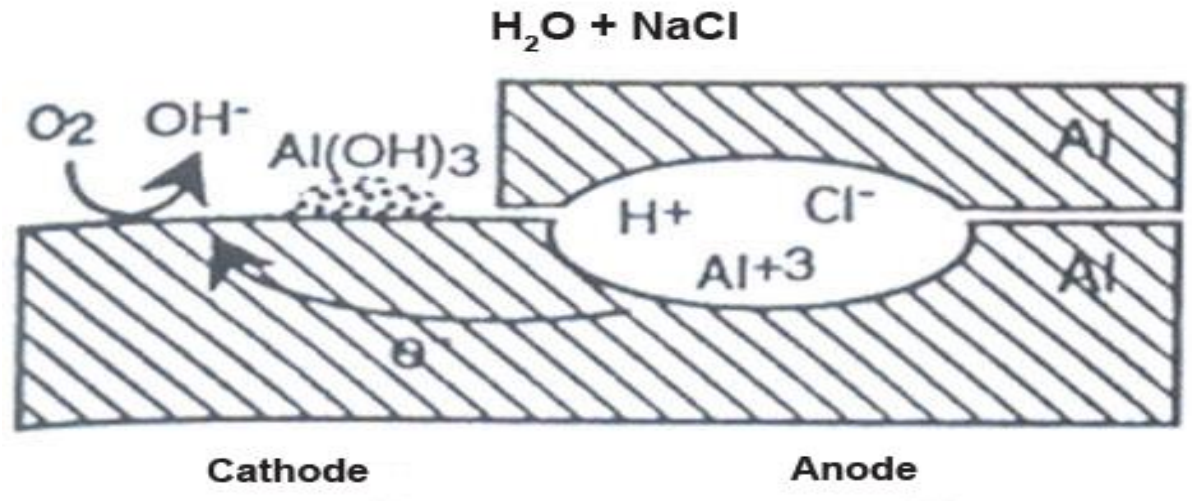

Figure 2. 20: Corrosion mechanism on aluminium [75].

2.1.6. Corrosion theory

2.1.6.1. Kinetics

Kinetic models can be used to further expound on corrosion process. Temperatures associated with the environment greatly influence the rate of corrosion. The higher the temperature, the faster the corrosion rate. The lower the temperature, the slower the rate of corrosion [76]. Before the formation of corrosion products, the process of corrosion passes through the activated complex like other chemical reactions. The minimum required energy is needed for the transition of the reactants to the activated complex. With the use of the Arrhenius equation (2. 5), the activation energy (E_a) can be determined.

$$\log C_R = \log A - \frac{E_A}{2.303RT} \tag{2.5}$$

where C_R is the rate of corrosion, Arrhenius pre-exponential factor is denoted by A, E_a is activation energy of the corrosion process, R is the gas constant denoted by R and the absolute temperature is denoted by T.

Corrosion kinetics bring an elucidation regarding corrosion rate at a specific time and environment. Corrosion reaction undergoes a redox reaction of which the electrons involved can be further quantified as current. The corrosion behaviour of the metals in an electrolyte can be examined through temperature effect [77]. Regarding Equation 2.1, the corrosion rate increases with an increase in temperature, E_a and A can be varied with temperature. Depending on the analysis method, the rate of corrosion is measured differently.

2.1.6.2. Adsorption isotherms and thermodynamic parameters

Adsorption studies assist by elucidating the adsorption mechanism of the inhibitor compound on the metal surface. This adsorption process depends on the metal type, inhibitor structure, and the electrolyte type [78]. There are several adsorption isotherms tested on the studies of corrosion such as Langmuir, Temkin, Frumkin and

Freundlich isotherms [79]. The type of the adsorption isotherm is determined from the surface coverage obtained in gravimetric analysis [80]. The isotherm with large regression coefficient of approximately 0.99 is most preferred and this best fit the Langmuir adsorption isotherm. From Equation 2.6, the Langmuir adsorption isotherm is given from which the equilibrium constant of adsorption or desorption is obtained.

$$\frac{C_{inh}}{\theta} = \frac{1}{K_{ads}} + C_{inh} \tag{2.6}$$

C_{inh} is the inhibitor concentration, Θ is the surface coverage degree, and K_{ads} is the equilibrium constant of adsorption.

With the assistance of chemical stability of the species and reactions involved, the process of corrosion can further be defined. The thermodynamic control concept can further help in understanding corrosion process although the rate of corrosion process cannot be evaluated by thermodynamic calculations. The theoretical activity of the metal can be calculated with the application of thermodynamics when the composition of the surrounding is known. The equilibrium constant of adsorption relates to change in Gibbs free energy of adsorption (ΔG_{ads}) by Equation 2.7:

$$K_{ads} = \frac{1}{55.55}\exp(-\frac{\Delta G}{RT}) \tag{2.7}$$

ΔG is the adsorption Gibbs free energy, R is gas constant, T is temperature and 55.5 is the water concentration of solution. With the help of Equation 2.7, the Gibbs free energy values of adsorption (ΔG_{ads}) can be easily determined. Mostly, negative values of the Gibbs free indicate that a spontaneous process occured. A negative value of change in free Gibbs energy (ΔG_{ads}) implies the spontaneity of corrosion process and a good adsorption stability at the inhibitor metal interface [81]. The varience between free Gibbs energy and temperature is explained in two ways:

i. Exothermic process occurs when ΔG_{ads} increase as the temperature increases.
ii. Endothermic process occurs when ΔG_{ads} decrease as the temperature increases.

The values of the free Gibbs energy play an important role in figuring out the kind of adsorption process that is taking place on the surface of the metal. In addition, the type of adsorption process can either be physisorption, which is also known as "physical adsorption," or chemisorption (chemical adsorption). The values of G_{ads} that range from -40 kJ. mol^{-1} and above in a direction that is negative represent the chemisorption process that ultimately results in chemical bonding. In addition, if the value of G_{ads} is less than -20 kJ. mol^{-1} and goes in the positive direction, this indicates a physisorption process rather than a chemical bonding activity since it indicates a weak van der Waals interaction [82]. There are other thermodynamic parameters which can be derived, such as adsorptive enthalpy, ΔH^o and the standard entropy, ΔS^o. With the help of the Van't Hoff equation, adsorptive enthalpy can be deduced:

$$\frac{dInK_{eq}}{dt} = \frac{\Delta H^{\theta}}{RT^2} \tag{2.8}$$

The adsorptive constant is denoted by K.

Using the equation below, the standard entropy, ΔS^o can be calculated:

$$\Delta G^o{}_{ads} = \Delta H^o{}_{ads} - T\Delta S^o{}_{ads} \tag{2.9}$$

Using the Equation 2.10, the equilibrium constant (K_{eq}) for the reaction is calculated. Faraday's constant is denoted by F:

$$RTInK_{eq} = -\Delta G^o = nF\Delta E^o \tag{2.10}$$

2.1.7. Electrochemistry

According to Equation 2.11, positively charged metal ioins propagate into an electrolyte and in turn electrons cleaves on the oxide-free metal surface resulting in metal dissolution [83].

$$M \rightarrow M^{n+} + ne^- \tag{2.11}$$

An atom in metal surface is denoted by M, an ion in solution is denoted by M^{n+} and electrons in a metal are denoted by ne^-.

Owing to a negative charge on the metal surface from residual electrons, the potential difference between the metal surface and the solution increases and this potential is the metal's potential as the working electrode. The change in potential hinders further metal dissolution and in turn favors the deposition of metal ions from an electrolyte to cleave back on the metal surface which is the reverse of Equation 2.11. The continuiety of degradation and deposition processess of metal ions would enhance the metal reaching its potential stability tenderly resulting in equal rates of the dissolution and deposition processes [84]. This metals's potential is entitled reversible protential (E_r) having a concentration dependent value of dissolved metal ions and the standard reversible potential (E˚) for unit activity from dissolved metal ions, $a_{M^{n+}}$:

$$M^{n+} + ne^- \leftrightarrow M \tag{2.12}$$

$$E_{r,M^{n+}/M} = E^{o}{}_{M^{n+}/M} + \frac{RT}{nF} \ln a_{M^{n+}} \tag{2.13}$$

Gas constant is denoted by R, Absolute temperature is denoted by T, Faraday constant denoted by F and the number of electrons transferred per ion is denoted by *n*. Once a reversible potential is reached, no further net dissolution of metal takes place. In addition, the net dissolution of the metal is generally slow in this process. The potential of the metal in most cases do not attain a reversible potential although the potential of the metal is positive because due to the fact that when different reactions are involved electrons can be eradicated from the metal surface [85]. In addition, a reaction between electrons and hydrogen ions can occur in acidic solution with electrons adsorbing on the metal surface resulting in hydrogen evolution (Equation 2.14).

$$2H^+ + 2e^- \rightarrow H_2 \tag{2.14}$$

The reaction above permits continuiety of the same metal ions quantity into solution which results in a metal corrosion with the reversible potential given in Equation 2.14.

$$E_{r,H^+/H_2} = E^o_{H^+/H_2} - \frac{RT}{F}\frac{InP^{0.5}_{H_2}}{a^+_H} \quad (2.15)$$

P_{H2} is the hydrogen gas partial pressure. If hydrogen partial pressure is permitted to build up, the reversible potential of reaction (Equation 2.14) could be attained. Due to the absence of further net reaction of hydrogen ions, the net metal dissolution would cease effectively.

In neutral solutions, the concentration of hydrogen ions is to permit reaction (Equation 2.14) to progress at a significant rate. Nevertheless, the electrons on the metal can react with oxygen molecules from air into solution effectively to produce hydroxyl ions as demonstrated in Equation 2.16.

$$O_2 + 2H_2O + 4e^- \rightarrow 4OH^- \quad (2.16)$$

The potential of the working electode (metal) remains more than the reaction's reversible potential (Equation 2.17):

$$E_{r,O_2/OH^-} = E^{o}{}_{O_2/OH^-} - \frac{RT}{4F}\ln\frac{a_{OH^-}{}^4}{P_{O_2}} \quad (2.17)$$

Once Equation 2.11 and 2.16 couples, corrosion process can proceed. In the electrochemical terminology, the electrode on which oxidation reaction occurs is called anode. The dissolution of the metal is as the result of the loss of electrons on the surface of the metal thus oxidation process (Equation 2.11). In electrochemical terminology, the gaining of electrons is called a reduction occurring at the cathode [86].

2.1.8. Corrosion inhibitors

Inhibitors are used extensively in the manufacturing of chemicals, as well as in water treatment facilities, oil and gas exploration, and other related fields. The use of chemical corrosion inhibitors is the method that has seen the greatest amount of use for the purpose of preventing the corrosion process. These inhibitors are utilised in a wide variety of settings and can limit the pace of corrosion. Inhibitors can be

categorised in several different ways, including as mixed types and as adsorption inhibitors. In the case of adsorption inhibitors, cathodic and anodic inhibitors are slowed down by mixed-type inhibitors, and the adsorbed inhibitor on the metal surface produces a thin coating that prevents the metal from corroding [87]. In different situations, different types of metals require different inhibitors to be applied. Most organic corrosion inhibitors, such as ionic liquids and green inhibitors, have the advantage of being environmentally friendly and economically effective. This is especially true with organic corrosion inhibitors.

2. 2. SELECTED CORROSION INHIBITORS

2.2.1. Some organic compounds as corrosion inhibitors

2.2.1.1. Plant extracts as corrosion inhibitors

In recent years, phytocompounds and extracts derived from herbs have garnered an increasing amount of attention in the field of environmentally friendly products. When evaluating some plant extracts, the total phenolic content should be employed, and the relationship between the extract outline and the corrosion inhibitive impact should be considered. It was discovered that there was a correlation between the overall phenolic content of the plant extracts and the efficiency with which they inhibited corrosion. The extracts' inhibitory effectiveness increases in direct proportion to the total phenolic content of the plant material. When screening plant extracts for inhibitory effects, it is likely that the total phenolic content can be utilised as a reference [88]. This is because total phenolic content includes both monomeric and polymeric phenolics [88].

2.2.1.2. Extraction methods used to obtain plant extracts.

Throughout the course of the last several decades, several articles on the isolating and fractionating of diverse compounds, including plant extracts, essential oils, and chemicals that have been purified, have appeared. The chemical composition of the drug, the particle size of the sample, and the presence of interfering compounds are

all factors that influence the selectivity of an extraction process [89]. This method is used to profile the target content of plant species. The market niche of the compound of interest and the needed level of purity both have an impact on the choice of extraction process, which in turn influences the rate, yield, and purity of the extracted substance. The quantity of a chemical that can be extracted from plant material is susceptible to being significantly influenced not only by the type of solvent that is used for the extraction process but also by the procedures that are used to isolate the substance after it has been extracted. Because of the influence that these operational variables have on both the concentration of the extract and its antioxidant activity, each extraction method has its own distinct set of variables that need to be optimised. The primary factors that influence the extraction kinetics are the extraction time, temperature, the ratio of solvent to feed, the number of sample repetitions, and the choice of extraction solvent. The degree to which temperature and the amount of time required to extract a substance both play a significant role in determining solubility. The viscosity and surface tension of the solvents both decrease when the extraction temperatures are raised, which in turn has the effect of accelerating the rate at which mass is transferred [90]. Another factor that can influence the extraction kinetics is the pretreatment of the material. This factor has an impact not only on the sample's matrix but also on the particle size and distribution, as well as the amount of moisture that is contained within the sample.

Because of the ease with which they can be implemented, the reliability with which they are endowed, and the adaptability with which they are endowed, the liquid-liquid and solid-liquid extraction strategies that have been present for a protracted time are still widely used today. These traditional approaches do, however, come with their own individual advantages and disadvantages that should not be overlooked. The amount of material that can be extracted is improved when various solvents are used in the process. One of the most significant drawbacks of this method is that it makes use of traditional solvents, such as alcohols (methanol, ethanol, and isopropanol), acetone, diethyl ether, and ethyl acetate, all of which are frequently mixed with varying amounts of water for the purposes of sample preparation, separation, and detection. In addition,

this method also requires the use of ethyl acetate. Not only are these solvents a problem for the environment, but they are also a problem for the economy. In order to satisfy the requirements, set forth by the regulatory body, it is necessary to carry out additional purification steps utilising membranes. It is possible for active chemicals to undergo rapid chemical degradation if they are subjected to higher temperatures for an extended period. The traditional method of extraction takes an extremely long time, which is another one of the many drawbacks associated with the method. The extraction process itself also takes an extremely long time. The modern extraction techniques place an emphasis on applications that are beneficial to the environment, techniques that are based on sorption, techniques that reduce the amount of solvent that is used, and techniques that make use of both solid and liquid materials [91,92].

In comparison to organic solvent technology, solid-phase extraction, also known as SPE, pressurised liquid extraction, also known as PLE, microwave-assisted extraction, also known as MAE, and solid-phase microextraction, also known as SPME, all have several significant advantages. The ease of product fractionation is just one of these benefits, along with the product's positive impact on the surrounding environment. These techniques are simple, the extraction process with them takes less time, and they produce fewer harmful pollutants because they use a lower percentage of organic solvent. This is because the organic solvent is used as a carrier. Because of this, they have seen an increase in their level of popularity. The most significant benefit that the SFE has to offer is the selective extraction of components or the fractionation of the total extracts [93]. Both processes are possible with the SFE. This can be achieved by altering the process parameters or by utilising a variety of gases with the intention of isolating components or fractionating them. Both methods are viable options. It is common knowledge that subcritical and supercritical fluids are types of solvents that do not cause cancer, do not cause genetic mutations, do not cause fires, and are thermodynamically stable. Additionally, it is also common knowledge that these types of solvents do not cause fires. Any substance that has been brought to a temperature and pressure that are both greater than its critical point is a supercritical fluid. At this stage, the substance does not exist in a state that can

be classified as either liquid or gas. They function admirably as a suitable replacement for organic solvents, which, when they are brought to within a short distance of their critical point, exhibit a peculiar property in which even minute variations in temperature or pressure can result in significant variations in density. They do this because organic solvents approach their critical point. Because of this, the characteristics of the organic solvents can be altered in a wide variety of different ways. They are an adequate substitute for the original item. The point at which the boiling curve and the pressure-temperature phase diagram intersect is known as the critical point (Figure 2.21). At this point, both the liquid and gas phases vanish, and all that is left is the supercritical phase. On the pressure-temperature phase diagram, the region corresponding to gas and liquid are separated by the boiling curve.

The fundamental advantage of the extraction methods, on the other hand, is that they can be used to isolate both polar and non-polar molecules, and their selectivity can be adjusted by selecting the appropriate solvent and/or operating conditions. This ability to isolate both types of molecules is a fundamental benefit of the extraction methods. The extraction methods have the significant benefit of being able to separate both types of molecules, which is a significant advantage. According to research that was carried out on the components that make up corrosion inhibitors, it was discovered that chemicals that are either polar or non-polar can be effective at inhibiting corrosion. In addition to this, the techniques of extraction that have been covered up until this point offer economic benefits, which have been discussed up until this point. The findings of this review indicate that polyphenols are one of the primary ingredients that are included in environmentally friendly corrosion inhibitors. Other ingredients that are included in these inhibitors include: Although other solvents, like ethyl acetate or acetone, have been used extensively in the extraction of polyphenols from plants, the largest yields of polyphenols are typically obtained using ethanol, methanol, and their combinations with water. Other solvents, like ethyl acetate or acetone, have also been used extensively in this process. The reason for this is that these solvents have a higher boiling point than water, which makes it possible for them to dissolve a greater quantity of polyphenols [94–96].

Due to the intricacy of the subject matter, it is conceivable to make the assertion that there is still a "barrier" separating study and the application of the findings. This is something that can be said. Because this is something that is possible, it is something that can be said. To achieve quality control of vegetable extracts and the efficacy of specific phytocompounds, much more research needs to be done on analytical and microbiological characterisation assessments on vegetal extracts that are being tested as novel eco-friendly material-protecting products. These assessments must be performed on vegetal extracts that are being tested as novel eco-friendly material-protecting products [97,98]. These assessments need to be performed on vegetal extracts that are being tested as novel eco-friendly material-protecting products. These sorts of evaluations ought to be carried out on plant extracts that are currently being investigated for use as innovative environmentally friendly material protecting products. In the sections that are to follow, we will discuss in greater depth the research that has been carried out over the course of the past two decades on the use of plant extracts as corrosion inhibitors for aluminium and its alloys in a variety of corrosive environments. This research was conducted on the use of plant extracts as corrosion inhibitors for aluminium and its alloys in various corrosive environments. During this study, an investigation into the utilisation of plant extracts as corrosion inhibitors for aluminium and its alloys in a variety of different corrosive conditions was carried out. In addition to this, particulars pertaining to the extraction method itself as well as the key components of the extracts are broken down in this section of the article (as reported by the authors in the specific corrosion inhibition research or in studies not directly connected to corrosion research). Based on the solvents that were used during the extraction procedure, the extracts were divided up into four unique groups.

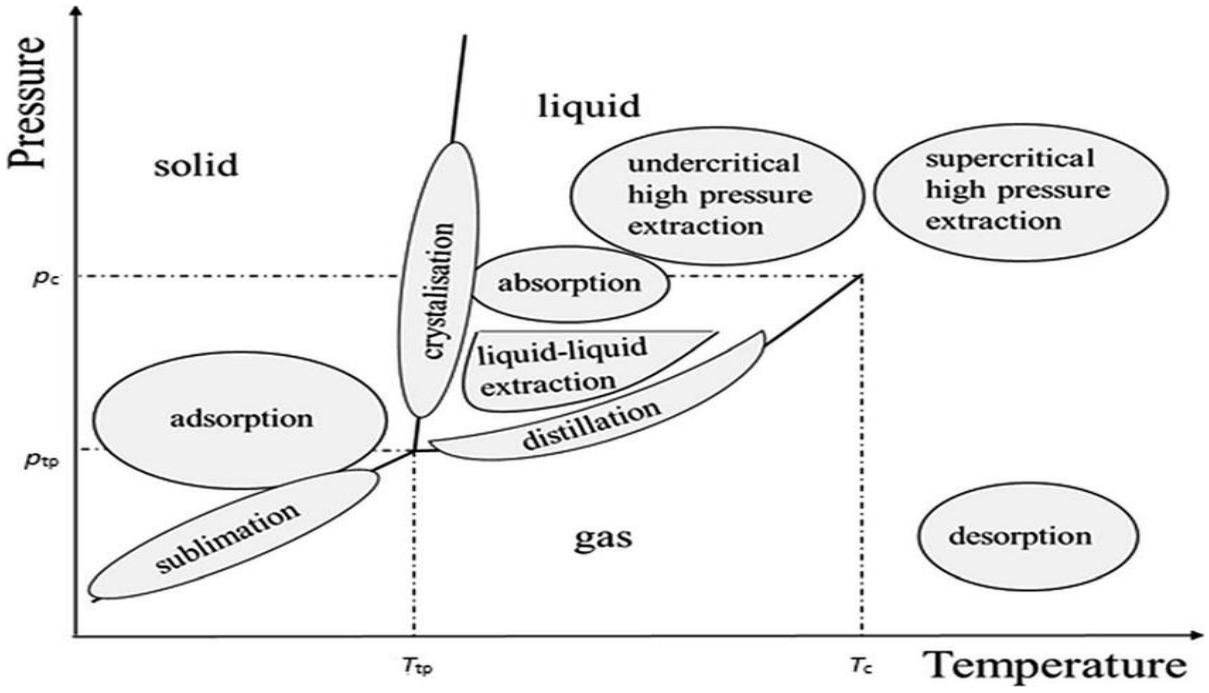

Figure 2. 21: p–T diagram of a pure substance and separation processes [55].

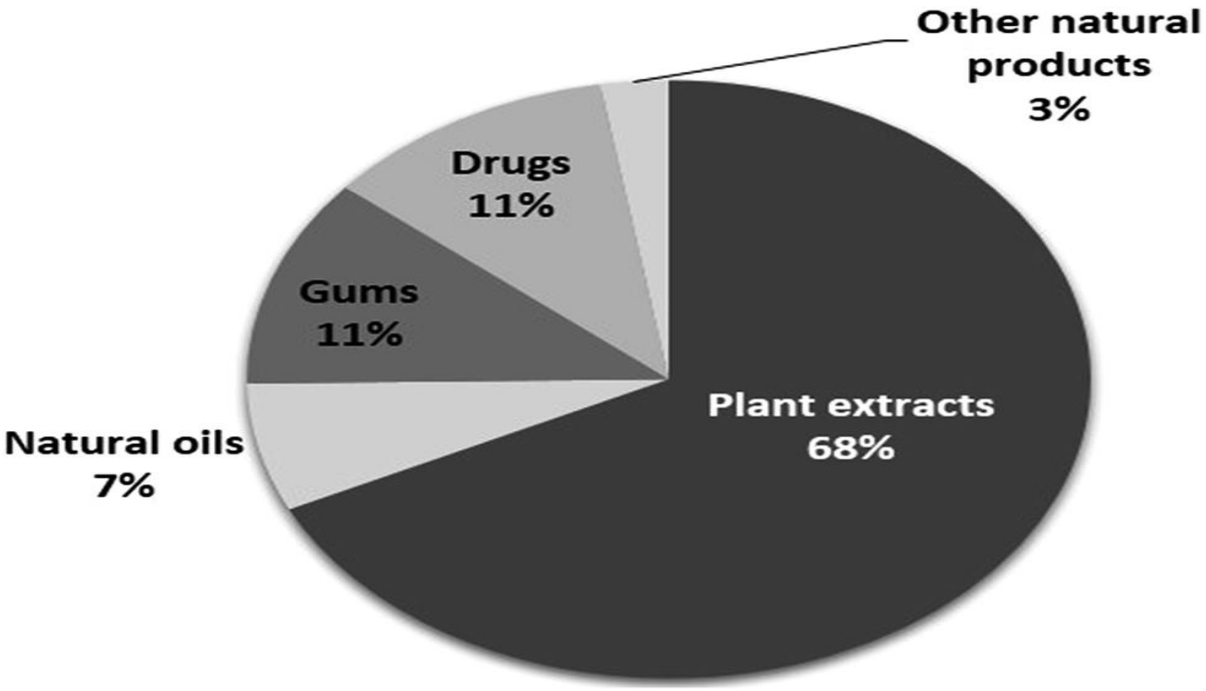

Figure 2. 22: Natural products as corrosion inhibitors for aluminium and its alloys [55].

Figure 2.22. shows different percentages of natural products as corrosion inhibitors.

2.2.1.3. Drugs as corrosion inhibitors for aluminium and its alloys

As was stated earlier, there was once a time when it was supposed that pharmaceuticals had the potential to act as corrosion inhibitors. This was especially true with regard to the protection of steel against corrosion [99]. The number of studies that describe drugs as corrosion inhibitors for aluminium and its alloys is relatively low; however, such research may become more appealing in the not-too-distant future. The chemical structures of all the anticorrosion medications that have been reported as being effective in this article are summarised in a condensed form [24,59,100–104].Antibacterial and antifungal drugs were among the compounds that had received the most attention from researchers up until this point because of their potential use as corrosion inhibitors for aluminium and the alloys of aluminium in a variety of different solutions [24,59,100–104].

This attention had been focused on these compounds since antibacterial and antifungal drugs were among the compounds that had received the most attention from researchers. However, there have also been a few studies done on the possibility of using antihypertensive and antiemetic drugs as corrosion inhibitors [55,105]. These drugs are used to treat high blood pressure and nausea, respectively. These medications are prescribed to treat high blood pressure and, respectively, nausea and vomiting. Both medications are prescribed to treat high blood pressure, as well as nausea and vomiting, respectively. When put through a series of tests in acidic solutions, every one of the medicines that were the focus of the investigation demonstrated an ability to prevent corrosion.

The WL method has been utilised quite extensively in recent research that has been carried out to evaluate the effectiveness of these compounds as inhibitors [59,100,101,103]. These studies have been carried out in recent times. The authors of each of the included studies arrived at the same finding, which was that the individual drugs tested acted as mixed-type inhibitors. This was the consensus reached by the researchers who carried out the studies. The incorporation of polarisation methods into several the research projects ultimately led to the formation of this conclusion.

According to the findings of all the research that has been carried out and published about the use of drugs as corrosion inhibitors, the efficiency of the inhibition increased proportionally with the drug concentration, but it decreased as the temperature increased. This was the conclusion that was reached after all the research on the topic had been carried out and published. This was the realisation that came about as a result of all the investigation that was carried out. The authors suggested mainly physisorption as a possible adsorption mechanism for all of the drugs that were studied, with the exception of Bhat and Alva's work [24,59,100,102,104,105], which suggested a mixed-type adsorption (physisorption and chemisorption) for meclizine hydrochloride. This work was the only one that suggested this type of adsorption

mechanism. Although Bhat and Alva's research was the only one that suggested a mixed-type adsorption, this was still the result.

This result was reached as a direct consequence of the thermodynamic calculations that were carried out and their outcomes. On the other hand, these authors reported that physisorption was the most important part of the overall mechanism [106]. Gece has compiled a thorough review article in which he compares medications that are categorised into a variety of pharmacotherapeutic categories [99]. Although each of these pharmaceuticals has a completely unique biological mechanism of action, it is still possible to apply any of them to the treatment of corrosion in a wide variety of materials. However, it is essential to keep in mind that the pharmacodynamic, and consequently the pharmacologic action that the drugs have on the body, have, in essence, nothing to do with the mechanism of their potential to inhibit corrosion.

In addition, rather than classifying these drug-based corrosion inhibitor candidates according to their biological activity, it is more useful to consider their general molecular properties (such as the presence of heterocycles in their structures or reactive centres such as O, N, and/or S atoms with lone pairs of electrons, which can aid in their adsorption onto metal surfaces). In addition, it is ideal to classify medications in accordance with the pharmacotherapeutic groups to which they belong to perform an analysis (or categorisation). Not only is this ideal in the context of describing the drugs, but also in the context of the potential for corrosion inhibition that the drugs possess.

Particularly, carrying out these steps makes it much simpler for a researcher with a background in the biological sciences to search for their potential dual application in clinical settings. This is because these steps are performed. This is because of the fact that carrying out these steps enables one to better organise the information that is being gathered. This is especially true for medical implants, like metal-based hip prostheses, where antimicrobial drugs (like antifungals and antibiotics) or anti-inflammatory drugs can make a big difference in preventing corrosion while the implant

is exposed to the harsh biological environment of the body for a long time as shown in figure 2.23. They can also help the body accept the implant by preventing infections or making them less likely [99].

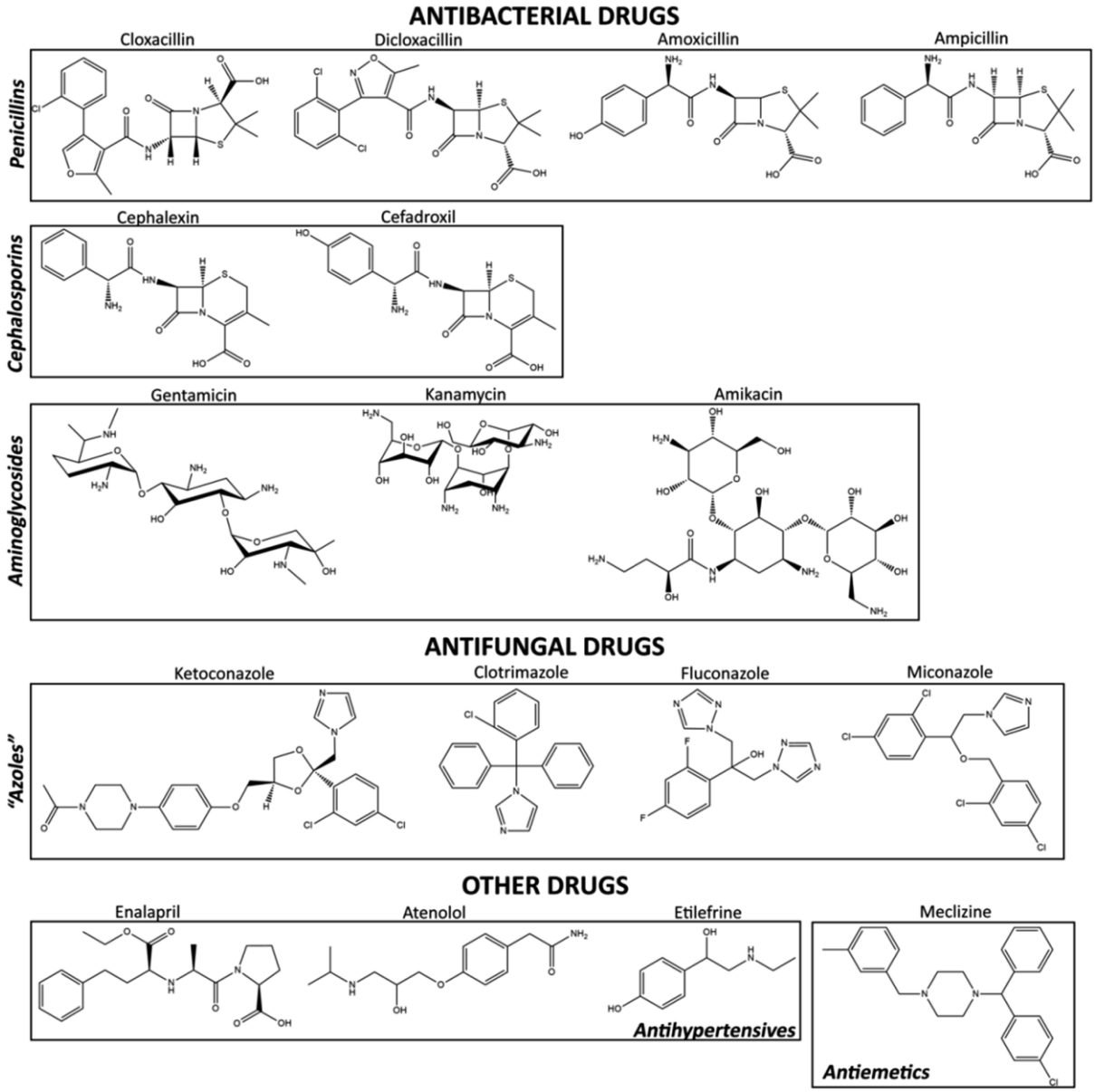

Figure 2. 23: Tested drugs [55].

2.2.1.4. Gums as corrosion inhibitors

Plant-based gums are made up of a combination of long-chain polysaccharide compounds, which are formed either naturally because of the gummosis, as a result of injury to the bark or stem, or as a result of microbial attack. Gummosis is the process by which plant-based gums are produced. The production of gums derived from plants takes place through a process known as gummosis. The term "gummosis" can refer to either the process of the decomposition of plant tissue or an injury to the bark or the stem of the plant. Gummosis is a term that is used in botany. Gums have a wide variety of applications, some of which include the preservation of food, work in the cosmetics and pharmaceutical industries, and work in the cosmetics industry (fungi and bacteria) [107].

Most of the time, oils and organic solvents will not cause them to dissolve. When other gums are put in contact with liquid water, the water is either absorbed by the gum, causing it to swell, or the gum is dispersed in the water, causing it to produce a solution that is jelly-like or viscous. On the other hand, when they encounter water, certain gums dissolve very quickly and easily. The hydrolysis of these gums results in the production of glucuronic acid in addition to the simple monosaccharides galactose, mannose, and arabinose as a byproduct [107,108]. The stem of plants, particularly those belonging to the families Leguminosae and Sterculiaceae, is the source of most gums, with only a small percentage coming from other plant parts. This is especially true of plants that are legumes and sterculiaceous.

This is particularly true of legumes and other plants in the sterculiaceous family. This is especially the case with gum tragacanth, which is a substance that can be found in plants that are members of the legume and sterculiaceous families (roots, leaves, and seeds). In addition to their well-known applications in the pharmaceutical and food industries [109–112], gums can also be used as corrosion inhibitors for a wide variety of metals in a number of different environments [108], where corrosion is prevalent. These gums can be used in a variety of settings, including marine environments, chemical environments, and food environments. These gums have applications in a

variety of different environments, including chemical environments, food environments, and marine environments, among others [108].

These gums have a variety of different applications that can be used in a wide range of environments. These gums contain a high concentration of nitrogen and oxygen atoms, which can be found in the polysaccharide compounds that are found in the gums. Additionally, these gums contain a high concentration of carbon atoms. These polysaccharide compounds perform the function of adsorption centres, and as a result, they have the capacity to stop corrosion from occurring. In addition to this, gum-metal complexes will begin to form, and these complexes will work as a protective barrier layer to separate the surface of the metal from the corrosive environment. This will prevent the surface of the metal from being corroded.

In addition to this, gums have a low level of toxicity, they are biodegradable, and they are beneficial to the environment. Gums are a natural substance that can be found in many plants. Gums are a naturally occurring substance that can be discovered in a wide variety of plant species. The utilisation of gums is a more responsible choice for the environment. In order to determine whether or not a variety of gums have the potential to act as corrosion inhibitors for aluminium and the alloys that are made of aluminium, a variety of gums have been tested in a variety of different solutions [108,113,122,114–121]. The results of these tests will determine whether a variety of gums have this potential.

None of the three types of gums—xanthan gum, Commiphora pedunculata gum, or arabic gum—went through any additional purification steps before being put to use [114,115,117]. In the earlier studies that came before, the other gums were purified utilising one of two approaches [117,123] that could not be more dissimilar from one another. The purification processes for Raphia hookeri [113], Pachylobus edulis [116], and Dacroydes edulis [124] all made use of the same method, which consisted of dissolving the gums in an ethanol solution that contained 95% of the gums' original

concentration. This method was utilised in all three of the purification processes. This approach was utilised in each one of the different purification procedures.

Eddy *et al*. [108,118,120,123], were able to successfully purify the gum by first dissolving it in ice-cold distilled water and then centrifuging the resulting solution to form a thick gel. This process was successful in removing impurities from the gum. Using this process, they were able to eliminate any impurities that might have been found in the gum. This procedure has been carried out successfully on several different occasions. After the addition of watered-down hydrochloric acid, the pH of the supernatant was brought to a state in which it had a value that was more comparable to that of an acidic solution. This was accomplished by lowering the concentration of the acid. After that, an extremely slow addition of ethanol with a concentration of 80% was made, and the gum that had precipitated was obtained by centrifuging the mixture.

In the end, the gum was cleaned with alcohol, then it was cleaned with ether, and in the end, it was allowed to dry out before it was used. Before it was used, the gum was cleaned with alcohol, then it was cleaned with ether. The gums that were used in the studies that were carried out independently by Eddy *et al*. were purified by using the same method that was used to purify the gums. Traditional methods such as WL, HE, and thermometric testing were the only methods that were used in any of these studies to determine how effective the gums being evaluated were at preventing the growth of microorganisms. The only methods that were used to determine how effective the gums being tested were at inhibiting the growth of microorganisms were these methods (no electrochemical analysis was reported).

Two of the materials that are put through the most exhaustive testing and inspection procedures are aluminium in its purest form as well as alloys of aluminium in the 1xxx series [108,115,118–120]. In each of the studies, the investigators discovered that increasing the gums' concentration led to an increase in the effectiveness of their inhibitory properties. The results of all of the studies came to the same conclusion regarding this finding. In each and every one of the studies that they analysed; the

results consistently pointed to the same conclusion. In the research carried out by Arukalam *et al*. [125], Eddy *et al*. [122]., Umoren *et al*. [113]., and Umoren, it was found that an increase in temperature led to an increase in the effectiveness of the inhibition, whereas in other studies, it was found that the opposite was true. Umoren *et al*., and Umoren were the researchers who made this discovery.

According to the findings of the study that Eddy *et al*. [118] conducted, the progression of the change in inhibition effectiveness for Ficus tricopoda gum followed an unpredictable pattern as the temperature increased. However, the authors found that the effectiveness of the inhibition increased with an increase in temperature for higher gum concentrations. This was the case even though the gum concentrations remained the same. This was the case despite the consistency of the gum concentrations remaining unchanged. They discovered that the effectiveness of the inhibition decreased when the temperature was elevated for concentrations of up to 0.3 g. L^{-1} gum added; however, they discovered that the effectiveness of the inhibition increased when the temperature was elevated for higher gum concentrations.

For gum addition concentrations up to 0.3 g. L^{-1}, the efficiency of the inhibition reduced with increasing temperature, as reported by Eddy *et al*. [122]. The effectiveness of xanthan gum as a corrosion inhibitor of 98.08 percent aluminium alloy in a 0.5 M HCl solution at temperatures between 28 ^{o}C and 60 ^{o}C was published by Arukalam *et al*. [125]. Their studies centred on how well the gum worked as a heat-resistant corrosion inhibitor for the metal. Their primary focus was on learning if the gum worked as a corrosion inhibitor. They concluded that the process of inhibition occurs because protonated and molecular species can adsorb on the cathodic and anodic sites of the corroding metal surface.

As a result of these findings, they concluded that inhibition is a real phenomenon. In the experiments that Umoren [124] and Ebenso [114] carried out, they found that the exudate gum of Raphia hookeri was effective as a corrosion inhibitor for aluminium. This was one of the discoveries that came about because of the experiments. They

came to this realisation because of their investigation (the composition of the experiment was not given). To verify the accuracy of the method, tests were carried out at temperatures ranging from 30-60 ^{o}C using solutions of 0.1 M and 2. 0 M HCl. The findings substantiated the validity of the methodology. According to the authors, the exudate gum produced by Raphia hookeri is composed of D-mannopyranose and D-galactopyranose, both of which are connected to one another. The authors have been very generous in providing us with this information.

The findings that were presented by the authors [113,126] indicated that the addition of potassium halides led to an even more significant increase in the effectiveness of the inhibition (KI, KCl, and KBr). It was discovered that the synergistic effect of the halides decreases as one moves from iodine to bromine to chlorine. This was a finding that came about because of the research that was conducted. The authors of the study held the belief that the order could be explained by the fact that the radii of the halide ions and the electronegativity of the halide ions both played a role in the process of adsorption. Specifically, they believed that the order could be explained by the fact that the radii of the halide ions were greater than the electronegativity of the halide ions. They were, however, unable to provide any evidence to back up this hypothesis in any way. They thought that the order could be explained by the fact that the radii of the halide ions were increasing from lowest to highest. This was the order in which the radii were found. In a separate piece of research, Umoren *et al*. [127] compared the efficacy of the exudate gums from Raphia hookeri and Pachylobus edulis in inhibiting the corrosion of AA1060 aluminium alloy (98.5% purity) in 0.1 M and 2. 0 M HCl solutions at temperatures ranging from 30-60 ^{o}C. They found that the exudate gums from Raphia hookeri were more effective than the exudate gums from Pachy. They discovered that the gums obtained from Raphia hookeri were significantly more effective than those obtained from Pachylobus edulis. They made the discovery that the exudate gums from the Raphia hookeri species were significantly more effective at inhibiting corrosion than the exudate gums from the other Raphia species.

The findings of the study indicate that Raphia hookeri performs its role as an inhibitor in a manner that is more efficient than that of Pachylobus edulis does. In solutions of 1. 0 M and 2. 0 M NaOH, at temperatures of 30-40 ^{o}C, Umoren *et al*. [124], investigated the efficacy of gum arabic as a corrosion inhibitor for AA1060 aluminium alloy. The results of the research were positive. According to the findings conducted by Umoren *et al*. [113], gum arabic was successful in both concentrations. They were taken aback by the results of their investigation, which showed that gum arabic had a significant inhibitory effect. The scientists who conducted the research and wrote up the study are of the opinion that the ability of this gum to prevent corrosion is due to the adsorption of its primary constituents on the surface of the aluminium alloy.

This substance contained a variety of primary constituents, some of which were glucoproteins, arabinoglactan, oligosaccharides, and polysaccharides. Umoren [127] carried out a series of experiments to evaluate the efficacy of gum arabic as a corrosion inhibitor. The tests were carried out with the same aluminium alloy and temperatures in solutions that contained lower concentrations of sodium hydroxide (i.e., 0.1 M NaOH). Based on the findings of the study, gum arabic was found to be an effective substance in inhibiting corrosion. The author discovered that the variation in the efficacy of the inhibition with gum concentration and temperature followed the same pattern as what was discovered in the earlier work. This pattern was found to be true. The author is credited with discovering this pattern. The addition of 0.5 M KI led to an increase in gum arabic's already remarkable capacity to inhibit the growth of KI, which ultimately led to an improvement in gum arabic's capacity. This resulted in an increase in gum arabic's ability to inhibit the growth of KI. Umoren [127] conducted experiments to determine whether or not gum arabic had the potential to be used as a corrosion inhibitor for the same aluminium alloy. The gum arabic was heated to temperatures ranging from 30-60 ^{o}C and then immersed in a solution of 0.1 M H_2SO_4.

According to Umoren's [127] research, gum arabic exhibited positive characteristics in this regard. The gum arabic was being evaluated for its quality at various points

throughout the course of the investigation. In contrast to what was stated about alkaline solutions, it was discovered that the effectiveness of the inhibition decreased as the temperature increased. This was the case even though the temperature was not a factor in the initial discovery. This was the case even though the temperature was not a variable in the experiment that was initially conducted. The investigation that Ameh [117] and Eddy [118] commissioned the former to carry out found that the exudate gum from Commiphora pedunculata was effective as a corrosion inhibitor for AA3001 aluminium alloy when used in a solution of 0.1 M HCl at temperatures of 30-60 ^{o}C.

Ameh tested the efficacy of Commiphora kestingii gum exudate as a corrosion inhibitor for 96.65% aluminium alloy in 0.1 M H_2SO_4 solution at 30-60 ^{o}C. The data demonstrated the efficacy of the gum exudate. He found that the gum exudate worked just as well in cool temperatures as it did in hot ones. Besides octadecanoic acid, alpha camphorenal, nerolidolisobutyrate, diisopropenyl-1-methyl-1-vinyl cyclohexane, and abetic acid, the author says that this gum also included a significant amount of sucrose". In addition, all of these parts and pieces were physically present. Based on the discovery that the efficacy of the inhibition varied with temperature, the scientists concluded that chemisorption might be a potential adsorption mechanism for Commiphora kestingii gum exudate. So, they were able to deduce that chemisorption is a potential adsorption process for Commiphora kestingii gum exudate.

Due to this, the authors were able to arrive at the conclusion that chemisorption is a mechanism that has the potential to be used for the adsorption of Commiphora kestingii gum exudate. To put it another way, the authors arrived at their conclusion by basing it on the observation that the temperature influenced how effectively the inhibition performed. To put it another way, the authors found that the temperature influenced how effectively the inhibition worked. In an earlier piece of research, Umoren *et al*. [113], made the hypothesis that the adsorption of gum arabic on the surface of AA1060 aluminium alloy in NaOH solution would occur using the same mechanism. This hypothesis was tested and found to be correct.

Eddy *et al*. [122], conducted an experiment at temperatures of 30-60 ^{o}C to determine the efficacy of using Ficus tricopoda gum as a corrosion inhibitor for a 96.65% aluminium alloy that was dissolved in 0.1 M H_2SO_4 solution. The result of the experiment was to determine whether the gum was effective in preventing corrosion. The purpose of the experiment was to determine whether the utilisation of this gum produces the desired results. Camphene, sucrose, 2-methylene cholestan-3-ol, and 7-hexadecenal are some of the components that the gum is said to be made up of, at least according to the authors of the study that was carried out on the gum. The study was carried out to investigate the gum. It has been determined that the gum contains these constituents in its composition.

The findings of the authors indicate that the adsorption of Ficus tricopoda gum was endothermic up to 0.3 g. L^{-1} but exothermic at higher gum concentrations. This was the case regardless of the initial gum concentration. This was true even though the gum concentration at the beginning varied. Futhermore, the same group investigated the efficacy of Ficus thonningii gum as a corrosion inhibitor for 96.65% aluminium alloy in 0.1 M H_2SO_4 solution at both 30-60 ^{o}C. The gum was tested at both temperatures. Both temperatures were evaluated for their effect on the gum. The researchers [113] concluded that inhibition effiency was not affected by the temperature at any point. By employing a technique known as gas chromatography-mass spectrometry, the researchers were able to determine that the primary components of this gum include, among other things, 16-methyl-octadecanoic acid, abietic acid, n-hexadecanoic acid, and andrographolide (GCMS).

The researchers were able to use this information to determine the composition of the gum. Eddy *et al*., tested the effectiveness of Ficus benjamina gum as a corrosion inhibitor for 96.65% aluminium alloy in 0.1 M H_2SO_4 solution at temperatures of 30 and 60 ^{o}C as the final step of their experiment. During this experiment, the anti-corrosion qualities of the gum were investigated in detail and analysed. According to the authors [119], the majority of the gum is composed of the two sugars sucrose and D-glucose,

while the gum also contains a variety of carboxylic acids in smaller amounts. In addition, the authors state that the gum contains no protein or fat. Additionally, the gum has a flavouring component in it. These carboxylic acids include hexadecanoic acid, octadedecanoic acid, and 6, 13-pentacenequinone. From this study it was concluded that inhibition action of Ficus Benjamina gum, gum arabic and Commiphora kestingii gum is brought on by multiple-layer adsorption brought about by the various components of the gum itself [118]. The general mechanism as mentioned above is common to both types of gums.

Ameh postulated that the very same mechanism might be at work when gum arabic was considered. Umoren *et al*. [113], conducted a series of tests in order to evaluate the efficacy of Dacroydes edulis exudate gum as a corrosion inhibitor for AA1060 aluminium alloy in a 2. 0 M HCl solution at temperatures ranging from 30-60 ^{o}C. The purpose of the tests was to determine whether the gum was effective in preventing corrosion. Although the authors of the study suggested physisorption as a potential mechanism for this gum, based on the thermodynamic calculations, there was no specific indication given as to which of the gum components adsorbed on the surface of the aluminium. From these results, it was ascertained that physisorption is the best mechanism for this type of corrosion inhibition.

The critical take home message about the physisorption pathway has not been convincely dealt with. This then led to the plausible explanation about the conclusion thereof, more about the physisorption mechanism. This is something that needs to be dealt with in depth, in order to remove any doubt about this conclusion. It was hypothesised that the gums Raphia hookeri gum, Pachylobus edulis gum, Commiphora pedunculata gum, Ficus benjamina gum, Ficus thonningii gum, and gum arabic all used the same mechanism known as physisorption when exposed to an acidic solution. Several tests were carried out in order to investigate this hypothesis which conclusively proved that physisorption is the main mechanism of interest. Additionally, gum arabic yielded the same results making it a very ideal alternative.

Exudate gum from Gloriosa superba, which has a pH of 2, was tested by Eddy *et al*. [118], at temperatures of 30 and 60 ^{o}C to determine whether or not it is effective as a corrosion inhibitor for 96.65% aluminium alloy in 0.1 M HCl solution. The results of these tests showed that the exudate gum is effective. According to the findings, the gum had a beneficial effect. The authors [118] made the discovery that using the gum as a form of protection against corrosion worked effectively, which led to the conclusion that this method should be used more often. The results of a GC-MS analysis show that 1-piperoylp, 1-penta-decarborxylic acid, 9-octadecenoic acid, and stigmasta-5, 22-dien-3-ol are the primary components of the gum that is produced by the Gloriosa superba plant. Quantum chemical research and the relative calculations has revealed that the adsorption of this gum is caused by the presence of an amide group in stigmasta-5, 22-dien-3-ol and a hydroxyl group in 1-piperoylp. Both groups contribute to the structure of stigmasta-5, 22-dien-3-ol. The structure of stigmasta-5, 22-dien-3-ol includes contributions from both groups. These two groups, individually and collectively, contribute something to the gum's overall structure. The stigmasta-5, 22-dien-3-ol molecule contains trace amounts of both groups. A mechanism for the adsorption of Gloriosa superba gum onto the surface of aluminium that was of the mixed-type variety was proposed by the authors [118]. The thermodynamic calculations that were performed served as the foundation for this mechanism (physisorption and chemisorption). A mixed-type adsorption mechanism was also proposed for both the Ficus tricopoda gum and the gum arabic adsorption mechanisms when they were applied to the AA1060 aluminium alloy in NaOH solutions. This mechanism was applied to the adsorption of both gums.

2.2.1.5. Natural oils as corrosion inhibitors

Essential oils are highly concentrated hydrophobic liquids that contain monoterpene and sesquiterpene hydrocarbons in addition to oxygenated compounds. They are also known as volatile oils or ethereal oils. These will include compounds such as alcohols, aldehydes, ketones, acids, phenols, oxides, lactones, ethers, and esters". They are oxygenated compounds which give essential oils their unique flavours, colours and aromas. Aromatherapy is a holistic healing treatment that uses natural plant extracts

to promote health and well-being, this exploits the chemical properties of essential oils as a healing treatment. Some use essential oils for massaging and relaxation to treat fatigue and stress. Most of essential oils are used in perfumes or air fresherners. Avocado extraction of essential oil in addition, a mechanical extraction is utilised for recovering oil from ripe avocados, with the supplementary step for removing both the skin and seed. This is because most flowers do not contain enough oil that is volatile to be expressed, and because the chemical components of flowers are too delicate and easily denatured by the high heat used in steam distillation [128], a solvent such as hexane or SC-CO_2 is used to extract the oils from the crude plant material.

In recent years, the supercritical fluid extraction (SFE) method of extracting essential oil components has garnered a lot of interest, particularly in the food, pharmaceutical, and cosmetics industries. This is because the SFE method is a more environmentally friendly alternative to traditional methods such as organic solvent extraction and steam distillation. A lot of people are interested in the process of extracting essential oil components using SFE because it uses safer and less harmful solvents than traditional methods, and these solvents are also easier to remove or recover. This is one of the reasons why the process has garnered so much interest.

Essential oils are suitable for use as corrosion inhibitors for a variety of metals in several different environments. This is because essential oils contain the components described in earlier discussion within this document, and because essential oils have a low toxicity level and are readily available. It is this particular chemical character that they are appropriate to be used as corrosion inhibitors [105,129–131]. However, research on the effectiveness of various oils as corrosion inhibitors for aluminium and its alloys [55,132–134] has only been conducted on a small subset of these oils. Most of the studies have been performed using acidic solutions as the medium for the experiments. This has been the case for almost all the studies. In solutions containing 3% sodium chloride, the essential oils of Lavandula angustifolia L. and Laurus nobilis L. prevented the corrosion of AA5754 aluminium alloy and aluminium, respectively. On the other hand, Fayomi [134] and Popoola [132] found that green roasted Elaeis

guineensis oil successfully inhibited the corrosion of AA6063 aluminium alloy when it was exposed to a 3.5% sodium chloride solution [55,132].

The purest form of aluminium as well as various alloys of aluminium drawn from the 5xxx and 6xxx series were both put to the test and included among the materials that were analysed for their performance. When it came to the other naturally occurring compounds, it was found out that the efficiency of the inhibition is directly proportional to the concentration of all oils that were investigated. This was the case regardless of which naturally occurring compounds that were being studied. From their research work, Halambek *et al*. [133], investigated the effect of temperature on the efficacy of the inhibition provided by three oils that had been dissolved in ethanol at a concentration of 30 vol%. Their research showed that increasing the temperature led to an increasing in the effectiveness of the inhibition to a greater degree.

The ability of the essential oil of Ocimum basilicum L to act as a corrosion inhibitor for 99.85% aluminium in a solution of 0.5 M HCl was investigated by Halambek *et al*. [135], at temperatures ranging from 30-85 ^{o}C. The researchers found that the essential oil of Ocimum basilicum L had inhibitory effect to a great extend. However, there is an optimum temperature beyond which the efficacy is nullified. The temperature beyond the optimum one degrades polyphenols, particularly when they are exposed for a greater amount of time. In this instance, it is evidence that temperatures lower than the “degradation temperature” would be preferred. On the other hand, deterioration does not take place instantly; as a result, it is possible that a shorter exposure time is not as dangerous as a longer one. According to the researchers [55] of the study, linalool is the component of the oil that has the highest concentration. Eugenol, 1, 8-cineole, and geraniol come in descending order of concentration, following linalool.

In a solution of 1. 0 M hydrochloric acid, Halambek and Berkovi'c [135] conducted an experiment with temperatures ranging from 25-75 ^{o}C to determine whether or not the oil that was extracted from the plant Anethum graveolens L. was effective as a corrosion inhibitor for 99.85% aluminium. The experiment was carried out at

temperatures ranging from 25-75 ^{o}C (this upper temperature limit might also contribute to the degradation of these compounds, as discussed earlier). According to what was reported by the authors [135], the primary components of the oil are said to be limonene and carvone. The effectiveness of the oil that was extracted from the Lavandula angustifolia L plant as a corrosion inhibitor for Al–3Mg (95.5% Al) in a solution that contained 3% NaCl was investigated in an experiment that was carried out by Halambek *et al*. [133], at temperatures ranging from 25-60 ^{o}C.

According to the findings of the researchers, the primary components of the oil that was extracted from Lavandula angustifolia L were found to be linalyl acetate and linaalool. This information was gleaned from the study of the essential oil. The researchers of each of the three studies found that an increase in temperature resulted in a decrease in the effectiveness of the inhibition provided by the various oils. This was the case even though the studies were carried out at different temperatures. The process of decomposition might have to do with the decline in effectiveness that are being observed. The researchers Halambek *et al*. concluded that this behaviour could be explained by the inhibitor molecules desorbing from their positions as a result of the higher temperature.

Popoola *et al*. [132], and Abdulwahab *et al*. [132], conducted research to investigate how the presence of a corrosive environment affected the efficacy of inhibition provided by two different oils. The oils in question were olive oil and castor oil. In solutions containing 2. 0 M HCl and 2. 0 M HNO_3, the first group of authors investigated the efficacy of Arachis hypogeae natural oil as a corrosion inhibitor for 99.01% aluminium at a temperature of 25 ^{o}C. Above-mentioned authors conducted their tests in aqueous solutions. Using the natural oil from Arachis hypogeae, the solutions were evaluated to determine how effective they were at preventing corrosion. In their review article, the researchers Capuzzo *et al*. [128], described a method for SFE and the identification of volatile flavour components in roasted peanuts (Arachis hypogaea).

A group of compounds include hexanol, hexanal, methylpyrrole, benzene acetaldehyde, methylpyrazine, 2, 6-dimethylpyrazine, ethylpyrazine, 2, 3-dimethylpyrazine, 2, 3, 5-trimethylpyrazine, 2-furancarboxaldehyde, and 2-ethyl-5-trimethylpyrazine. Popoola *et al*. [132], discovered that the natural oil of Arachis hypogeae was an inhibitor that was more effective in HNO_3 solution than it was in HCl solution. The ability of ricinus communis oil to act as a corrosion inhibitor for a 99.01% aluminium alloy was evaluated by Abdulwahab *et al*. [132], using solutions of HCl and H_3PO_4 at a concentration of 2 millimolar. The experiment was conducted at a temperature of 25 ^oC.

Hexane was used as the solvent throughout the entire process, as stated in the Danlami *et al*. [136], report, which states that the Soxhlet method was utilised in order to extract this oil. According to what was found, the oil had a quantity that was rich in unsaturated fatty acids (rich in ricinoleic acid), followed by a quantity that had saturated fatty acids at a level that was only marginally higher than the unsaturated level (palmitic, stearic, linoleic, linolineic, and dihydroxylstearic acids). According to the findings of the study that Abdulwahab *et al*. [137], carried out, they found that the performance of the oil in either of the two acid solutions did not significantly differ from one another.

According to what has been reported, electrochemical techniques such as PDP, Rp, and EIS have been used in conjunction with the conventional WL technique in order to evaluate not only the effectiveness of the oils as corrosion inhibitors but also to Figure out how much influence the oils have on the reactions that lead to corrosion. This was done in order to evaluate not only the effectiveness of the oils as corrosion inhibitors but also to Figure out how much influence the oils have on the reactions that lead to corrosion. The purpose of this was to determine how much of an influence the oils have.

Based on the PDP readings, the scientists concluded that both the Arachis hypogeae oil and the green-roasted Elaeis guineensis oil operated as mixed-type corrosion

inhibitors for the various forms of aluminium. These two oils originated in the seeds of the Arachis hypogeae plant. Next, it was reported by Halambek *et al*., [133] that oils from Ocimum basilicum L., Anethum graveolens L., Laurus nobilis L., and Lavandula angustifolia L. all served as cathodic-type corrosion inhibitors. Results from an experiment by Halambek *et al*. [133] investigated the effectiveness of an ethanol solution of laurel oil as a corrosion inhibitor for 99.85% aluminium and AA5754 aluminium alloy in 1% acetic acid solution at 25 ^{o}C. Above-mentioned authors did this testing in order to determine whether the laurel oil inhibited the corrosion of the materials.

The effectiveness of the solution was evaluated while both unrefined aluminium and the alloy were present. Capuzzo [128] discovered that supercritical carbon dioxide extraction (SC-CO_2) was an effective method for isolating volatile and xed oils from dried berries of L. nobilis. The aim of this technique was to isolate volatile and xed oils. The extracts contained a sizeable amount of the volatile fraction, which was primarily made up of (E)-b-ocimene, 1, 8-cineole, a-pinene, b-pinene, blongipinene, linalyl acetate, d-cadinene, a-terpinyl acetate, and a-bulnesene. The volatile fraction also contained a-bulnesene. In addition, a considerable amount of a-bulnesen was found in the extracts. According to the findings of the authors, an ethanol solution of laurel oil protects the AA5754 aluminium alloy more effectively (has a higher inhibition effectiveness) than 99.85% pure aluminium does.

When compared, the two compounds proved to be very different. The ethanol solution of laurel oil inhibited the corrosion of 99.85% aluminium in the same way that it inhibits the corrosion of AA5754 aluminium alloy, but in a different way. This was confirmed by the PDP's measurements. The authors offered many potential pathways that could explain the inhibitory action of the oils that were evaluated. These mechanisms may be at work to account for the suppressive effect. Based on their thermodynamic calculations, Halambek *et al*. [133], determined that the adsorption of the ethanol solution of laurel oil on the surface occurred via a mixed-type process. A protective layer is produced on the surface of the aluminium and alloy as a direct result of this

process. According to the findings of Halembek *et al*. [133], the primary component of Laurus nobilis L. oil, 1, 8-cineole, has the potential to adsorb via the lone pair electrons present in oxygen atoms. The protective layer (film) that is already there will have this added on top of it. Linalool, which is the primary component of Ocimum basilicum L. oil and originates from the basil plant, was found to be responsible for the inhibitory effect that the oil of Ocimum basilicum L. possesses. The latter, in addition to protonating in an acid solution, possesses within its structure OH groups and double bonds, both of which are likely candidates for adsorption centres. Additionally, the structure protonates in an acid solution.

In addition to that, there are double bonds present in the structure. The hypothesis put forth by the researchers who carried out the study was that the inhibitory effect of the oil was exerted on the process in a series of two discrete stages. The initial step in the reaction is the adsorption of positively charged chloride ions onto the positively charged metal surface via electrostatic forces. The initially positively charged metal surface ends up with a negative net charge because of this stage of the reaction, which is the consequence of the initial stage of the reaction. During the second stage of the process, the protonated linalool had an electrostatic interaction with the negatively charged surface. Because of this, a protective layer formed on the surface of the aluminium as a byproduct of the process. This occurred because the aluminium was heated.

The authors formed the hypothesis that the active components of the oil physisorbed on the surface of the aluminium based on the findings of the thermodynamic experiment. This hypothesis was supported by the results of the experiment. Halambek and Berkovi'c [135] came up with a mechanism for the adsorption of oil from Anethum graveolens L. onto the surface of aluminium that was of the mixed type and was very similar to the mechanism that was described above. Halambek and Berkovi'c [135] are the ones responsible for developing this mechanism. The authors claim that chemisorption can occur in one of two ways: either by the electrons of the aromatic ring forming donor-acceptor bonds with the p-orbitals of the aluminium, or by

the displacement of water molecules from the surface of the aluminium and the sharing of electrons between the oxygen atoms and the aluminium.

The exchange of electrons is a central component of both mechanisms. Because chloride ions are present, there is a possibility that physisorption will occur between protonated species and the negatively charged surface of the aluminium. This will cause the protonated species to take on the charge of the aluminium. An experiment was carried out by Fayomi [132] and Popoola [132] at a temperature of 30 ^{o}C to investigate the efficacy of using green roasted Elaeis guineensis oil as a corrosion inhibitor for AA6063 aluminium alloy. The experiment was carried out in order to find out more information regarding this topic. The amount of sodium chloride present in the solution was 3.5% of its total volume. Carotene, vitamin E, sterols, and squalene were found to be the most abundant components of the oil that was obtained from Elaeis guineensis by using the SC-CO_2 extraction method. This was demonstrated in the introduction. Squalene was also found to be present in significant amounts.

The oil was still able to provide an adequate level of protection even after being submerged for a total of 216 hours (between 68% and 78%). Based on the data, it can be concluded that the inhibitory action of this oil is due to the adsorption of surfaceactive chemicals and oxide on the surface of the aluminium, which changes the wettability and the interface. It was also shown that the adsorption of surfaceactive chemicals and oxide on the surface of the aluminium was responsible for the inhibitory activity of this oil.

In addition to the primary groups of eco-friendly inhibitors that were discussed earlier, a small number of naturally occurring substances have also been investigated for their potential to prevent corrosion of aluminium in alkaline and chloride-containing solutions. This work was done in addition to the primary groups of eco-friendly inhibitors that were discussed earlier. The findings of these studies have demonstrated that the naturally occurring substances do not possess the capability to prevent corrosion in each environment. It was discovered that increasing the product

concentration led to an increase in the effectiveness of inhibition for each of the natural products that were tested. This was true for all the natural products that were examined.

The findings of an investigation that was carried out by Rosliza *et al*. [55], into the potential of natural honey to act as a corrosion inhibitor for an aluminum–magnesium–silicon alloy (97.36% aluminium) in seawater at 25 ^{o}C are presented here. The investigation was carried out in order to determine whether natural honey can prevent corrosion of the alloy. Gudi'c *et al*., evaluated the effectiveness of five different types of honey as corrosion inhibitors for AA5052 aluminium alloy in 0.5 M NaCl solution at 20 ^{o}C. These honeys were extracted from oak trees (H1), coniferous honeydew trees (H2), winter savoury trees (H3), alder buckthorn trees (H4), and carob trees (H5). Oak honey (H1) was found to be the most effective corrosion inhibitor, it was discovered that oak honey (H1) is the most effective corrosion inhibitor so far.

The honey that was collected from oak trees had the highest level of inhibition, followed by the honey that was collected from coniferous honeydew trees. The effectiveness of the inhibition gradually decreased from H3 to H5 to H4 to H2 to H1 respectively as it moved down the list. When PDP measurements were carried out on different kinds of honey, it was discovered that all the honey acted as a mixed-type inhibitor. This was the case in both studies. On the other hand, Gudi'c and his coworkers discovered that the anodic reaction was primarily influenced by each of the various kinds of honey that were put to the test. This was an important finding as the inhibition action brought on by the various types of honey was due to the formation of a surface layer “a thin film” on the surface of the aluminium materials, which prevented further attack on the aluminium.

The thermodynamic calculations that were carried out by both teams of researchers indicated that physisorption was a candidate for the role of adsorption mechanism for each of the different kinds of honey that were researched. After boiling animal connective tissue for a considerable amount of time, Abdallah *et al*. [138], tested the

glue that they obtained as a corrosion inhibitor for aluminium and aluminium alloys containing AA6063 and 20556 (92.47% aluminium) at a temperature of 30 ^{o}C using a 0.1 M solution of sodium hydroxide. The tests were performed at a concentration of 0.1 M. The results showed that the glue was effective in inhibiting the corrosion of aluminium and aluminium alloys. A concentration of 0.1 M was used for all the tests that were carried out. The findings of the tests indicated that the adhesive was effective in protecting aluminium and aluminium alloys from corrosion.

The effectiveness of the inhibition decreased in proportion to the increasing silica content, and the progression followed the order aluminium > AA6063 alloy > 20556 alloy. It was demonstrated that the efficiency of the inhibition would decrease in a manner that was directly proportional to the rate at which the temperature would rise. The results of the PDP tests suggested that the animal glue exhibited properties that were comparable to those of a mixed-type inhibitor. In their hypothesis, the authors of the study hypothesised that the adsorption of animal glue on the surface of materials made of aluminium is caused by the substitution of water molecules for those that are already present there.

CONCLUSION

From the cited studies, it has been well established that natural products do serve as important corrosion inhibitors. This is much more pronounced when taking into con sideration the different parameters required for each. This opened a new research avenue into compounds that are environmentally friendly. It opened the possibility of several potential research niche, one of which is into corrosion inhibitors. However, for these inhibitors to be utilised in actual industrial applications, several factors must first be taken into consideration. This is necessary in order to proceed with this important research which highlights its contribution to environmental care and rehabilitation. It is essential to engage in this type of research that aligns with green chemistry and all documented benefits.

Due to the fact that a higher percentage of the reviewed literature gave very little attention to the tests of these extracted compounds [132]. These opened avenues for future research meant to evaluate their efficiency. On the other hand, given that the extracts were taken from the plant based. Since they are of natural origin that are not tempered with, there is a great potential that they do not pose any kind of health risk in any way. Some of them have already been put to test in the application of various substances and it was confirmed that they indeed do not pose or contaminate fauna and the immediate natural environment respectively. This was done in order to ensure that they were safe to use in the applications that were being considered.

This is also true for the medications that were discussed, as each one has been shown to be safe through clinical testing and is, in fact, still being utilised in pharmacotherapy procedures that involve human patients at the present time. On the other hand, the latter facts simply cannot be contested, even though it is self-evident that the actual dose of exposure or intake is an essential component to take into consideration. In addition, as was demonstrated in the review article [99], the body of knowledge derived from the research concerning the use of pharmaceuticals as corrosion inhibitors for aluminium and its alloys is very limited. In this manner it is quite evident that there is still room for further research, mybe even escalate it to a critical research niche.

Utilising the German WGK (Wassergefahrdungsklassen) classification is one method that can be utilised to quickly determine whether a substance is safe for the environment. The overwhelming majority of chemical manufacturers and distributors have ease of access to the data that is associated with this classification. Depending on their toxicity, chemicals are placed into one of three categories under the national German VwVwS regulation: WGK 1, WGK 2, and WGK 3. Where WGK 1 is the least toxic and WGK 3 as the highest toxic with reference to water.

This procedure is carried out in order to ensure that all requirements of the national German VwVwS regulation are met. There is not much of a threat to people's health posed by the WGK 1 classification, which is the one that is regarded as being the

safest all around. The LC50 and EC50 categories, also known as the lethal or effective concentrations in 50% of the tested subjects, respectively, provide an additional method for determining toxicity. LC50 and EC50 are abbreviated from "lethal concentration" and "effective concentration," respectively. Within each of these categories, the chemicals are ordered from the most toxic to the least toxic to the almost entirely non-toxic in descending order.

In the South African context, they are still designing guidelines for quantifying contaminants emanating from corrosion inhibitors. For the moment we are all guided by National Environmental Management Act No. 107 of 1998. 29 January 1999 (NEMA). It is of high priority that a scaling system the same as the WGK one will be designed and effected in South Africa.

The ability of a substance to biodegrade is typically evaluated based on the percentage of that substance's components that are still detectable in the environment after a period of time equal to or equal to twenty-eight days [139]. This evaluation is done to determine whether the substance can be considered to have biodegraded. Another factor that plays a role in determining the rate at which bioaccumulation takes place is referred to as the partition coefficient, and it is denoted by the symbol Po/w (partition between 1-octanol and water). If the compound in question has a high partition coefficient, then there is a greater possibility that it will be bioaccumulated in living organisms. In this field it was established that despite many research ventures concerning corrosion inhibition of this type has not been fully investigated, there is therefore a wide gap that needs to be attended to through a holistic approach. There is therefore most compounds that have not been reported on.

Prior to testing an extract's ability to inhibit corrosion effectively, it would be beneficial to separate and analyse the extract's individual components using methods such as high-performance liquid chromatography mass spectrometry (HPLC-MS) or gas chromatography mass spectrometry (GC-MS). With these components isolated it becomes evident which ones are responsible for the corrosion inhibitory effect.

This confluence of factors such as extended periods of time and high temperatures has the potential to produce a wide range of complications. Due to these issues, there is an urgent need to encourage the development and implementation of alternative extraction methods that do not call for harsh processing conditions such as high temperatures during the manufacturing process or potentially hazardous organic solvents. The extraction method is carefully chosen to yield the ideal component that specifically display the highest inhibition of metal corrosion. These methods should be developed and implemented as quickly as possible.

The fulfilment of this prerequisite is a precondition to be attained before an essential requirement can be satisfied. A method known as the supercritical fluid extraction method is an alternative to the extraction techniques that have been summarised in the review. This method is one of the alternatives that can be used. It enables the separation of naturally occurring compounds from natural materials in a selective manner at temperatures that are more manageable. Considering the studies that have been carried out and reported on the use of pharmaceuticals belonging to a variety of pharmacotherapeutic groups as aluminium corrosion inhibitors, there are a few aspects that need to be clarified more thoroughly before this field can be given the recognition that it justifiably deserves.

These aspects include antimicrobial drugs, which are antibacterial and antifungal drugs, have the highest potential out of all the different types of drugs that have been tested as potential corrosion inhibitors for aluminium. Out of all the different types of drugs that have been tested, antimicrobial drugs have the highest potential as corrosion inhibitors for aluminium. Yet it depends where they are going to be used whether the antimicrobial activities are concerned or not. Since there are a great many questions about the mechanism by which these compounds inhibit corrosion that are still unanswered, it is necessary for the interaction that these compounds have with aluminium on the molecular level to be investigated in greater depth. Before the use of these drugs can become more prevalent, there is an urgent need to carry out an in-

depth investigation into the ways in which the effectiveness with which they prevent corrosion is affected by a variety of physicochemical factors including temperature, pH level, ionic concentration, and other factors of a similar nature. There is a need to think about the quantity that is used (which is typically quite a lot when one takes into consideration the fact that large metallic surfaces need to be protected against corrosion), in addition to the potential effects that this could have on the environment that is all around us.

In addition, as Gece has already pointed out, not all pharmaceuticals are easily biodegradable, and the byproducts of their transformation may be just as hazardous to the environment [139]. Due to this, additional research needs to be carried out before corrosion inhibitors of this kind can be regarded as being friendly to the environment. Despite this, we are confident that Gece's review has the potential to be of significant assistance in the process of finding potential candidates for subsequent tests, which are very expensive (e.g., biodegradability, toxicity, and bioaccumulation).

On the other hand, when one considers the possible applications of aluminium and the alloys of aluminium in the field of medicine (for instance, orthopaedic implants), drugs that inhibit corrosion appear to have an even greater appeal. As a result of this, the additional testing that is required to address the issues that have not yet been resolved will most likely be carried out rather quickly as opposed to being postponed until a later date. This is because this will most likely address the concerns that have not yet been resolved.

Most of the studies fail to mention the procedure that was followed in order to extract the natural oils from the plant material. Utilising high-pressure extraction with supercritical fluids is one of the simplest and most effective methods for removing these oils from plant materials at lower temperatures. Because this method reduces the amount of damage caused by heat and does not require the application of any potentially harmful solvents, it is one of the most useful and effective methods that can be used. When it comes to choosing solvents, SC-CO_2 is by far the option that is used

the most. This is because it possesses a high solvent power and can easily penetrate plant material.

One of SC-major CO_2's limitations is that it can only be used to treat dry raw materials and compounds with low polarity and low molecular weight. Co-solvents and other supercritical fluids as potential alternatives, such as propane, argon, or SF_6, could be used to get around these limitations if they were to be implemented. For example, propane is a supercritical fluid, whereas argon and SF_6 are not. In the process of modifying the polarity of the solvent, water, which is the most common and inexpensive solvent, can be used as an additional alternative solvent or co-solvent.

In recent years, there has been a rise in interest in the utilisation of subcritical water extraction as an alternative method for the process of phenolic compound extraction. This extraction method is an alternative to subcritical solvent extraction. The United States of America has been the only country to observe this pattern. When heated to well above 100 ^oC, the dielectric constant of water decreases while the ionic product of water increases. This happens because the ionic product of water is more stable at higher temperatures. This occurs due to the presence of a negatively charged ionic product produced by water. What this means is that both inorganic and organic compounds can share a common solvent that can be utilised to isolate the desired component.

The most significant barrier that needs to be traversed is represented by the extremely high amount of energy that is needed in order to warm up the medium. In addition, water that has been heated beyond its critical point, which is determined to be 374 ^oC and 221 bars of pressure, possesses a nature that is highly corrosive. This point can be determined by comparing the temperature of the water to the pressure that is being applied to it. The high-pressure apparatus that is used to obtain the products that are desired may experience difficulties as a result of this issue. There is unquestionably room for improvement in these environmentally friendly corrosion inhibitors in terms of their functional capabilities in relation to the environment. On the other hand, the

utilisation of actual formulations for corrosion inhibition would make these corrosion inhibitors even more effective than they already are . In addition, it is suggested that techniques of electrochemical and surface analysis be considered for the purpose of carrying out a more in-depth analysis of the inhibition mechanisms.

2.3. CORROSION TESTING

2.3.1. Gravimetric analysis

The broadly used inhibition method is the gravimetric or weight loss method. The method offers simplicity and dependability in several corrosion monitoring programs. Weight loss is known as metal mass loss during the process of corrosion. Furthermore, the rate of corrosion is measured as the ratio of weight loss to the product metal's surface area and the exposure time.

2.3.2. Adsorption studies

During corrosion testing in the presence of the inhibitor compound, an adsorptive film forms on a metal surface and an oxide layer is further characterised using the FTIR technique which is very essential in the adsorption film [140]. This technique caters for the analyses of both liquid and solid samples. In FTIR technique, infrared absorption spectrum is measured, and another advantage is that the technique is fast in processing data. Furthermore, with the help of FTIR qualitative analysis are examined such as the functional groups of the samples.

Analysing the adsorption layer created during the process, FTIR is applied to the powder for analysis [141]. Spectra can be collected and analysed from both liquid and solid samples using this method. This method of determining the infrared absorption spectrum is quick and precise. Its primary application is in qualitative research, where it helps classify samples into meaningful categories.

Inhibitory mechanism on a metal [142]:

i. The inhibitor chemically adsorbs via chemisorption resulting in the formation of a thin protective oxide film.
ii. The inhibitor adsorbs on the metal surface via physisorption (Van der Waals).
iii. The inhibitor further reacts with the potential corrosive medium after all the metal active sites are fully occupied to form a complex.
iv. Most studied inhibitors ideally undergo the Langmuir adsorption isotherm.

2.4. ANALYTICAL TECHNIQUES

2.4.1. Ultraviolet-visible spectroscopy (UV-vis)

Absorption spectroscopy in the ultraviolet-visible (UV-vis) range is known as UV-vis spectroscopy. Ultraviolet–visible spectroscopy is essentially an investigation of electronic changes within molecules under illumination by light. The ultraviolet or visible light when directed to π electrons or non-bonding electrons it gets absorbed resulting on the excitation of electrons from the ground state to higher energy [143]. Furthermore, this technique is utilised for quantitative analysis and qualitative analysis for the charecterisation of solutes under study. The number of impurities in organic solvents can also be determined by Uv-vis.

2.4.2. Fourier transform infrared spectroscopy (FTIR)

Using infrared light to obtain the absorption or emission spectra from interacting with the sample of interest, Fourier transform infrared spectroscopy is an analytical technique used to examine distinct functional groups found in chemical substances. The IR's frequency is often measured between 400 and 400 cm^{-1}. Analyte spectra are corrected by first recording the background emission spectrum of the IR source. The ratio of the sample spectrum to the background spectrum is related to the absorption spectrum of the sample. The sample's chemical composition can be deduced from the

resulting absorption spectrum, which is based on the bond natural vibration frequencies [4].

2.4.3. X-ray diffraction (XRD)

X-ray diffraction (XRD) is an analytical technique used to provide the information on unit cell dimensions and for phase indentification of a crystalline material. The mean bulk composition is determined after the analyte is finely grounded and homogenised. When Bragg's law ($n\lambda=2d\sin\theta$) condition is satisfied, constructive interference and a diffracted ray are produced due to the interaction of the incident rays with the analyte. With XRD, data interpretation and identification of unknown materials are relatively straight forward. Peak overlays have been a great disadvantage in XRD utility resulting in a detection limit of ~2% analyte for high angle reflections and that for fixed analytes [4].

2.4.4. Thermogravimetric analysis (TGA)

In an inert atmosphere (such as nitrogen, helium, vacuum, or air), thermogravimetric analysis can be used to determine the physical and chemical changes that take place in a material as a function of temperature or time. Inorganic materials, polymers, plastics, ceramics, glasses, and composites are analysed [144]. Thermogravimetric analysis (TGA) combined with differential scanning calorimetry (DSC) identifies the properties of a chosen material, including melting and recrystallization transitions, weight loss or gain owing to chemical reactions, and oxidation, dehydration, and breakdown [145].

2.4.5. Electrochemical techniques

Analytes can be analysed using electrochemical techniques, which involve the measurement of potential (volts) and/or current (amperes) in an electrochemical cell that contains the analyte of interest. Depending on the controlled and measured aspects, electrochemical methods can be categorised. Three main techniques in electrochemistry are potentiometry (measures the difference in electrode potentials), coulometry (measures the cell's current over time), and voltammetry (measures the

cell's current while actively changing the cell's potential) [146]. In addition, redox reactions occur during the operation of the above-mentioned techniques. The typical structure of an electrochemical cell will be that one containing two electrodes separated by a salt bridge immersed in an electrolyte solution. On the surface of the electrodes, chemical reactions mainly occur resulting in half reactions. Three main elcetrodes in the electrochemical cell are working electrode (WE), counter electrode (CE) and reference electrode (RE) [147]. On the working electrode is where a chemical reaction occurs, for an example, in this study the metal is the working electrode. In addition, the reference electrode is where standardization process occurs. Furthermore, a fixed potential on the reference electrode is evidenced while on the working electrode is where a change in potential is monitored. The commonly used reference electrode is saturated calomel electrode (SCE) and silver/silver chloride (Ag/AgCl) electrode both are the commonly used reference electrodes. Finally, the electrode where electrons sink for the flow of current from the external circuit is called an auxiliary electrode also known as the counter electrode.

2.4.5.1. Potentiodynamic polarisation (PDP)

To obtain the relevant electrochemical parameters such as the E_{corr}, i_{corr}, anodic Tafel slope, b_a and cathodic Tafel slope, b_c, the potentiodynamic polarisation method is used. According to Equation 2.18, current densities measured are used to calculate the percentage inhibition efficiency of the chemical corrosion inhibitor compound [148]:

$$\%IE_{PDP} = \left(\frac{i^{0}{}_{corr} - i^{i}{}_{corr}}{i^{0}{}_{corr}} \right) \mathrm{X}100 \tag{2.18}$$

Corrosion current density values are denoted by $i^{0}{}_{corr}$ and $i^{i}{}_{corr}$ denoting the corrosion current density in the absence and in the presence of inhibitor respectively.

2.4.5.2. Electrochemical impedance spectroscopy (EIS)

To investigate the charge transfer resistance that develops as metals corrode in corrosive settings, scientists utilise electrochemical impedance spectroscopy. Additionally, EIS can be used to probe other electrochemical parameters such as charge transfer resistance (R_{ct}) in the presence and absence of an inhibitor, double layer capacity (d_{ll}), constant phase element (CPE), and exponents. Furthermore, according to Equation 2.19, R_{ct} and R^{o}_{ct} are used to calculate the inhibition efficiency [149]:

$$\%IE_{EIS} = \left(1 - \frac{R^{0}{}_{ct}}{R_{ct}}\right) \mathrm{X}100 \tag{2.19}$$

OVERALL CONCLUSION

In conclusion, the purpose of this chapter was to provide a review of the relevant literature regarding the study of corrosion. This chapter provided an overview of the various classifications, forms, and rates of corrosion, as well as the method for preventing it. When a substance is subjected to air and moisture, a process known as corrosion can take place. This process involves the interaction of oxygen and water molecules, which ultimately results in the production of hydrogen. In addition, this chapter sheds light on how mild steel, aluminium, and zinc react to corrosion. In this body of research, the anti-corrosion properties of inhibitors, which are substances that are applied in extremely low concentrations, have been investigated.

Gravimetric analysis and electrochemical techniques are just two of the many methods that can be utilised in the research on corrosion; however, this chapter will focus on discussing just those two methods. Gravimetric analysis, also known as weight loss, outlines three essential parameters, including corrosion rate, surface coverage, and inhibition efficiency. The percentage of inhibition efficiency is the only parameter that can be determined using electrochemical techniques and weight loss methods. The literature review is summarised in this chapter, and the compound glycerol stearate

(GS) was chosen as the inhibitor compound of interest. In addition, the literature review revealed that analytical techniques including gravimetric method, UV-vis, FTIR, XRD, TGA, PDP, and EIS can be utilised to evaluate the electrochemical and structural properties of the GS. These are just some of the techniques that were presented.

CHAPTER THREE

EXPERIMENTAL

3.1. MATERIALS

3.1.1. Glycerol stearate (GS) synthesis [150]:

Firstly, we will have glycerol as the starting material, followed by the glycerol protection method through a refluxing for 6 hours a mixture of acetone (36 g), $CHCl_3$ (156 g), glycerol (30 g) and p-toluenesulfonic acid (1.2 g). After a reaction mixture is cooled, there will be an addition of Na_2CO_3 (1.3g) which will be stirred for 30 minutes. To obtain pure 1, 2-O-isopropyl-idene glycerol, the reaction mixture will be vacuum distilled (10 mmHg). Furthermore, in the presence of Na_2CO_3 (0.5g) for 6 hours at 140 ^oC stirred will be a mixture of methyl stearate (43 g, 0.15 mole) and 1, 2-O-isopropylidene glycerol (30 g, 0.23 mole). A continuous removal of methanol will be done by evaporation under atmosphere. After the completion of a reaction, excess 1, 2-O-isopropyl-idene glycerol will be obtained under vacuum (10 mmHg) and the remains will be dissolved, washed in ether and water, respectively, to remove Na_2CO_3. Moreover, a deprotection method will be done through the immersion of 1, 2-O-isopropyl-idene in ethanol (95%, 40 mL) and refluxed for 3 hours in the presence of Amberlyst 15 (wet) ion exchange resin (1.0g). Finally, a reaction mixture will be filtered, and the filtrate will be concentrated to give glycerol stearate as a product.

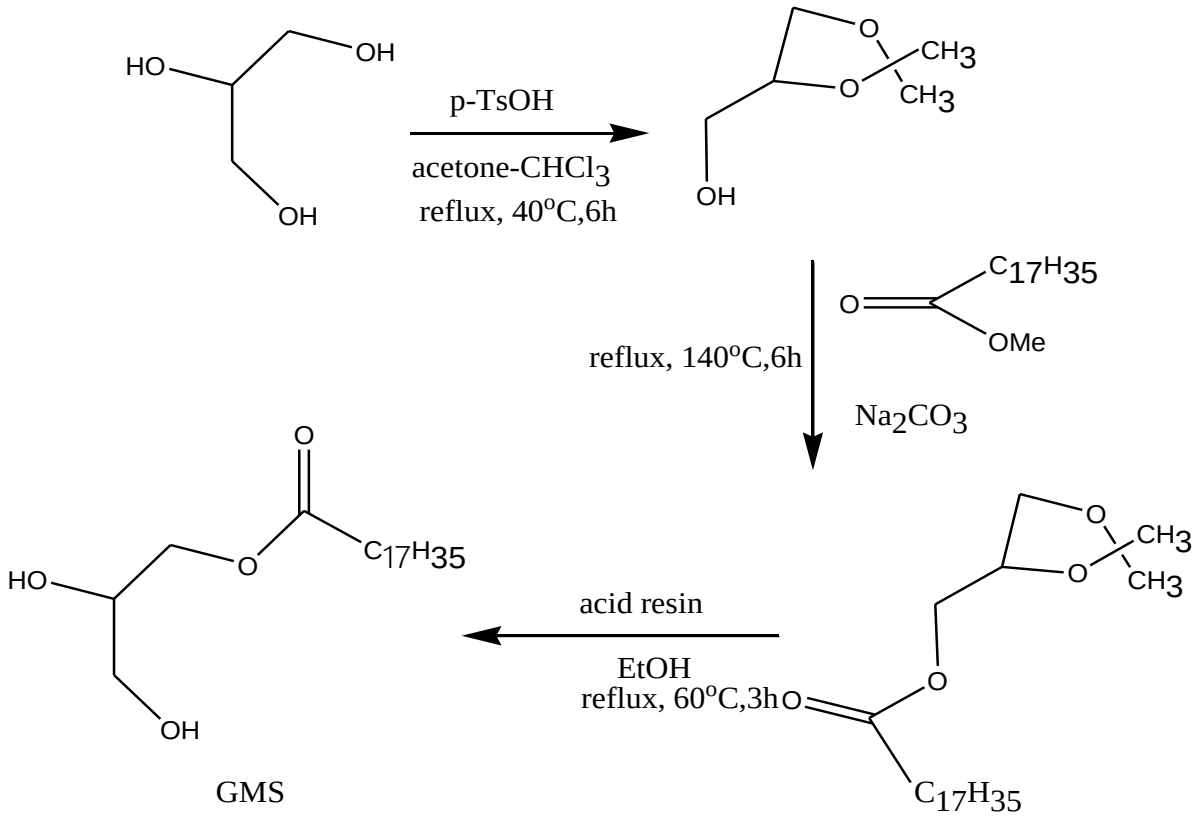

Figure 3. 1 : Synthesis of glycerol stearate.

3.1.2. Gravimetric analysis (Weight loss measurements):

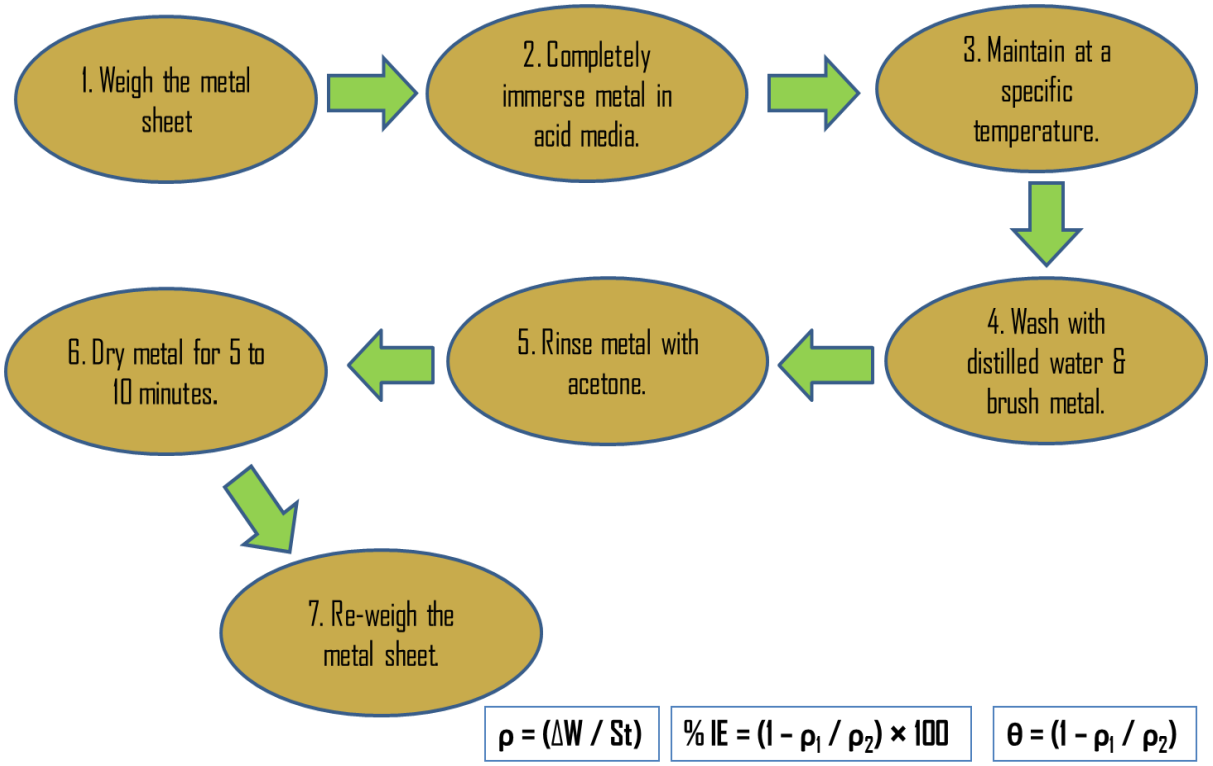

Figure 3. 2: Schematic procedure for weight loss measuerements.

About 50×10^{-5} M of glycerol stearate was prepared and from it 30×10^{-5} M and 10×10^{-5} M was prepared. Three thermostats at different temperatures; 318 K, 328 K and 338 K degrees celcius were used. Initial masses of three metals; aluminium, mild steel and zinc will be recorded before corrosion testing.The immersion time for the corrosion testing will be 3 hours both in the absence of the inhibitor and the presence of the inhibitor. After corrosion testing, metals were washed with distilled water and then left to dry. After drying the metals, final masses were recorded, thus mass loss was calculated and from then the corrosion rate, percentage inhibition efficiency and surface coverage were determined.

3.2. CHARACTERISATION TECHNIQUES

The inhibitor formation was confirmed by the Spectrum II FTIR spectrometer (PerkinElmer). The spectra were within 500 and 4500 cm^{-1} at 25 ^{o}C. Collected were 32 scans with 4 cm^{-1} resolution. Optical absorption spectra were recorded between 200 – 800 nm at room temperature using a Lambda 365 UV/vis spectrophotometer. The surface morphology was investigated using a scanning electron microscope (SEM).

3.3. COMPUTATIONAL STUDIES

The computational methodology adopted in this study was based on density functional theory dispersion corrected (DFT-D) [151], which are essential for the accurate description of the organic molecules within the $DMol^3$ [152] code embedded in the Materials Studio 2020 version. Geometry optimisations of the inhibitor were performed to calculate the energies of the highest occupied molecular orbital (HOMO) and lowest unoccupied molecular orbital (LUMO). These were performed using the generalised gradient approximation (GGA) [153] of Perdew-Wang 91 exchange-correlation functional [153], [154] (GGA-PW91). The Tkatchenko and Scheffler (TS) [155] dispersion correction to the PW91 was adopted. The convergence tolerances for energy, force and displacement were 2.0×10^{-5} Ha, 0.004 Ha. $Å^{-1}$ and 0.005 Å,

respectively. The double numerical plus polarisation (DNP) basis set with 4.4 Basis files will be set using DFT semi-core pseudopotentials.

With the aid of Koopmans's theorem, these parameters are often defined [156]:

Electronegativity (χ) was defined as the ability an atom has to attract electrons towards itself and it was determined using equation 3.1:

$$\chi \cong -1/2\ (E_{HOMO} + E_{LUMO}) \quad (3.1)$$

Global hardness (η) measured the resistance of an atom to a charge transfer and was estimated using equation 3.2:

$$\eta \cong -1/2\ (E_{HOMO} - E_{LUMO}) \quad (3.2)$$

Global electrophilicity index (ω) was estimated using a relationship between electronegativity and chemical hardness parameters in equation 3.3:

$$\omega = \chi^2/2\eta \quad (3.3)$$

Studies described that a high electrophilicity value showed a good electrophile and a small value showed a good nucleophile.

Global softness (σ), it showed the capacity of an atom or group of atoms to receive electrons [36], it was estimated through equation 3.4:

$$\sigma = 1/\eta \cong -2/\ (E_{HOMO} - E_{LUMO}) \quad (3.4)$$

Electron affinity (A) was defined as the energy released when an electron was added to a neutral molecule, it related with E_{LUMO} through equation 3.5:

$$A \cong -E_{LUMO} \quad (3.5)$$

Ionisation potential (I) was defined as the amount of energy required to remove an electron from a molecule, it related with E_{LUMO} through equation 3.6:

$$I \cong -E_{HOMO} \quad (3.6)$$

CHAPTER FOUR

RESULTS AND DISCUSSIONS

4.1. ALUMINIUM

OBSERVATION OF CORROSION RATE WITH TIME

Optical observations were made with Figure 4.1 showing aluminium metal before corrosion testing and from Figure 4.2-4.5 showing aluminium corrosion testing in (a) uninhibited solution and (b) inhibited solution. Results were taken after week, a month, 6 months and a year. The photographs of aluminium metal in the unhibited solution showed more rough surfaces as compared to those tested in the presence of glycerol stearate. By optical observations it showed that more pits were present on the surface of aluminium metal in the uninhibited solution. But the introduction of glycerol stearate did minimise the pits.

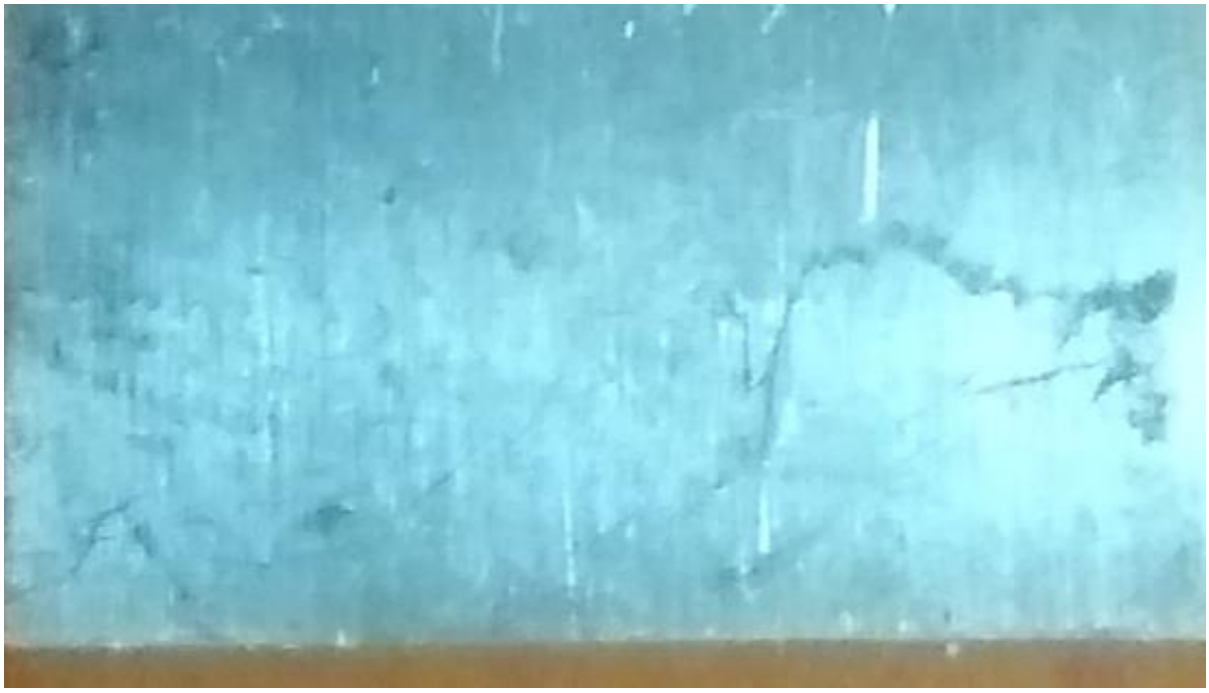

Figure 4. 1: Aluminium metal before corrosion testing.

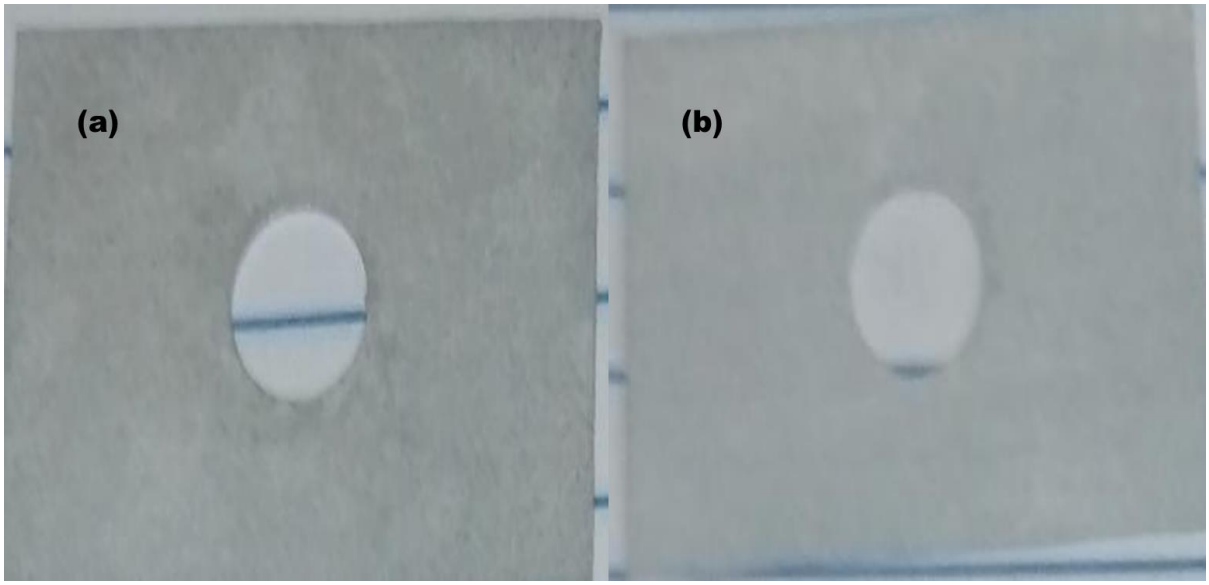

Figure 4. 2: Aluminium metal (a) Uninhibited solution after a week (b) Inhibited solution after a week.

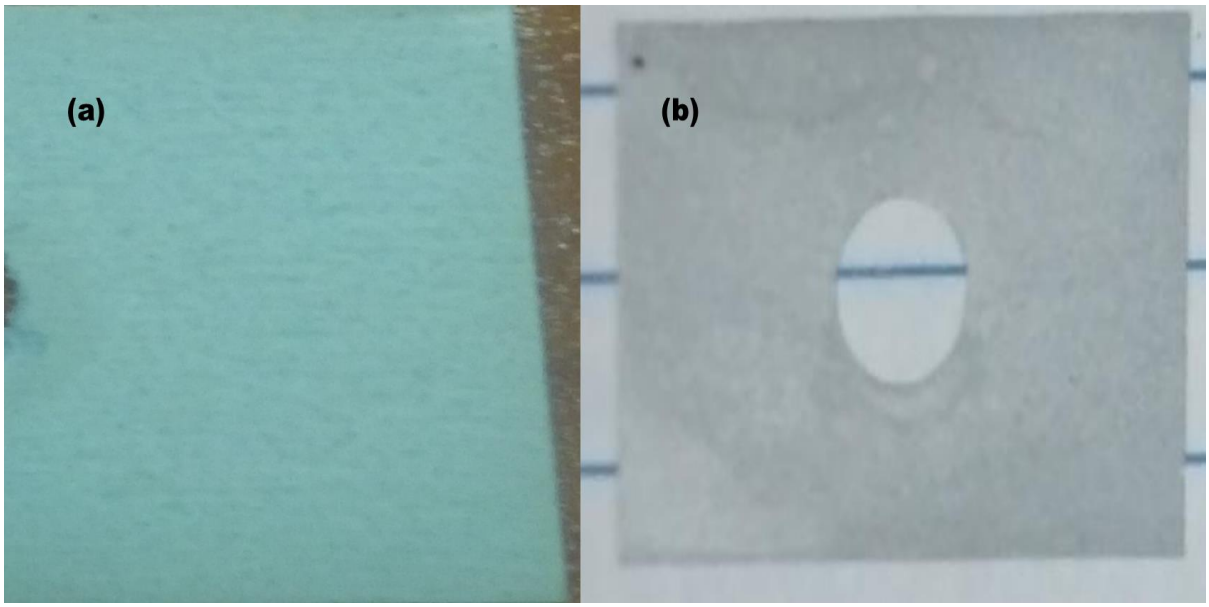

Figure 4. 3: Aluminium metal (a) Uninhibited solution after a month (b) Inhibited solution after a month.

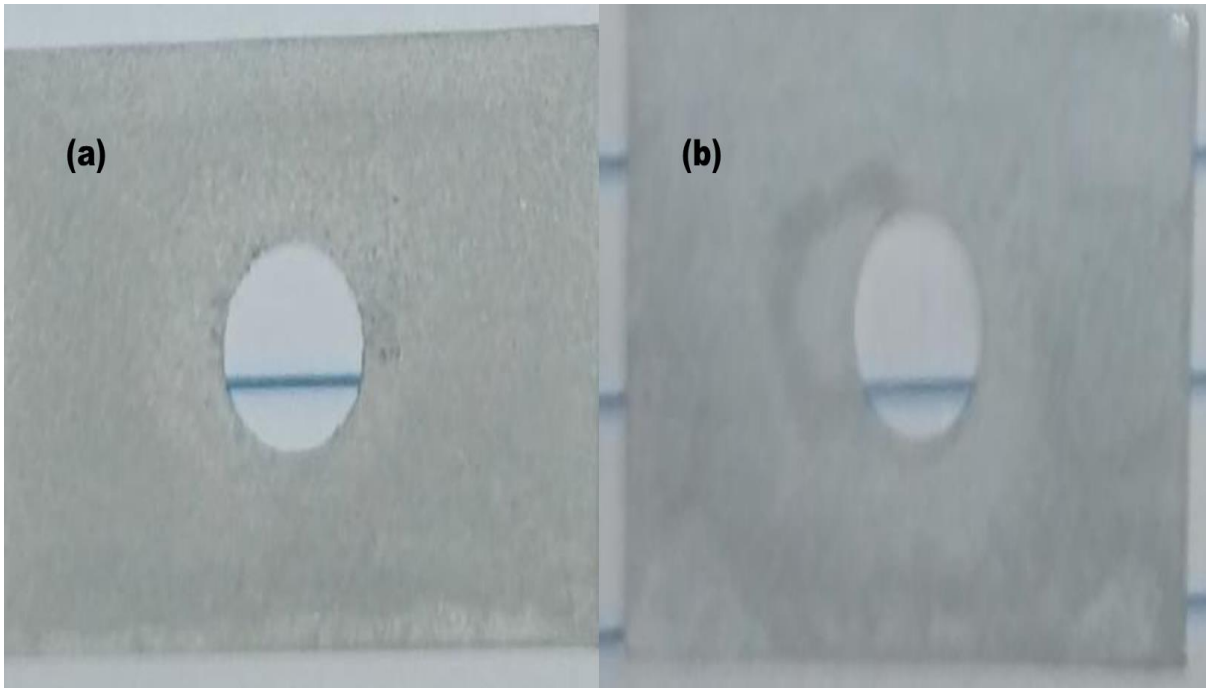

Figure 4. 4: Aluminium metal (a) Uninhibited solution after 6 months (b) Inhibited solution after 6 months.

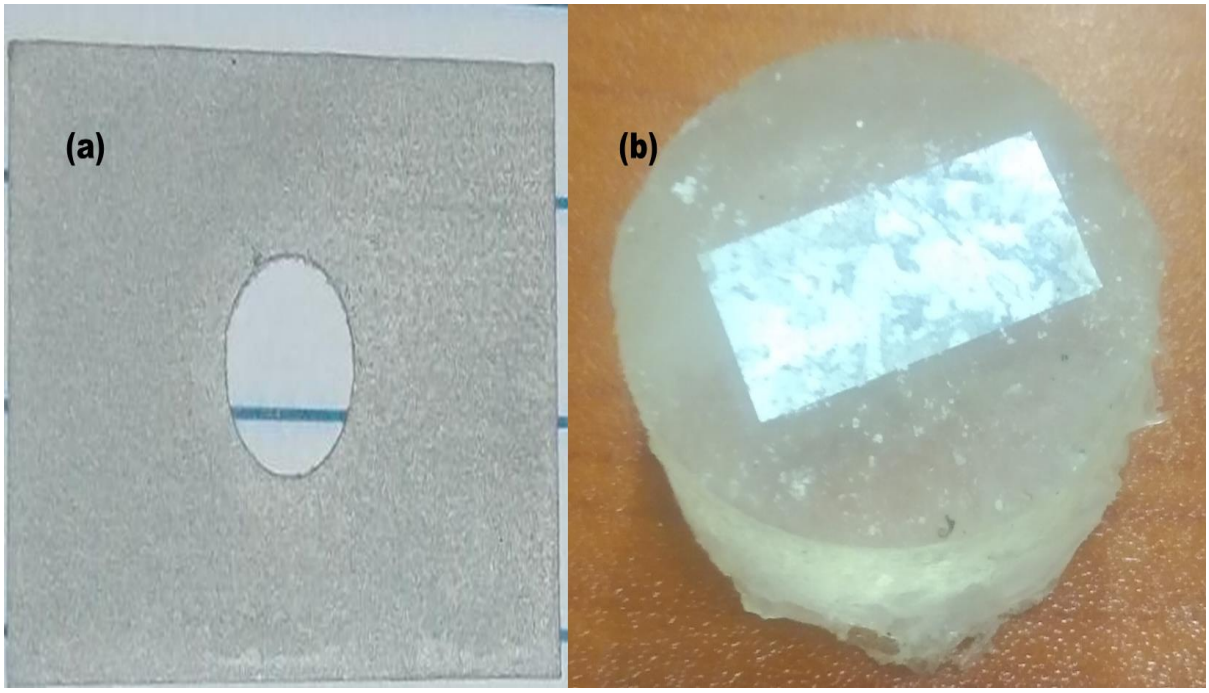

Figure 4. 5: Aluminium metal (a) Uninhibited solution after a year (b) Inhibited solution after a year.

4.1.1. Weight loss measurements

4.1.1.1. Glycerol stearate concentration and temperature effects on corrosion rate

Table 4.1 and in Figure 4.6, (a) shown are results of the rate of corrosion through weight loss measurements for Al in 1. 0 mol. L^{-1} HCl at various GS concentrations from 10 x 10^{-5}- 50 x 10^{-5} M and at 318 K, 328 K and 338 K. In addition, when 10 x10^{-5} M of inhibitor was added, the rate of corrosion decreased as compared to that for the uninhibited solution at three various temperatures, and there was a decrease in the rate of corrosion when 30 x10^{-5} M and 50 x 10^{-5} M of the inhibitor were added as noticed in Table 4.1. The rate of corrosion decreased as GS concentration increased since surface coverage (θ) of GS increased on the Al metal surface [114]. It was also noticed that the rate of corrosion, C_R was high for GS at 338 K as compared to 318 K and 328 K. In addition, corrosion rate decreased as GS concentration increased as shown in Table 4.1.

Figure 4.6(a) showed percentage efficiency of inhibition against GS concentrations at 318 K, 328 K and 338 K. At 50 x 10^{-5} M, the highest inhibition efficiency values were obtained. In addition, the %IE of GS increased with increasing inhibitor concentration. The donation of lone pairs from the O atoms into the unfilled orbit of the Al metal formed a coordinate bond. In addition, Cl^- ions were adsorbed on Al/solution interface [157–159].
Rate of corrosion (C_R in g. $cm^{-2}\cdot h^{-1}$), efficiency of inhibition (%IE), surface coverage (θ) were determined from the weight loss data [160,161].

At 50 x 10^{-5} M percentage inhibition efficiency of GS ranged between 55.40-98.51%. At 30 x 10^{-5} M percentage inhibition efficiency was between 52.70-97.01%. Finally, at 10 x 10^{-5} M percentage inhibition efficiency of GS ranged from 48.65-95.52%. The adsorption isotherm results were shown in Figure 4.6 (b). Langmuir adsorption isotherm and inhibitor surface coverage (θ) on Al surface related to GS concentration (C_{inh}) according to:

$$\theta = \frac{K_{ads} C_{inh}}{1 + K_{ads} C_{inh}} \quad (4.1)$$

The linear form is given by:

$$\frac{C_{inh}}{\theta} = \frac{1}{K_{ads}} + C_{inh} \quad (4.2)$$

Where C_{inh} denoted GS concentration, θ denoted surface coverage degree, K_{ads} denoted constant of equilibrium. Figure 4.6 (b), the plot of C_{inh}/θ against C_{inh} showed a linear graph with a positive slope. In Table 4.2, K_{ads} values were presented and were observed to decrease as the temperature decreased [162]. In this project, larger values of K_{ads} for GS indicated process of adsorption, which was favoured by larger values of K_{ads} [162]. In Figure 4.6. (b), Langmuir adsorption isotherm was followed by GS observed from data given by R^2 values closer to and at unity in Table 4.2. Furthermore, from slope values a monolayer adsorption was obtained [163,164]. From K_{ads} values obtained, free energy of adsorption ($\Delta G°_{ads}$) was determined using the Equation 4.3:

$$\Delta G^{o} = -2.303 RT \log(55.5 K_{ads}) \quad (4.3)$$

$\Delta G°_{ads}$ denoted adsorption Gibbs energy, 55.5 value represented molar concentration of water in solution, T denoted absolute temperature, and K_{ads} denoted constant of equilibrium for adsorption process. In Table 4.2, it was observed that $\Delta G°_{ads}$ values for GS inhibitor were less than -20 kJ. mol^{-1}, which indicated a physisorption mechanism of adsorption [163–165].

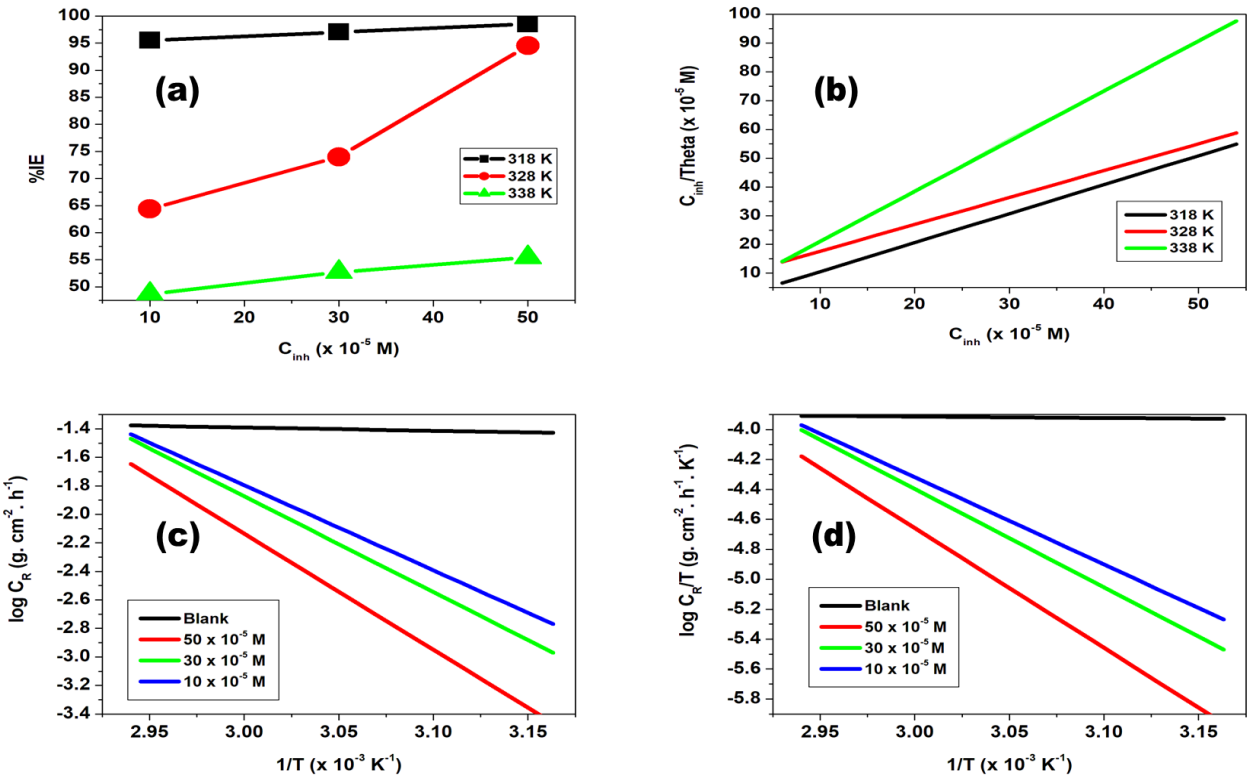

Figure 4. 6: Efficiency (%IE) versus GS concentration (M) plot for (a) GS; and Langmuir isotherm (b) GS inhibitor on Al metal sheet at 318 K, 328 K and 338 K. Arrhenius graphs for Al metal in 1. 0 M HCl with and without GS (c) Transition state graphs at differing GS (d).

Table 4. 1: Corrosion rate (C_R), efficiency of inhibition, (%IE) and surface coverage (θ) of GS at 318, 328 and 338 K for aluminium metal.

Inhibitor	Temperature (K)	Concentration (x 10^{-5} M)	Weight loss (g)	Corrosion rate (x 10^{-3} g. cm^{-2}. hr^{-1})	Inhibition efficiency (IE)	Surface coverage (Θ)	C/Θ x 10^{-5}
GS	318	0	0.67	37.22	_	_	_
		10	0.03	1.67	95.52	0.9552	10.4688
		30	0.02	1.11	97.01	0.9701	30.9231
		50	0.01	0.56	98.51	0.9851	50.7576
	328	0	0.73	40.56	_	_	_
		10	0.26	14.4	64.39	0.6439	15.5310
		30	0.19	10.6	73.98	0.7398	40.5540
		50	0.04	2.22	94.52	0.9452	52.8982
	338	0	0.74	41.11	_	_	_
		10	0.38	21.1	48.65	0.4865	20.5561
		30	0.35	19.4	52.70	0.5270	56.9245
		50	0.33	18.3	55.40	0.5540	90.2459

Table 4. 2: Adsorption parameters for glycerol stearate on Al metal.

Inhibitor	T (K)	K_{ads} (x10^5 L.mol^{-1})	R^2	$-\Delta G^o_{ads}$ (kJ.mol^{-1})
GS	318	2,0004	0.9999	-12.45
	328	0.2746	0.9994	-12.84
	338	0.1204	0.963	-13.24

4.1.2. Thermodynamic and activation parameters

The Arrhenius equation was used to evaluate temperature effect on the behaviour of the adsorption process and activation energy (E_a) parameters of corrosion process according to [81,166]:

$$\log C_R = \log A - \frac{E_a}{2.303RT} \quad (4.4)$$

C_R denoted rate of corrosion, E_a denoted energy of activation, R denoted molar gas constant (8.314 J. K^{-1}. mol^{-1}), and T denoted absolute temperature and A denoted frequency factor. The plot of log (C_R) against 1/T for aluminium in 1. 0 mol. L^{-1} HCl with and without GS was presented in Figure 4.6 (c). From slopes, values of the activation energy were obtained. Furthermore, from intercepts of regression lines frequency factor was obtained. Slope = $-E_a/2.303R$ and c = logA where c indicated regression line intercept. Adsorption process that occurred at metal surface/inhibitor interface could be either exothermic process where heat was given off or endothermic process where heat was absorbed. Table 4.3 showed that values of E_a in the inhibited solution were generally higher than that of the blank solution in all inhibitor concentrations. It was studied that physical adsorption was determined by higher E_a values while chemical adsorption was determined by lower E_a values [167]. Temperature effect on

inhibition efficiency for Al was used to obtain entropy ($\Delta S°$) and enthalpy values ($\Delta H_a°$) presented in Table 4.3. Positive values of $\Delta H_a°$ indicated that Al dissolution and GS undergo endothermic processes [87,168]. Positive values of ΔS^o in GS containing solution indicated that activated complex formation is dissociative rather than associative at the rate-determining step [124]. Measurements for $\Delta S°$ and $\Delta H_a°$ were determined using Equation (4.5):

$$log\left(\frac{\mathrm{CR}}{T}\right) = \left[\log\left(\frac{R}{hN}\right) + \left(\frac{\Delta S}{2.303R}\right)\right] - \frac{\Delta H}{2.303RT} \quad (4.5)$$

k_B denoted Boltzmann's constant: C_R indicated rate of corrosion and h denoted Plank's constant.

Figure 4.1 (d) showed log (C_R/T) versus 1/T graph for GS, showing linear graphs with $\left[\log\left(\frac{R}{hN}\right) + \left(\frac{\Delta S}{2.303R}\right)\right]$ as intercept. In addition, -ΔH°/R values were calculated from slopes. Furthermore, it was noticed that blank solution showed high C_R values as compared to GS inhibitor. Lower C_R values indicated that Al metal dissolution was minimised.

Table 4. 3: Presented are activation energy (E_a), entropy (ΔS^o) and enthalpy of activation (ΔH^o_a) values.

Inhibitor	**Concentration** (x10^{-5}M)	E_a **(kJ.mol^{-1})**	ΔH^o_{ads} **(kJ.mol^{-1})**	ΔS^o **(JK^{-1}.mol^{-1})**
GS	0	4.47	1.75	-267.28
	10	114.23	111.51	54.25
	30	128.61	125.88	95.88
	50	155.87	153.14	172.63

4.1.3. Potentiodynamic polarisation (PDP)

Aluminium potentiodynamic polarisation curves in 1. 0 M HCl in uninhibited and inhibited systems were presented in Figure 4.7. In Table 4.4, shown are values of inhibitor concentrations, E_{corr}, I_{corr}, Tafel slopes (b_a and b_c) anodic and cathodic respectively, and percentage inhibition efficiencies (%IE_{PDP}). Obtained current densities were by extrapolating curves of Tafel slopes to corrosion potential. It was observed in Table 4.4 that inhibition efficiency increases as inhibitor concentration increases and as corrosion current densities decrease. This was because of adsorption of GS on aluminium surface. Potentiodynamic polarisation study showed that GS inhibition efficiencies increased in the order: 10 x 10^{-5} M (51.37%), 30 x 10^{-5} M (78.80%) and 50 x 10^{-5} M (81.06%). Corrosion potential value of inhibited solutions against the blank plays an essential role in a sense that if E_{corr} is greater than 85 mV is given to either anodic or cathodic type inhibitors and if E_{corr} is less than 85 mV is accredited to a mixed type inhibitor mechanism [169]. Furthermore, it was observed in Table 4.4 that E_{corr} values were less than 85 mV with the cathodic inhibitor mechanism dominating inferring from the Tafel slopes.

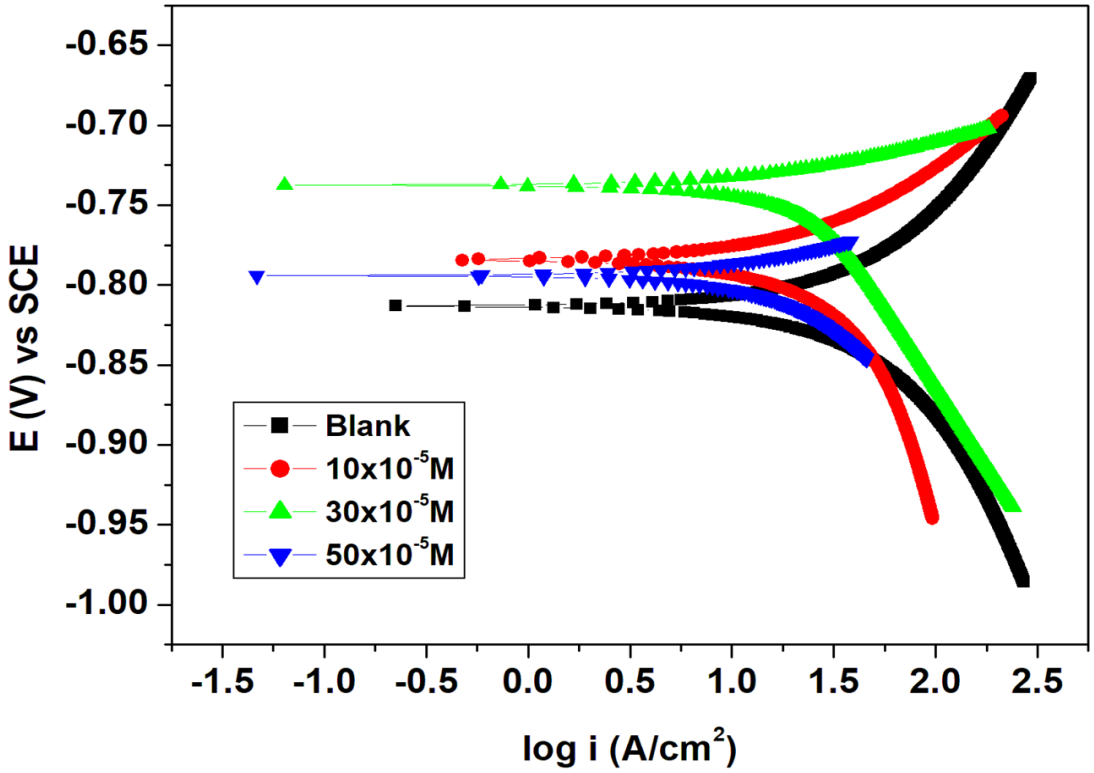

Figure 4. 7: Potentiodynamic polarisation plot for aluminium in 1. 0 M HCl in the uninhibited and inhibited solutions of GS different concentrations.

Table 4. 4 : Polarisation measurements such as E_{corr}, I_{corr}, b_a and b_c using different inhibitor concentrations.

Inhibitor	Concentration x 10^{-5} (M)	-E_{corr} (mV)	I_{corr} (mA.cm^{-2})	b_a (mV)	b_c (mV)	%IE_{PDP}
Blank		813.17	109.90	290.9	396.8	-
GS	10	784.10	53.44	134.8	594.4	51.37
	30	737.45	23.30	38.4	198.5	78.80
	50	793.74	20.82	52.1	145.4	81.06

4.1.4. Electrochemical impedance

Corrosion behaviour of aluminium in 1.0 M HCl and in the presence 10 x 10^{-5} M, 30 x 10^{-5} M and 50 x10^{-5} M GS concentrations was studied with the aid of the EIS. The Nyquist plot of aluminium without and with GS concentrations was presented in Figure 4. 8 with corresponding Bode plots in Figure 4.9 showing that the high frequency limit corresponds to the solution resistance R_s represented on the electric circuit shown on Figure 4.10. In addition, in Bode plots the low frequency limit represents (R_s + R_{ct}) from Nyquist and Bode plots are in good agreement. Table 4.5 showed that R_{ct} values increased in inhibited solutions and a decrease in C_{dl} values was observed as the inhibitor concentration increased. The increase in R_{ct} values was due to adsorption of GS molecules on aluminium metal thus retarding metal dissolution and hydrogen evolution, which are oxidation and cathodic processes occurring at metal solution interface [170]. Furthermore, Nyquist plots in Figure 4.8 showed a single depressed capacitive arc or semicircle due to metal surface roughness and this revealed that aluminium dissolution was by a single transfer process [171]. The impedance nature of GS was studied with the use of an electrical circuit comprising R_s, R_{ct} and C_{dl} shown in Figure 4.10.

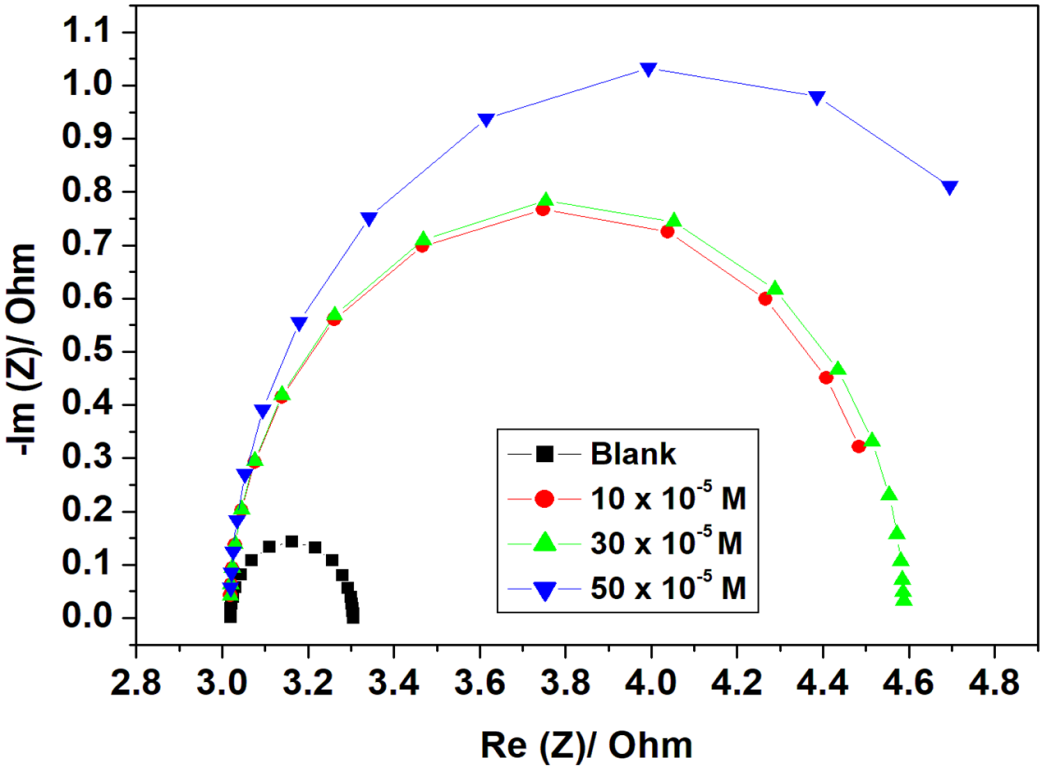

Figure 4. 8: Nyquist plot for aluminium in 1. 0 M HCl in the uninhibited and inhibited solution with different GS concentrations.

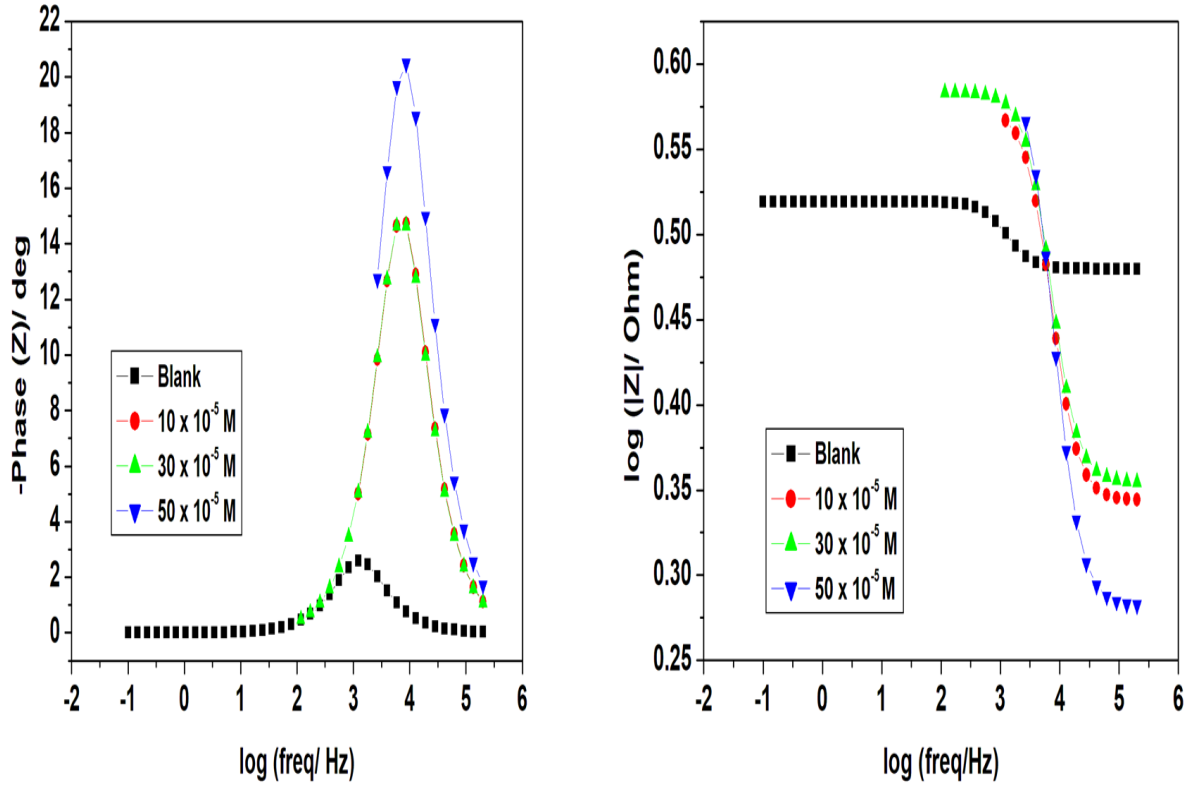

Figure 4. 9: Bode plots of aluminium in 1. 0 M HCl with and without glycerol stearate.

Table 4. 5: Electrochemical impedance parameters.

Inhibitor	Concentration x 10^{-5} (M)	R_s (Ω)	R_{ct} (Ω)	C_{dl} (x10^{-6} F)	%IE_{EIS}
Blank		3.019	0.286	451.2	-
GS	10	2.208	1.536	60.24	81.38
	30	2.262	1.570	59.71	81.78
	50	1.913	2.070	45.05	86.18

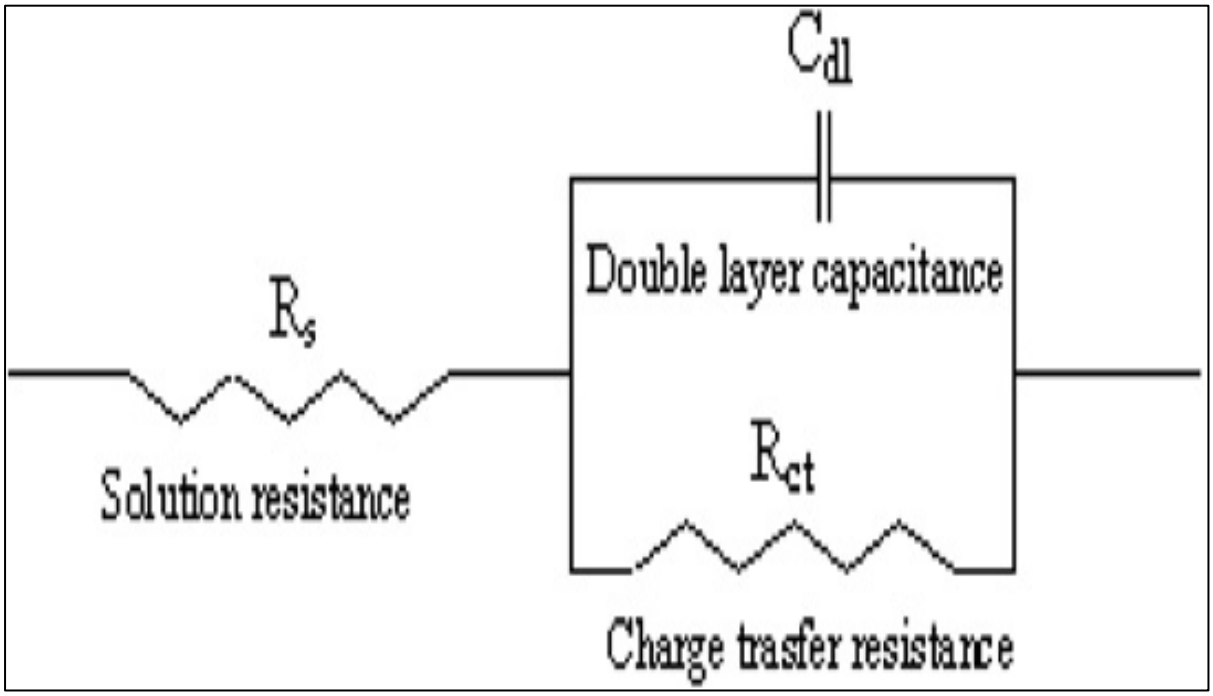

Figure 4. 10: The suggested electrical circuit for studied GS.

4.2. MILD STEEL

OBSERVATION OF CORROSION RATE WITH TIME

Visual observations were made with Figure 4.11 displaying mild steel before corrosion tests occurred. In addition, Figure 4.12-4.15 revealed that mild steel exhibited a redish-brownish colour owing to the formation of iron oxide especially in photographs for the unhibited solution. However, this rust was minimised after corrosion inhibitor was introduced. Observations were made after week, a month, 6 months, and a year.

Figure 4. 11: Mild steel before corrosion testing.

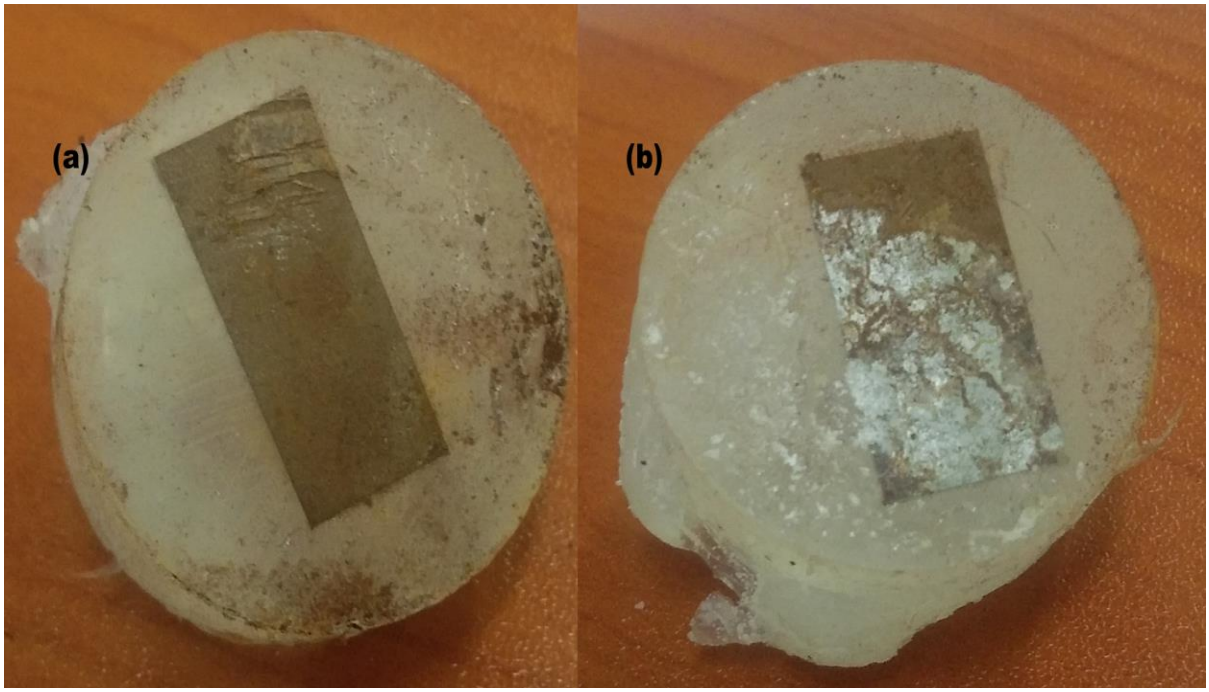

Figure 4. 12: Mild steel (a) Uninhibited solution after a week (b) Inhibited solution after a week.

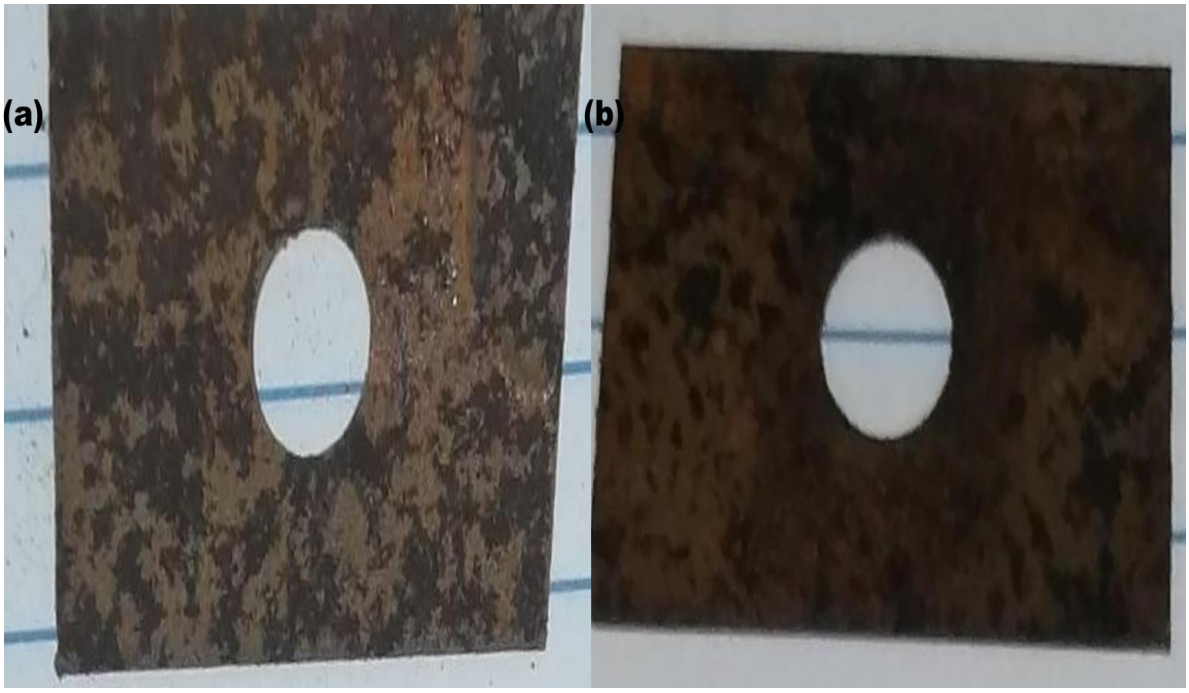

Figure 4. 13: Mild steel (a) Uninhibited solution after a month (b) Inhibited solution after a month.

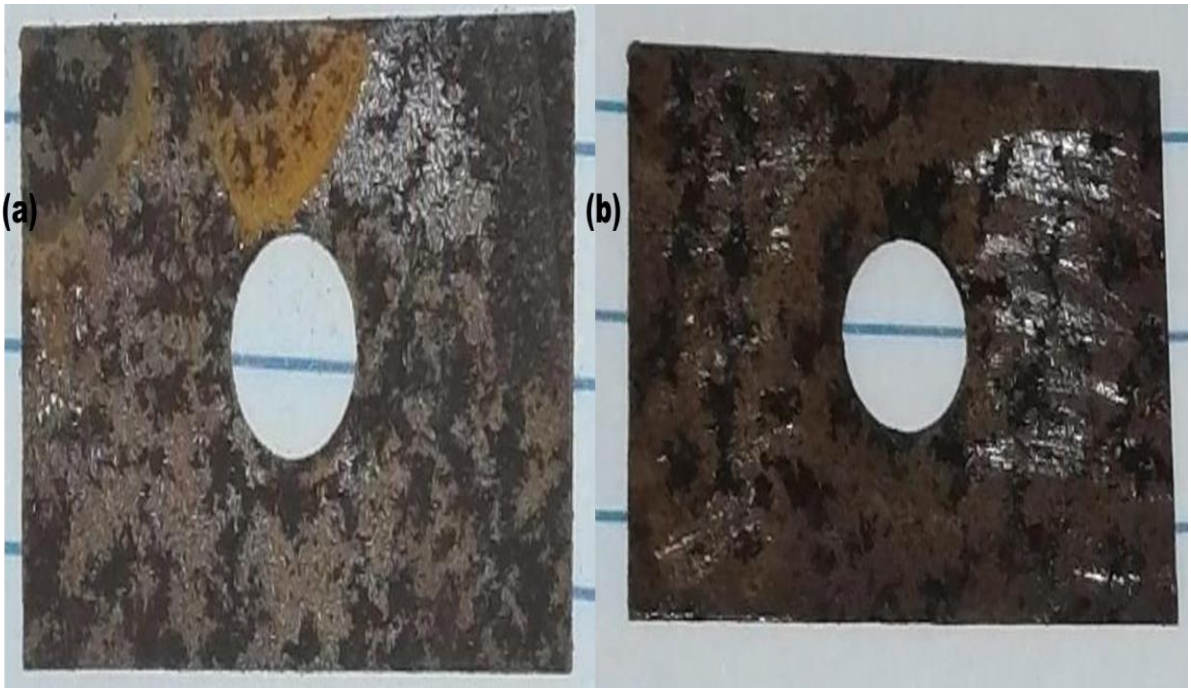

Figure 4. 14: Mild steel (a) Uninhibited solution after 6 months (b) Inhibited solution after 6 months.

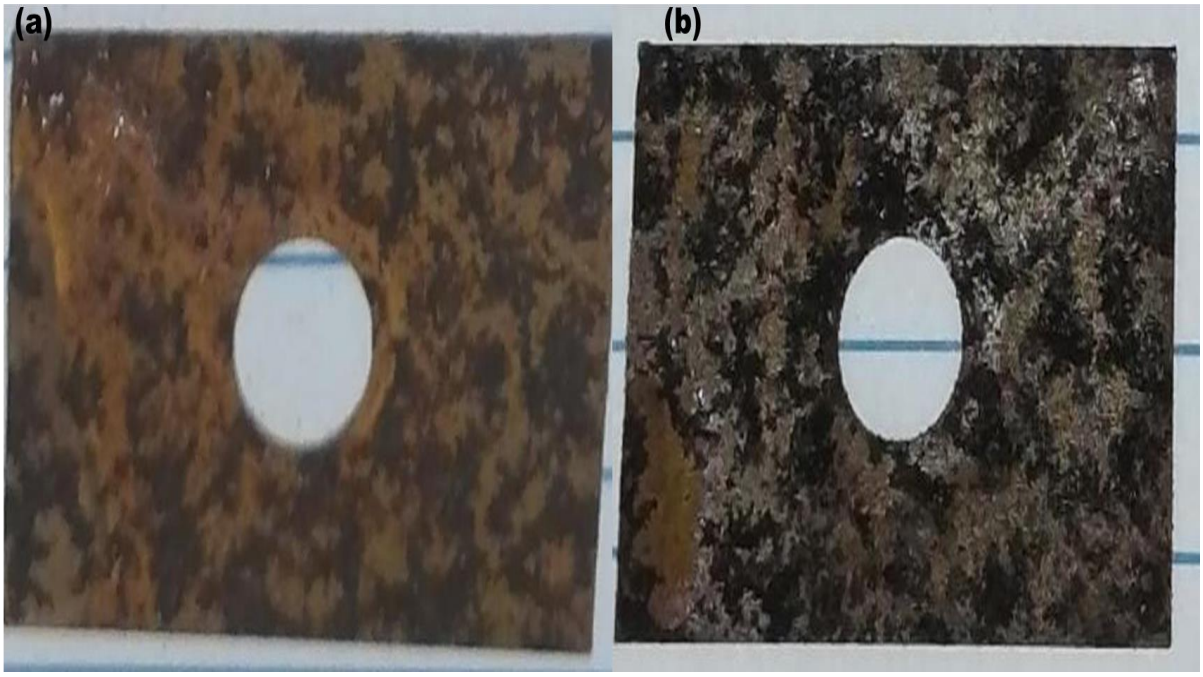

Figure 4. 15: Mild steel (a) Uninhibited solution after a year (b) Inhibited solution after a year.

4.2.1. Weight loss measurements

4.2.2. Effect of inhibitor concentration and temperature on corrosion rate

Figure 4.16 (a) is a display of the percentage inhibition efficiency (%IE) versus inhibitor concentration plots at various temperatures for GS. It is clearly shown from the results that the %IE increases as the concentration of the inhibitor increases. However, we observed an appreciable %IE of 92.73 % for 50 x 10^{-5} M at 328 K. This behaviour is due to more inhibitor molecules resulting in a larger surface coverage on the mild steel (MS) [172]. Furthermore, at 328 K we observed an appreciable reduced corrosion rates such as 4.44 x 10^{-3}, 3.89 x 10^{-3}, 2.78 g.cm^{-2}.h^{-1} at 10 x 10^{-5}, 30 x 10^{-5}, 50 x10^{-5} M.

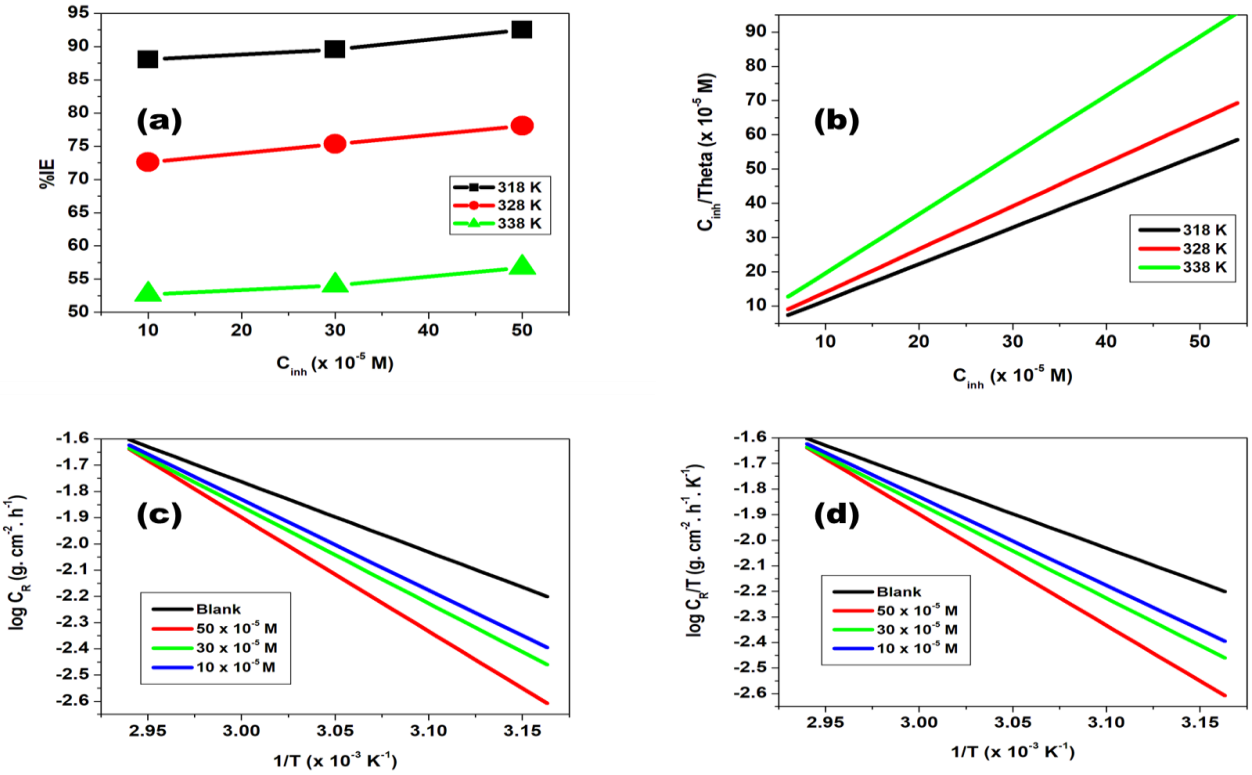

Figure 4. 16: Efficiency (%IE) versus GS concentration (M) plot for (a) GS; and Langmuir isotherm (b) GS inhibitor on MS sheet at 318 K, 328 K and 338 K. Arrhenius graphs for MS in 1. 0 M HCl with and without GS (c) Transition state graphs at differing GS (d).

Table 4. 6: Corrosion rate (C_R), efficiency of inhibition, (%IE) and surface coverage (θ) of GS at 318, 328 and 338 K for mild steel.

Inhibitor	Temperature (K)	Concentration (x 10^{-5} M)	Weight loss (g)	Corrosion rate (x 10^{-3} g. cm^{-2}. hr^{-1})	Inhibition efficiency (IE)	Surface coverage (Ɵ)	C/Ɵ x 10^{-5}
GS	318	0	0.13	7.28	_	_	_
		10	0.08	4.44	88.06	0.8806	11.3560
		30	0.07	3.89	89.55	0.8955	33.5002
		50	0.05	2.78	92.54	0.9254	54.0325
	328	0	0.22	12.2	_	_	_
		10	0.20	11.1	72.61	0.7261	13.7730
		30	0.18	10.0	75.35	0.7535	39.8168
		50	0.16	8.89	78.08	0.7808	64.0331
	338	0	0.41	22.78	_	_	_
		10	0.35	19.44	52.70	0.5270	18.9748
		30	0.34	18.89	54.05	0.5405	55.5013
		50	0.32	17.78	56.76	0.5676	88.0971

In order to obtain insight into the way the GS compound adsorbs on the surface of the metal, several different adsorption isotherms, including the Langmuir, Frumkin, Freundlich, and Temkin isotherms, have been investigated and fitted using data. In order to further understand the isotherm that determines the adsorption process, values at 318, 328, and 338 K for various inhibitor doses were considered. This was done while observing the surface coverage. The Langmuir adsorption isotherm suggests that the value is connected to the equilibrium adsorption constant, K_{ads}, as well as the concentration of GS (Equations 4.1). The results are shown in Table 4.7, and the data fit the Langmuir isotherm adsorption for GS inhibitor [173].

Table 4. 7: Adsorption parameters for glycerol stearate on MS.

Inhibitor	T (K)	K_{ads} (x10^5 L.mol^{-1})	R^2	-ΔG^o_{ads} (kJ.mol^{-1})
GS	318	1.0465	0.9995	-10.74
	328	0.4256	0.9989	-11.08
	338	0.6611	0.9996	-11.41

Equation 4.3 was used to determine the adsorption free energy denoted by G_{ads}. Electrostatic interaction between charged molecules and a charged metal surface (physisorption adsorption mechanism) is related with energies smaller than -20 kJ. mol^{-1}, as reported in the literature [174]. In difference, if the ΔG^o_{ads} values are less than -20 kJ. mol^{-1} or less negative is an indication that there is electrostatic interactions which signify a physisorption mechanism [19]. According to results on Table 4.2, it is noticed that GS inhibitor accounts for physisorption mechanism. In addition, a spontaneous adsorption process of GS was observed considering negative ΔG^o_{ads} values [175].

4.2.3. Thermodynamic and activation parameters

The Arrhenius equation was used to evaluate temperature effect on the behaviour of the adsorption process and activation energy (E_a) parameters of corrosion process according to [176,177]:

$$\log C_R = \log A - \frac{E_a}{2.303RT} \quad (4.4)$$

C_R denoted rate of corrosion, E_a denoted energy of activation, R denoted molar gas constant (8.314 J. K^{-1}. mol^{-1}), and T denoted absolute temperature and A denoted frequency factor. The Arrhenius Equation (4.4) and its transition state Equation were used to calculate activation energy, entropy, and enthalpy at various GS

concentrations (Equation 4.5). Part (c) of Figure 4.16 depicts an Arrhenius plot of log (C_R) vs reciprocal temperature (1/T), which was used to derive the activation energy estimates. S^o and H^o were determined by solving the transition state equation (4.5) [148]. Transition state graphs for GS at different temperatures are shown in Figure 4.16 (d). Activation energy, measured in joules per mole, is needed for any chemical reaction to take place. Increases in the activation energy barrier for the corrosion process, as measured at concentrations of 10 x 10^5, 30 x 10^5, and 50 x10^5 M, indicate that the GS compound is effective at inhibiting corrosion. [178]. The activation energy of the corrosion process is improved by increasing a double layer thickness which is associated with higher E_a values. Positive values of ΔH^o are the indication of an endothermic process [179,180]. Negative values of S^o are an indication that the formation of the activated complex during the rate-determining step is associative rather than associative. This indication can be further interpreted to mean that there is a decrease in disorderliness as the reaction progresses from reactants to activated complex [148]. A depiction of the various parameters taken from the Arrhenius plot and the transition state plot can be seen in Table 4.8.

Measurements for $\Delta S°$ and $\Delta H_a°$ were determined using Equation (4.5):

$$log\left(\frac{CR}{T}\right) = \left[\log\left(\frac{R}{hN}\right) + \left(\frac{\Delta S}{2.303R}\right)\right] - \frac{\Delta H}{2.303RT} \quad (4.5)$$

k_B denoted Boltzmann's constant: C_R indicated rate of corrosion and h denoted Plank's constant. Figure 4.16 (d) showed log (C_R/T) versus 1/T graph for GS, showing linear graphs with $\left[\log\left(\frac{R}{hN}\right) + \left(\frac{\Delta S}{2.303R}\right)\right]$ as intercept. In addition, -ΔH°/R values were calculated from slopes. Furthermore, it was noticed that blank solution showed high C_R values as compared to GS inhibitor. Lower C_R values indicated that Al metal dissolution was minimised.

Table 4. 8: Presented are activation energy (E_a), entropy (ΔS^o) and enthalpy of activation (ΔH^o_{ads}) values for GS on mild steel.

Inhibitor	**Concentration** (x10^{-5}M)	E_a **(kJ.mol^{-1})**	ΔH^o_{ads} **(kJ.mol^{-1})**	ΔS^o **(JK^{-1}.mol^{-1})**
GS	0	51.27	48.54	-134.03
	10	66.09	63.37	-90.85
	30	70.74	68.02	-77.41
	50	83.14	80.41	-41.02

4.2.4. Potentiodynamic polarisation (PDP)

The use of tafel slope analysis aided in determining corrosion current densities which were required for corrosion rates calculations. In addition, via the extrapolation of the tafel lines, electrochemical parameters such as corrosion potential (E_{corr}), anodic (b_a) and cathodic (b_c) tafel slopes and corrosion current density (I_{corr}) were obtained.

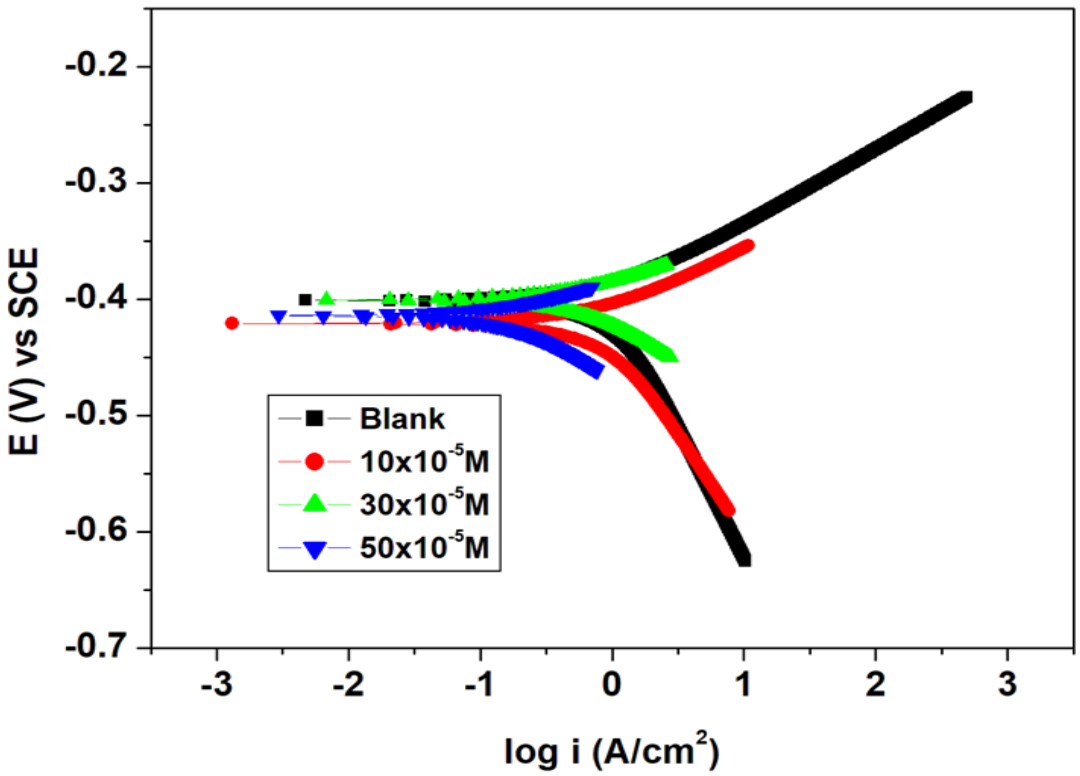

Figure 4. 17: Potentiodynamic polarisation plot for mild steel in 1. 0 M HCl in the uninhibited and inhibited solutions of GS different concentrations.

Figure 4.17: Potentiodynamic polarisation curves for mild steel in 1. 0 M HCl with and without the GS inhibitor concentrations ($10x10^{-5}$ M, $30x10^{-5}$ M and $50x10^{-5}$ M). From Figure 4.17 it is observed that different concentrations of GS reduced the corrosion current density (I_{corr}) values. The most essential trend observed was that the corrosion current density shifted to lower regions upon the introduction of GS inhibitor compound. The tafel curves showed that the I_{corr} values reduced with the increasing GS inhibitor concentrations. In addition, it is observed that the difference between E_{corr} values of the blank (1. 0 M HCl) and that of the inhibited solutions is less than 85 mV which signifies a mixed-type inhibition mechanism with the cathodic inhibition dominating as observed from the tafel slopes [181] . Furthermore, it is shown that the tafel slopes decreased upon the introduction of the inhibitor, thus confirming that GS has successfully adsorbed on mild steel surface retarding metal dissolution (anodic

process) and hydrogen evolution (cathodic process). The percentage inhibition efficiencies increased with the increase of the inhibitor concentration with the highest efficiency of 82.69% at $50x10^{-5}$ M.

Table 4. 9 : Polarisation measurements such as E_{corr}, I_{corr}, b_a and b_c using different inhibitor concentrations.

Inhibitor	**Concentration x 10^{-5} (M)**	**-E_{corr} (mV)**	**I_{corr} (mA.cm^{-2})**	**b_a (mV)**	**b_c (mV)**	**%IE_{PDP}**
Blank		401.15	1.04	65.6	225.5	-
GS	10	420.00	0.89	61.0	172.1	14.42
	30	400.59	0.61	45.7	74.6	41.35
	50	414.13	0.18	37.3	73.8	82.69

4.2.5. Electrochemical impedance

More insight regarding corrosion behaviour of mild steel in hydrochloric acid and inhibition by glycerol stearate was obtained with the aid of the electrochemical impedance spectroscopy. Nyquist graphs in Figure 4.18 are presented as imperfect semicircles together with their corresponding bode plots in Figure 4.19 which revealed that as the inhibitor concentration increased the phase angle increased which signifies the formation of the adsorptive film. In addition, the imperfect semicircles are a representation of mild steel impedance spectra in the uninhibited and inhibited solutions with different GS inhibitor concentrations. From the impedance spectra, it is observed that the diameter of the imperfect semicircles increased with the increase in the inhibitor concentration [182] and the imperfection of the semicircle is indicative of a charge transfer process governing the corrosion of mild steel [183] . Furthermore, to explain the impedance nature, an electric circuit comprising the solution resistor (R_s), charge transfer resistance (R_{ct}) and a double layer capacitance (C_{dl}) in Figure 4.20 was used.

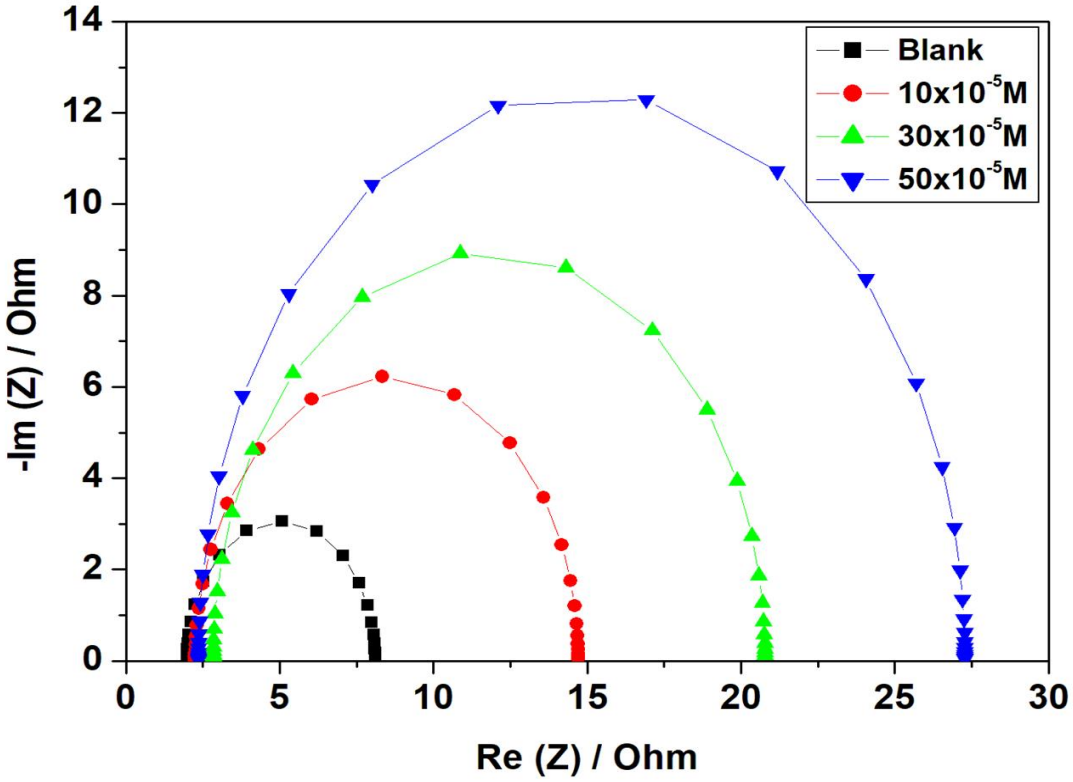

Figure 4. 18: Nyquist plot for aluminium in 1. 0 M HCl in the uninhibited and inhibited solution with different GS concentrations.

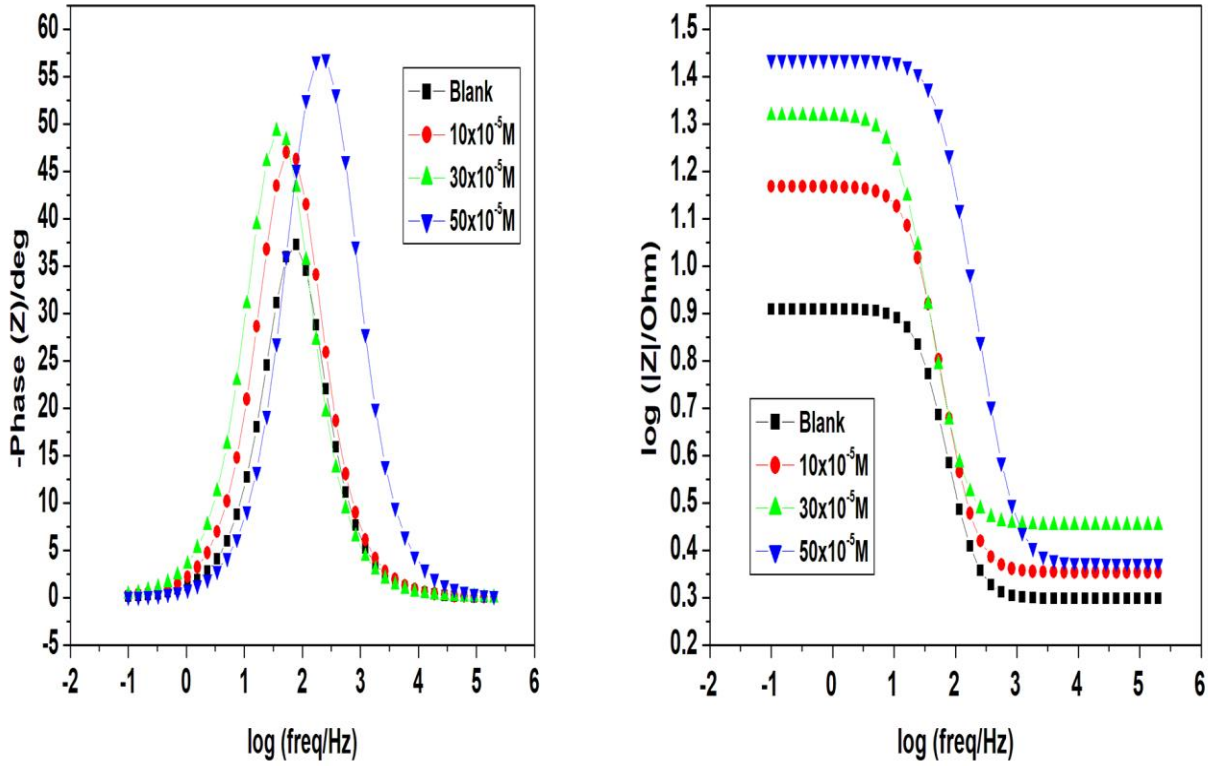

Figure 4. 19: Bode plots of mild steel in 1. 0 M HCl with and without glycerol stearate.

Table 4. 10: Electrochemical impedance parameters.

Inhibitor	Concentration x 10^{-5} (M)	R_s (Ω)	R_{ct} (Ω)	C_{dl} (x10^{-6} F)	$\%IE_{EIS}$
Blank		1.986	6.122	0.719	-
GS	10	2.256	12.45	0.540	50.83
	30	2.839	17.94	0.602	65.88
	50	2.357	24.93	0.102	75.44

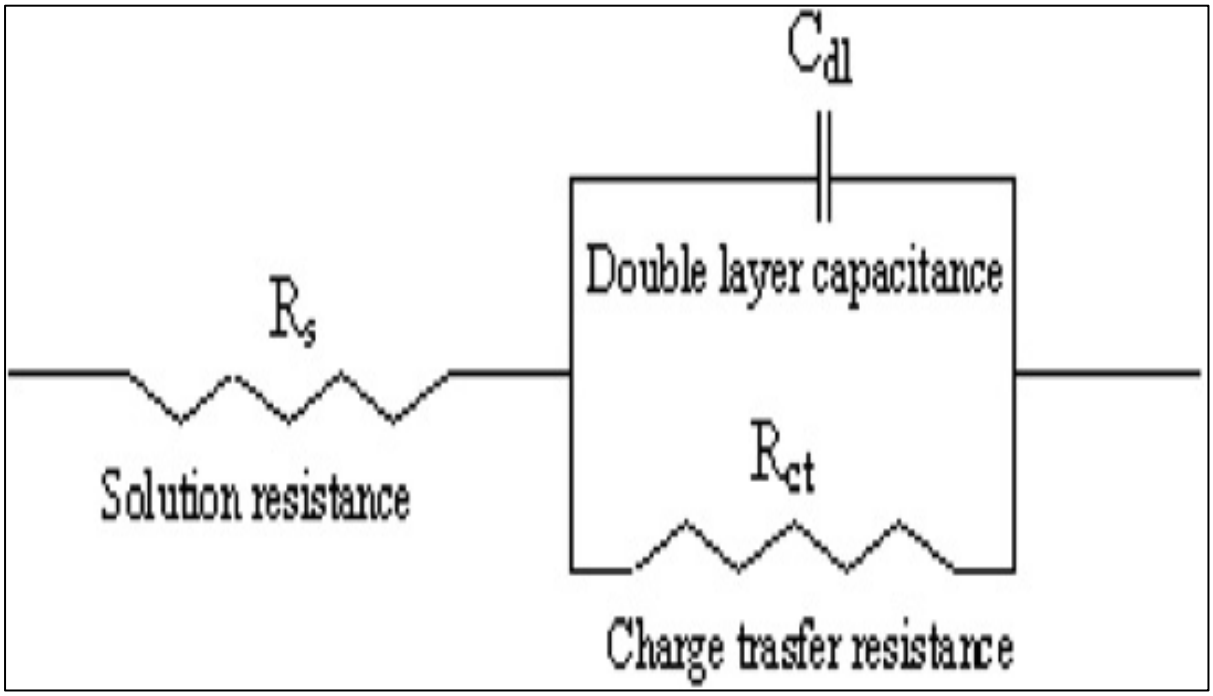

Figure 4. 20: The suggested electrical circuit for studied GS.

4.3. ZINC

OBSERVATION OF CORROSION RATE WITH TIME

Pictorial observations were performed on the zinc metal before corrosion tests were run as shown in Figure 4.21. When viewing zinc metal strictly in acidic medium (uninhibited solution) the entire metal accumulated stains on surface revealing a redish-brownish color as witnessed earlier with mild steel. However, after glycerol stearate (inhibitor) was introduced, zinc metal obtained clear surface on some parts of the metal especially when observations were made after a week. The same behaviour was observed although not very announced for after a month, 6 months and a year as compared to when observations were made after a week as shown from Figure 4.22-4.25.

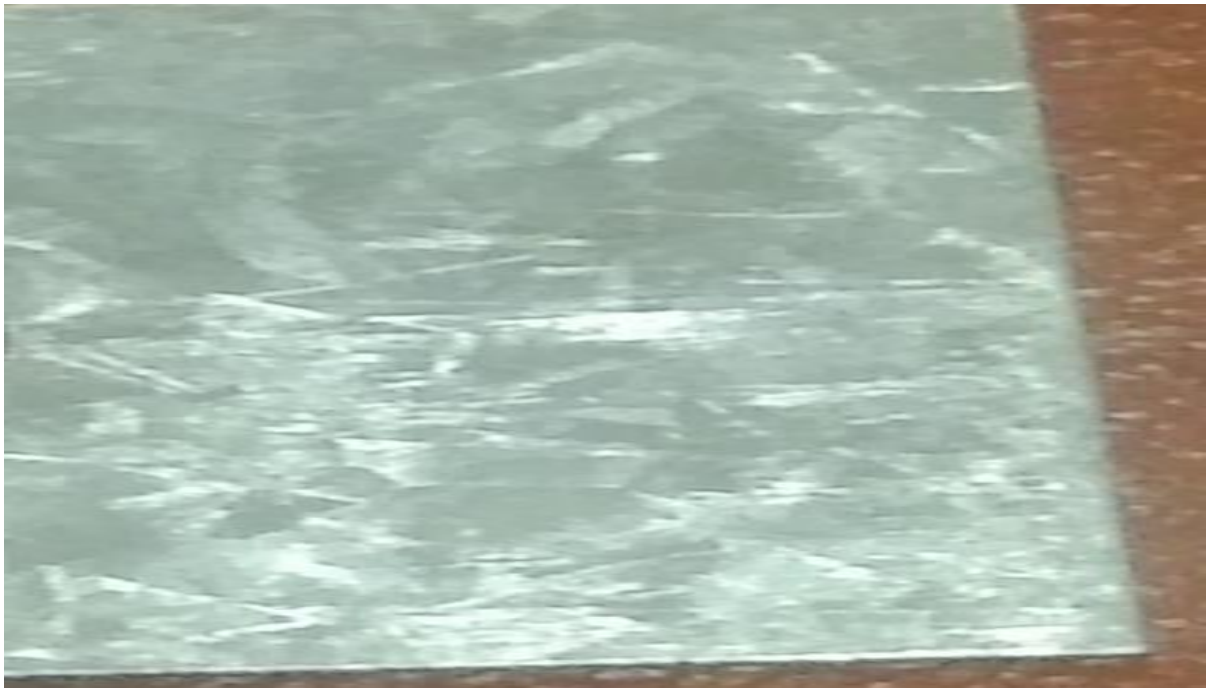

Figure 4. 21: Zinc metal before corrosion testing.

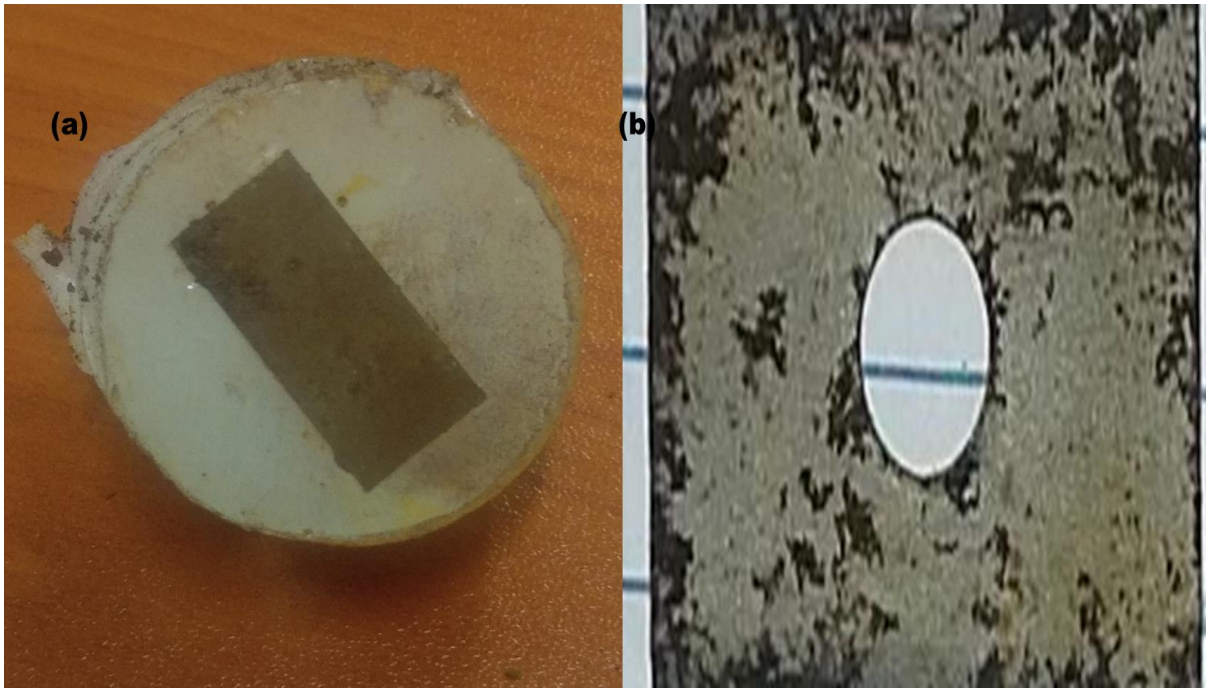

Figure 4. 22: Zinc metal (a) Uninhibited solution after a week (b) Inhibited solution after a week.

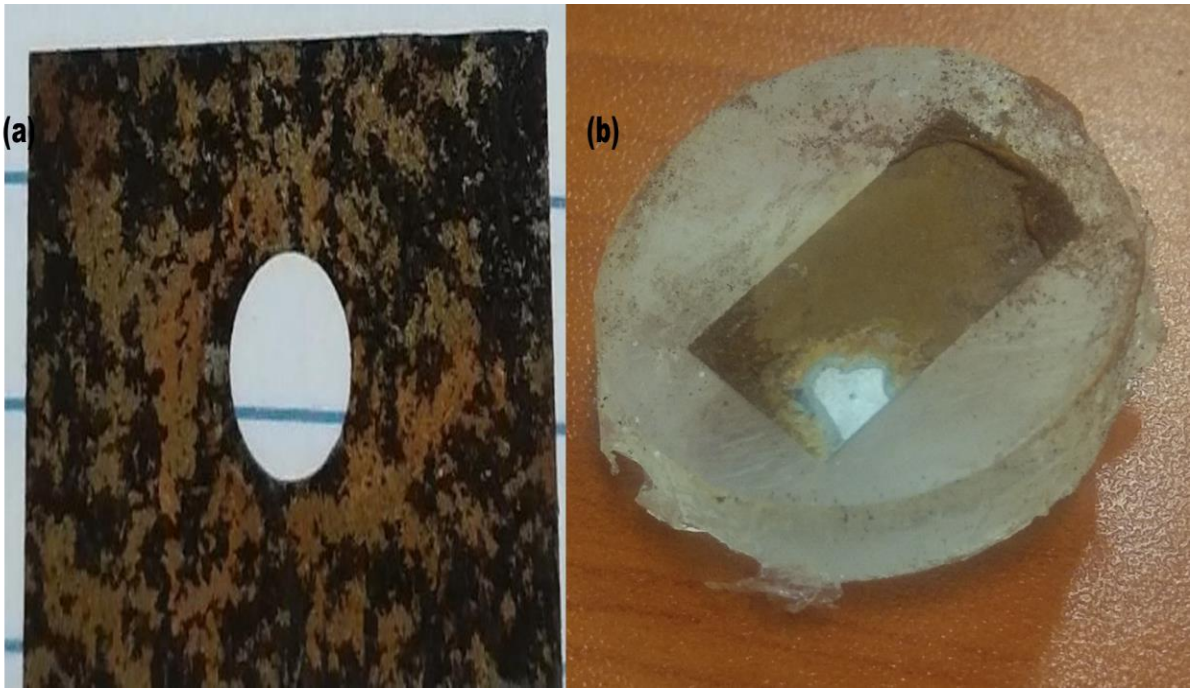

Figure 4. 23: Zinc metal (a) Uninhibited solution after a month (b) Inhibited solution after a month.

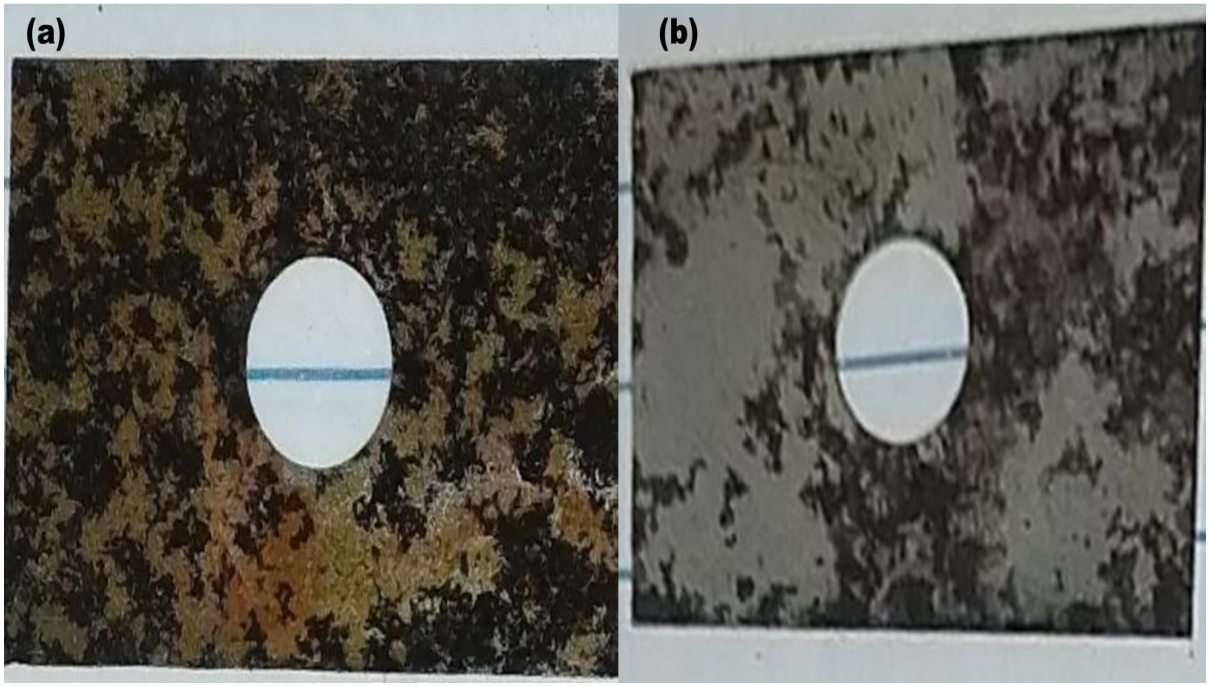

Figure 4. 24: Zinc metal (a) Uninhibited solution after 6 months (b) Inhibited solution after 6 months.

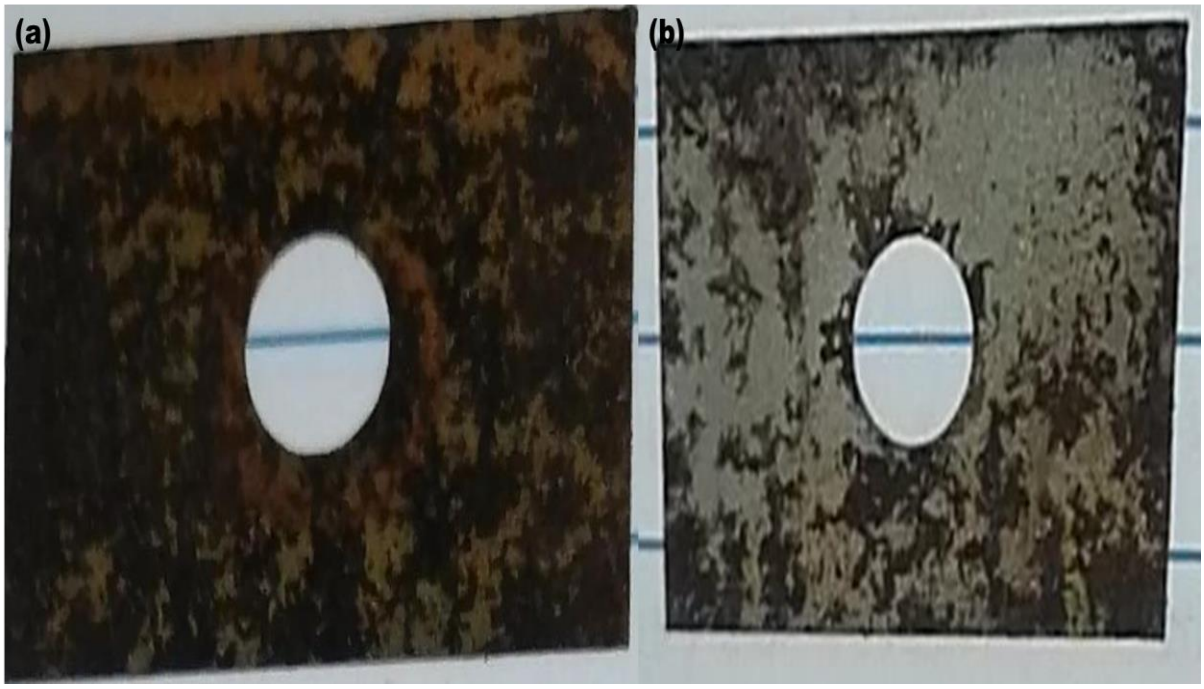

Figure 4. 25: Zinc metal (a) Uninhibited solution after a year (b) Inhibited solution after a year.

4.3.1. Weight loss measurements

4.3.2. Effect of inhibitor concentration and temperature on corrosion rate

The gravimetric experiments of Glycerol stearate (GS) inhibitor were presented by the percentage inhibition efficiencies (%IE) against inhibitor concentration plots at 318, 328 and 338 K as given in Figure 4.26 (a). The %IE is observed to increase at all temperatures the inhibitor concentration increases from 10 x 10^{-5} - 50 x 10^{-5} M, for GS. In addition, it is observed that the %IE increases with the increase in temperature. This observation could be due to the thermal stability of the GS and the adsorption nature of the inhibitor particularly on a zinc metal (Zn) [124]. The effect of temperature is showed by the %IE values for 10 x 10^{-5} M at 318 K, 67.16% while at 328 and 338 K, 68.65% and 73.13% were obtained respectively. The density of corrosion rate increases severely as the temperature increases.

As shown from studies, the rate of metal dissolution is hindered by increasing the inhibitor concentration [132]. The corrosion rate was found to be 15.56, 19.44 and 31.11 × 10^{-3} g.cm^{-2}.h^{-1} in the uninhibited solution at 318, 328 and 338 K, respectively. However, according to the observations on Table 4.11 it is observed that upon the introduction of the inhibitor in the solution, the rate of corrosion decreased. The similar behaviour was observed by Hong *et al*. [184], using fungicides and 4-amino-antipyrine on the corrosion of copper in NaCl solution, respectively. It was found that the metal dissolution decreased optimum to a value of 10.0× 10^{-3}g.cm^{-2}.h^{-1} in GS for 50 x 10^{-5} M inhibitor concentration at 318 K. Furthermore, metal mass loss decreased with a decrease in the rate of corrosion due to the inhibitor adsorption on Zn metal surface.

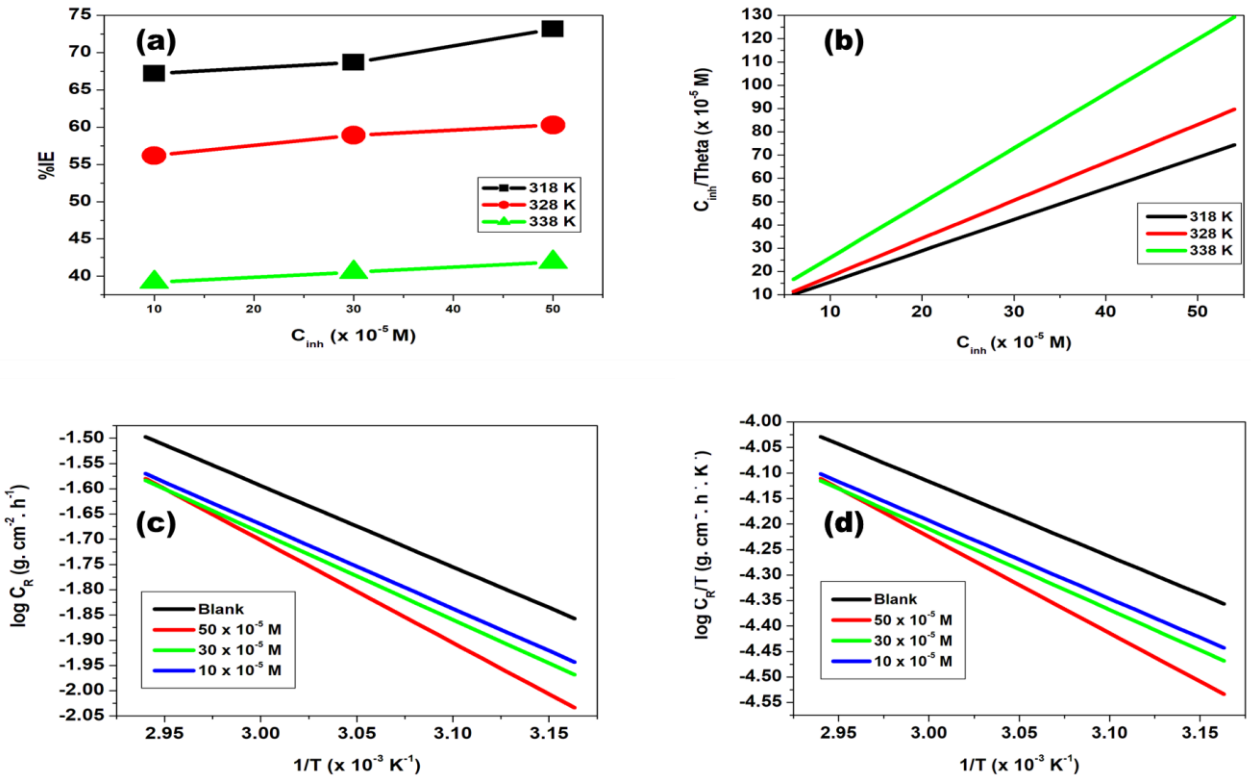

Figure 4. 26: Efficiency (%IE) versus GS concentration (M) plot for (a) GS; and Langmuir isotherm (b) GS inhibitor on zinc sheet at 318 K, 328 K and 338 K. Arrhenius graphs for zinc metal in 1. 0 M HCl with and without GS (c) Transition state graphs at differing GS (d).

The mechanism type followed during the process of adsorption at the inhibitor/metal interface has been investigated in a significant way by fitting various adsorption isotherms with the best regression line R^2 value. The surface coverage and inhibitor concentrations of the GS relationship followed the Langmuir equation, as expressed by Equation 4.2. Figure 4.26 (b) depicts a Langmuir adsorption isotherm plot with R^2 values ranging from 0, 9996 to 0, 9999. The Langmuir plots are enhanced by R^2 values close to unity. Table 4.12 shows the adsorption equilibrium constant and standard free energy of adsorption values.

The number of inhibitor layers that had been adsorbed on the metal surface was calculated by using the slopes of the regression lines. The standard free energy of adsorption [185] offers insight into the spontaneity of the inhibitory process as well as the stability of adsorption. According to the research that has been done [185], a

spontaneous process is characterised by having values of free energy of adsorption that are on the negative sign. A physisorption adsorption mechanism is indicated when the value of the free energy of adsorption is less than or equal to -20 kJ. mol^{-1}, whereas a chemisorption adsorption mechanism is indicated when the value is greater than or equal to -40 kJ. mol^{-1} in the negative direction [4]. GS supplied a physisorption process, which can be found displayed in Table 4.12, for Gibbs free energy values that were lower than -20 kJ. mol^{-1}.

Table 4. 11: Corrosion rate (C_R), efficiency of inhibition, (%IE) and surface coverage (θ) of GS at 318, 328 and 338 K for zinc metal.

Inhibitor	**Temperature (K)**	**Concentration (x 10^{-5} M)**	**Weight loss (g)**	**Corrosion rate (x 10^{-3} g. cm^{-2}. hr^{-1})**	**Inhibition efficiency (IE)**	**Surface coverage (Ɵ)**	**C/Ɵ x 10^{-5}**
GS	318	0	0.28	15.56	_	_	_
		10	0.22	12.22	67.16	0.6716	14.8893
		30	0.21	11.67	68.65	0.6865	43.6968
		50	0.18	10.0	73.13	0.7313	68.3688
	328	0	0.35	19.44	_	_	_
		10	0.32	17.78	56.17	0.5617	17.8034
		30	0.30	16.67	58.91	0.5891	50.9263
		50	0.29	16.11	60.28	0.6028	82.9486
	338	0	0.56	31.11	_	_	_
		10	0.45	25.00	39.19	0.3919	25.5183
		30	0.44	24.44	40.54	0.4054	74.0029
		50	0.43	23.89	41.89	0.4189	119.3593

Table 4. 12: Adsorption parameters for glycerol stearate on zinc.

Inhibitor	T (K)	K_{ads} (x10^5 L.mol^{-1})	R^2	$-\Delta G^o_{ads}$ (kJ.mol^{-1})
GS	318	0.4528	0.9989	-8.52
	328	0.5881	0.9999	-8.79
	338	0.3877	0.9996	-9.06

4.3.3. Thermodynamic and activation parameters

Metal dissolution increases with the increase in temperature, and as a result, there is a lower activation barrier [186]. By the help of Arrhenius equation and plot, the effect of temperature on the adsorption of GS onto the Zn surface is evaluated. The log C_R against 1/T plot as shown in Figure 4.26 (c). The plot assisted in calculating the values of the activation energy for the corrosion process. In Table 4.13 is the record of the calculated parameters of activation energy. The activation energy value in the uninhibited solution was less than those obtained in the inhibited solution. Higher activation energy values in the inhibited solution advocated to a prolonged rate of corrosion due to the formation of GS/Zn complex [187]. The entropy and enthalpy of activation can be used to investigate the inhibition efficiency of GS on Zn metal surface. Scientists have found that higher negative entropy values represent less surface destruction on metal, while higher positive entropy values represent greater disorder in the system [188].

Enthalpy values can represent either endothermic or exothermic reactions, depending on the sign of the value. Adsorption can be either physically or chemically involved in exothermic processes [40,189], while adsorption is used in endothermic processes. Plot of the transition is shown in Figure 5.26, which is based on Equation 5.4. (d) For GS.

Table 4. 13: Presented are activation energy (E_a), entropy (ΔS^o) and enthalpy of activation (ΔH^o_a) values for zinc metal.

Inhibitor	**Concentration** (x10^{-5}M)	E_a **(kJ.mol^{-1})**	ΔH^o_{ads} **(kJ.mol^{-1})**	ΔS^o **(JK^{-1}.mol^{-1})**
GS	0	30.85	28.13	-197.30
	10	31.98	29.26	-197.20
	30	33.03	30.30	-197.05
	50	38.94	36.21	-196.14

4.3.4. Potentiodynamic polarisation (PDP)

The polarisation parameters can be determined with the help of tafel plots. These include the corrosion potential (E_{corr}), the corrosion current density (I_{corr}), the anodic tafel slope (ba), and the cathodic tafel slope (b_c). Corrosion current densities were calculated by extrapolating tafel segments from anodic and cathodic curves. Coefficients of inhibition were found to be proportional to densities of corrosion currents (Equation 2.18) [148]. In Figure 4.27, we see a tafel plot for zinc metal in 1. 0 M HCl at varying concentrations of the GS inhibitor compound, both in its uninhibited form and its inhibited form. The addition of glycerol stearate corrosion inhibitor was found to decrease Icorr values. Inhibitor adsorption onto the zinc metal surface was observed, providing support for the adsorption mechanism [181]. Furthermore, the calculated E_{corr} difference between the blank (1. 0 M HCl) and the inhibitor solutions was less than 85 mV, indicating a mixed-type mechanism of inhibition with the cathodic mechanism dominating as observed from the tafel slopes at each inhibitor concentration [181].

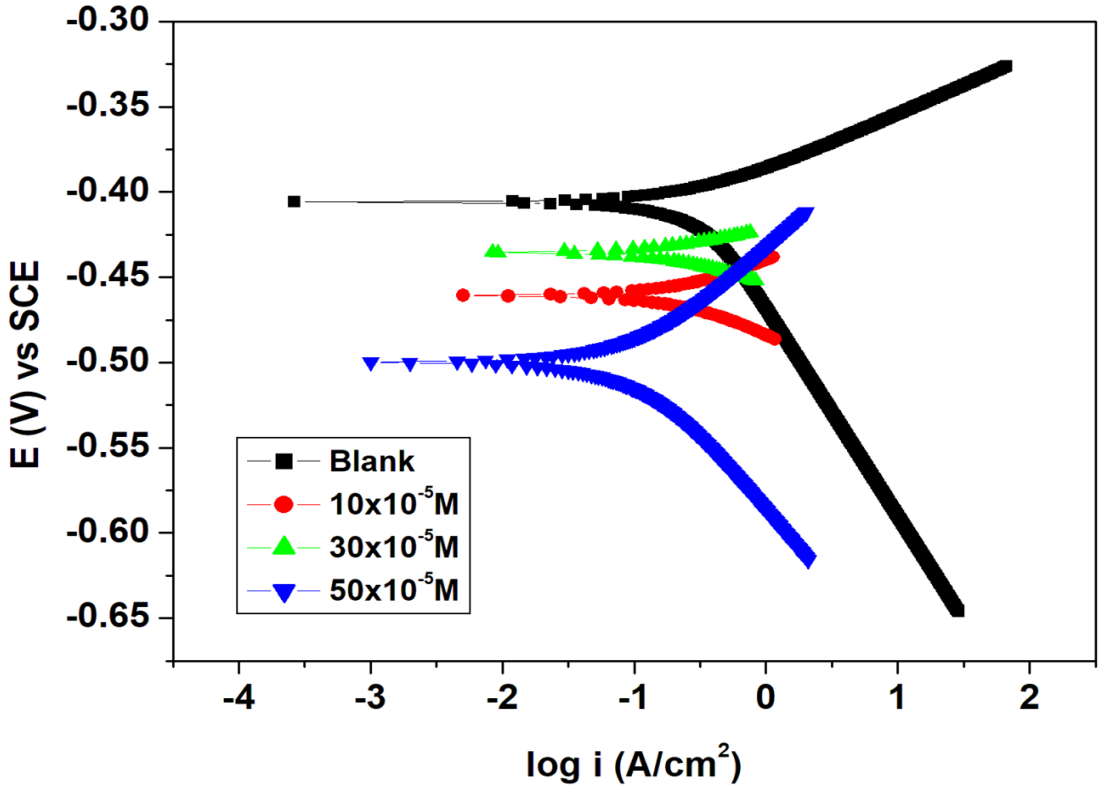

Figure 4. 27: Potentiodynamic polarisation plot for zinc in 1. 0 M HCl in the uninhibited and inhibited solutions of GS different concentrations.

Table 4. 14 : Polarisation measurements such as E_{corr}, I_{corr}, b_a and b_c using different inhibitor concentrations.

Inhibitor	Concentration x 10^{-5} (M)	-E_{corr} (mV)	I_{corr} (mA.cm^{-2})	b_a (mV)	b_c (mV)	%IE_{PDP}
Blank		445.25	0.38	70.3	97.5	-
GS	10	460.79	0.28	36.1	40.3	26.32
	30	435.47	0.19	18.5	25.3	50.00
	50	499.87	0.11	69.4	91.5	71.05

4.3.5. Electrochemical impedance

Further study of corrosion behaviour zinc metal in acidic medium in the uninhibited and inhibited solution of GS at different concentrations. In Figure 4.28-4.29 is a representation of Nyquist plot and its corresponding bode plot for zinc metal in the absence and presence of GS inhibitor compound. Bode plots revealed some information with regards to electrochemical behaviour of both the uninhibited and inhibited systems, it was revealed that at higher phase angle there was a frequency shift to higher frequency in the presence of glycerol stearate concenntrations. It is studied that the imperfection of the semicircles in the impedance spectra of zinc is due to the roughness and inhomogeneity on the metal surface [190]. From Table 4.15 is the impedance data for zinc metal obtained. Table 4.15 shows that the charge transfer resistance (R_{ct}) increased as the inhibitor concentration increased. The highest efficiency of 89.50% was obtained at $50x10^{-5}$ M. Moreover, to define the impedance nature, an equivalent electric circuit made up of the solution resistor (R_s), charge transfer resistance (R_{ct}) and a double layer capacitance (C_{dl}) in Figure 4.30 was utilised.

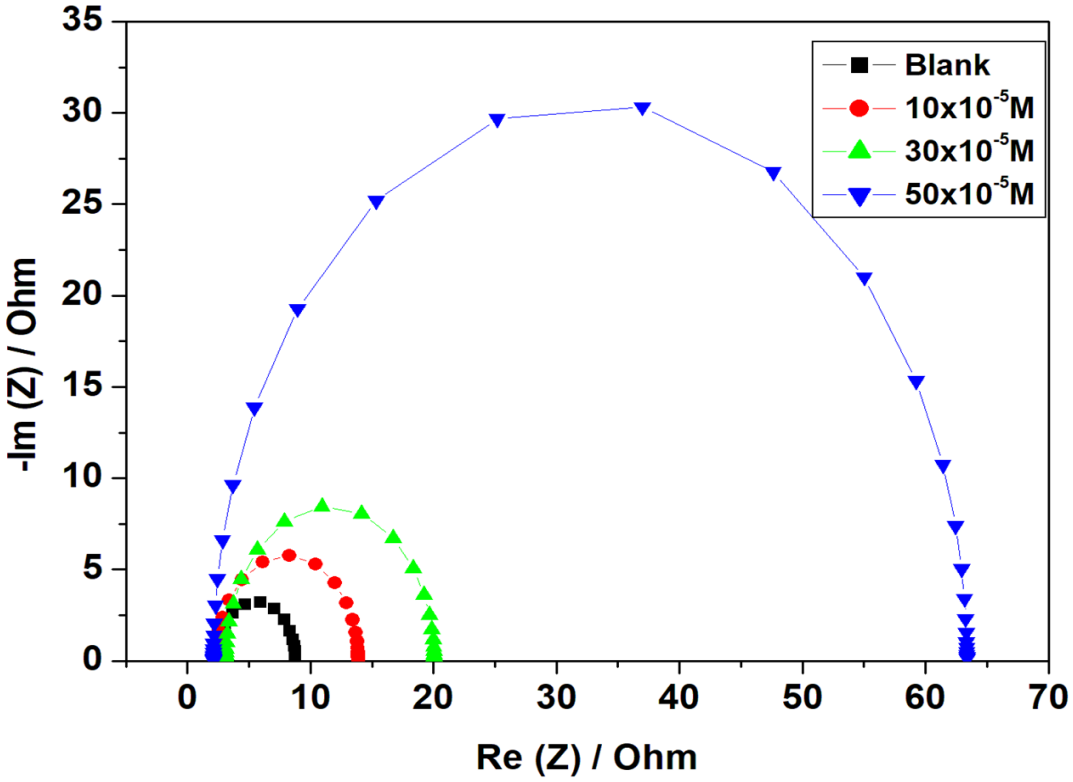

Figure 4. 28: Nyquist plot for zinc in 1. 0 M HCl in the uninhibited and inhibited solution with different GS concentrations.

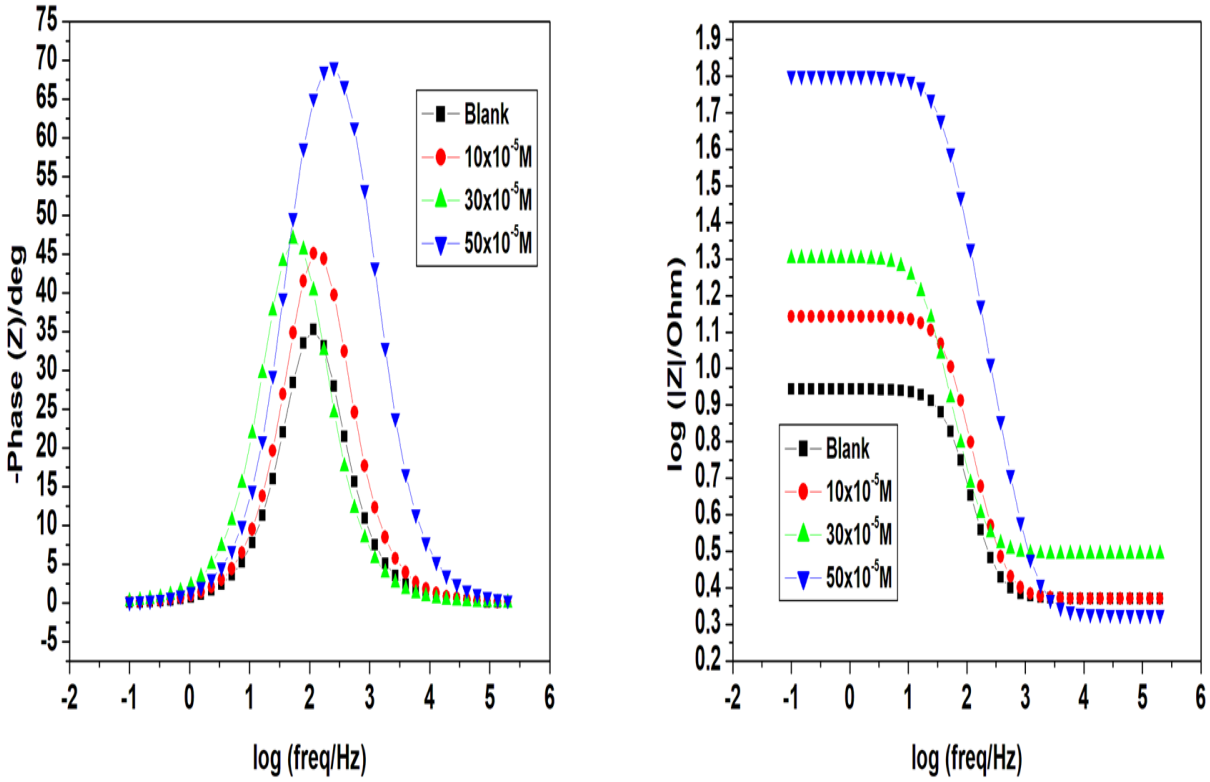

Figure 4. 29: Bode plots of zinc in 1. 0 M HCl with and without glycerol stearate.

Table 4. 15: Electrochemical impedance parameters.

Inhibitor	Concentration x 10^{-5} (M)	R_s (Ω)	R_{ct} (Ω)	C_{dl} (x10^{-6} F)	%IE_{EIS}
Blank		2.348	6.429	0.418	-
GS	10	2.344	11.54	0.252	44.29
	30	3.109	16.94	0.419	62.05
	50	2.121	61.24	0.006	89.50

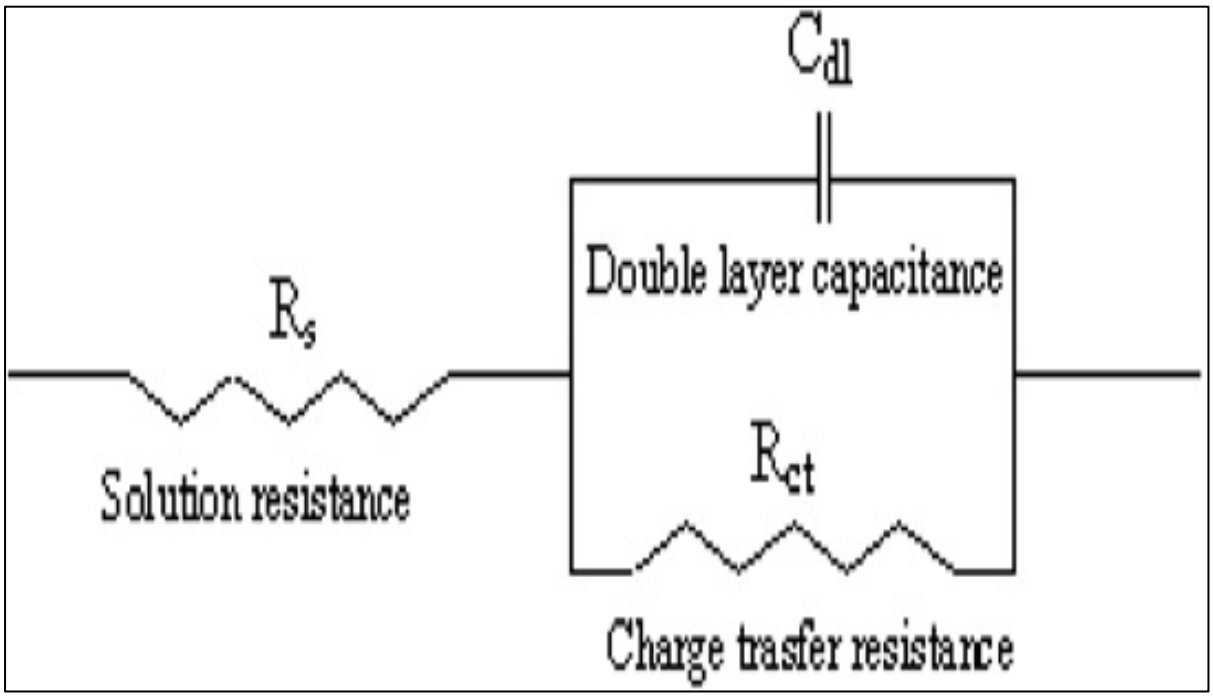

Figure 4. 30: The suggested electrical circuit for studied GS.

4.4. CHARACTERISATIONS

4.4.1. Fourier transform infreared spectroscopy (FTIR)

In order to study inhibitor adsorption film on the metal surface, fourier transform infrared spectroscopy (FTIR) was used [191]. The most region of interest is the high-energy region from 3000-4000cm^{-1} [192]. In actual fact, this region highly corresponds to the OH^-stretching vibrations [193]. Figure 4.31-4.33 displayed are IR spectrum of the adsorptive film and glycerol stearate (GS) for mild steel, aluminium and zinc. Each hydroxyl group formed hydrogen bonds which are detected by the peak at 3307 cm^{-1}, secondly followed by a band occurring at 3241 cm^{-1}. In addition, observing from a low energy region, there are two peaks occurring at 2914 cm^{-1} and 2849 cm^{-1} which represent the typical CH_2 stretch of alkyl carbon chains. Furthermore, another visible peak occurring at 1730 cm^{-1} is accredited to the C=O stretching mode. Moreover, on the adsorption film spectrum, the peak at around 590.34 cm^{-1} is accredited to the passivating iron oxide layer formed on the mild steel. When comparing glycerol spectrum and spectra for adsorptive films for mild steel, aluminium and zinc there is a

disappearance of glycerol stearate functional groups with respect to each adsorptive film formed on three specimen such as mild steel, aluminium and zinc and this imply that indeed the reactive heteroatoms have coordinated well on the surface of each metal.

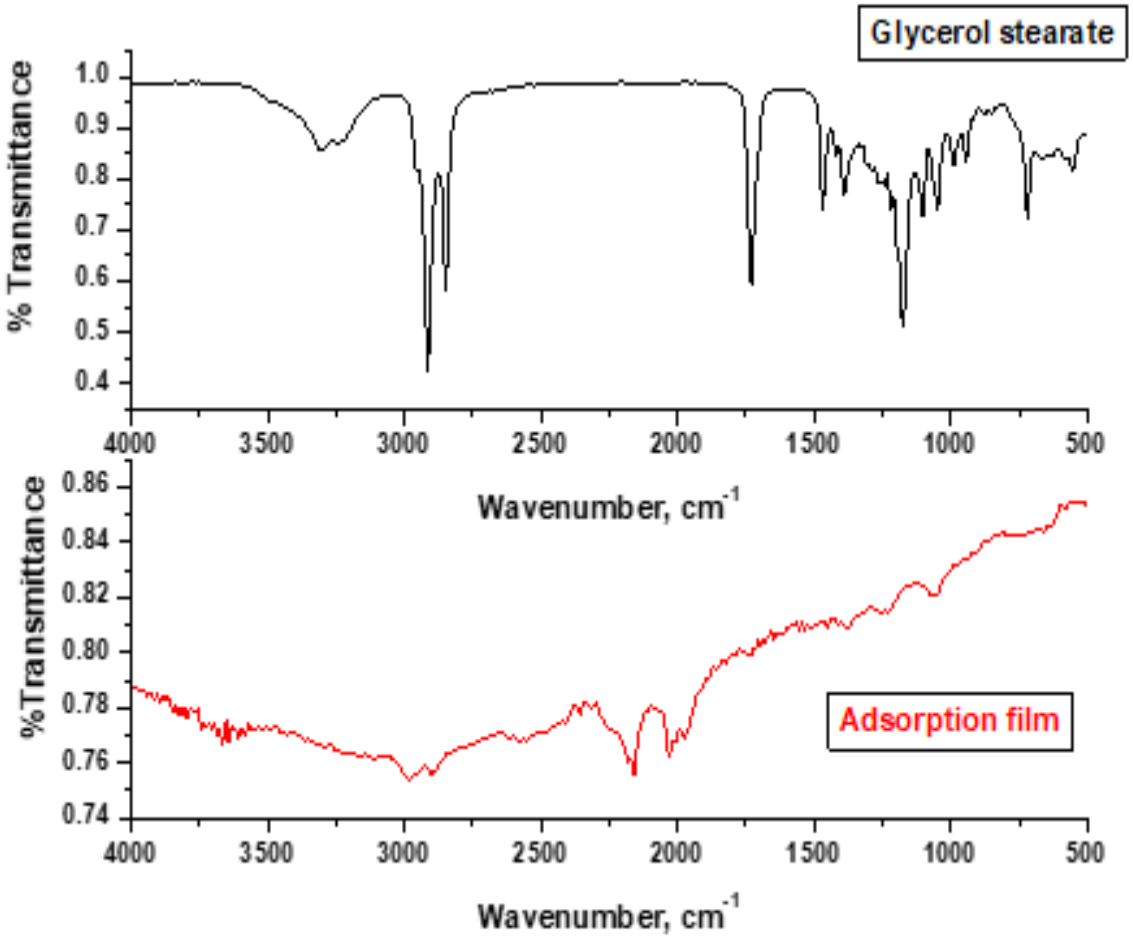

Figure 4. 31: FTIR spectra for glycerol stearate and adsorption film formed on aluminium.

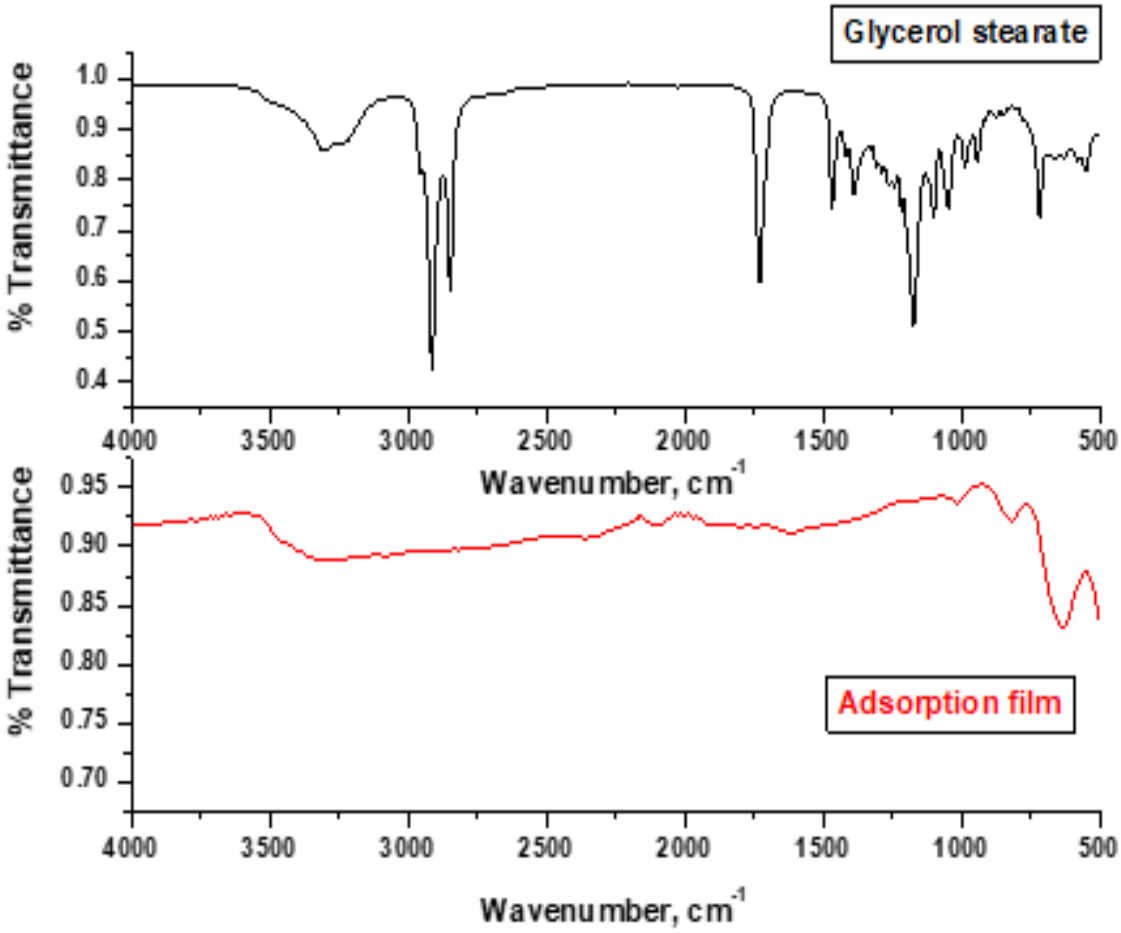

Figure 4. 32: FTIR spectra for glycerol stearate and adsorption film formed on mild steel.

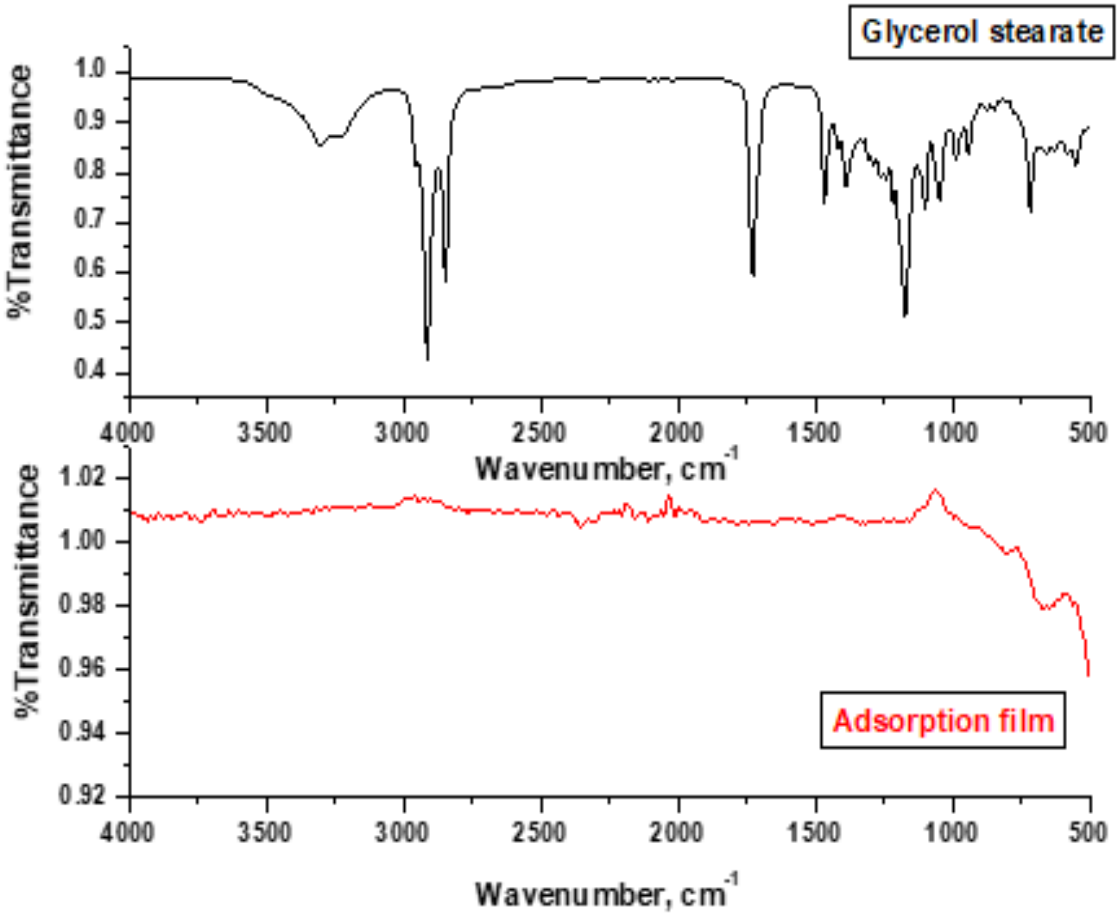

Figure 4. 33 : FTIR spectra for glycerol stearate and adsorption film formed on zinc.

4.4.2. Scanning electron microscopy (SEM) and energy dispersive spectroscopy (EDS)

In Figure 4.34, 4.37, 4.40, shown are smooth surfaces of aluminium, mild steel and zinc respectively before corrosion testing, any inhomogeneity revealed was due to abrasion with emery papers. Nonetheless in Figure 4.35, 4.38, 4.41 after immersion in 1. 0 M HCl aluminium, mild steel and zinc surfaces showed a rougher nature. These observations are substantiated by corresponding EDS spectra revealing the absence and presence of Cl^- that led to aluminium surface roughness [194]. However, introducing glycerol stearate inhibitor minimised more surface roughness when

comparing SEM micrographs in the absence and presence of inhibitor in 1. 0 M HCl solution as shown in Figure 4.36, 4.39, 4.42 for aluminium, mild steel and zinc.

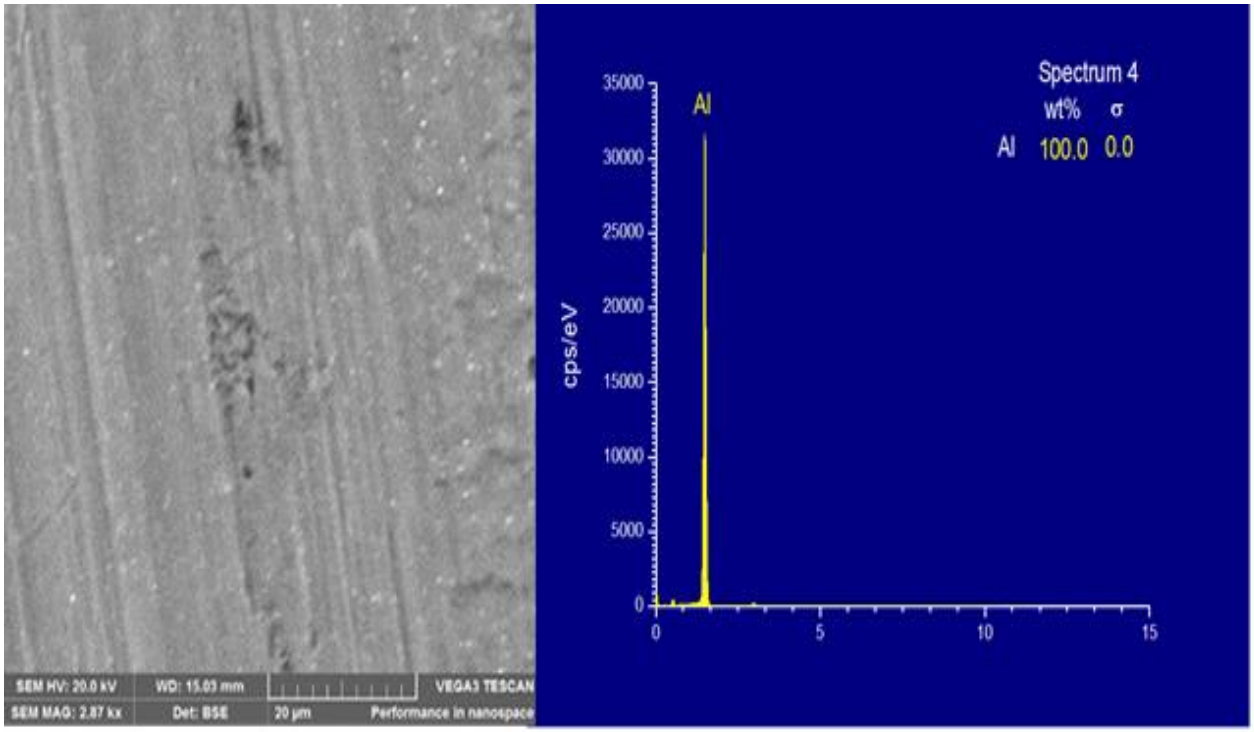

Figure 4. 34: SEM micrograph and EDS spectrum of pristine aluminium metal.

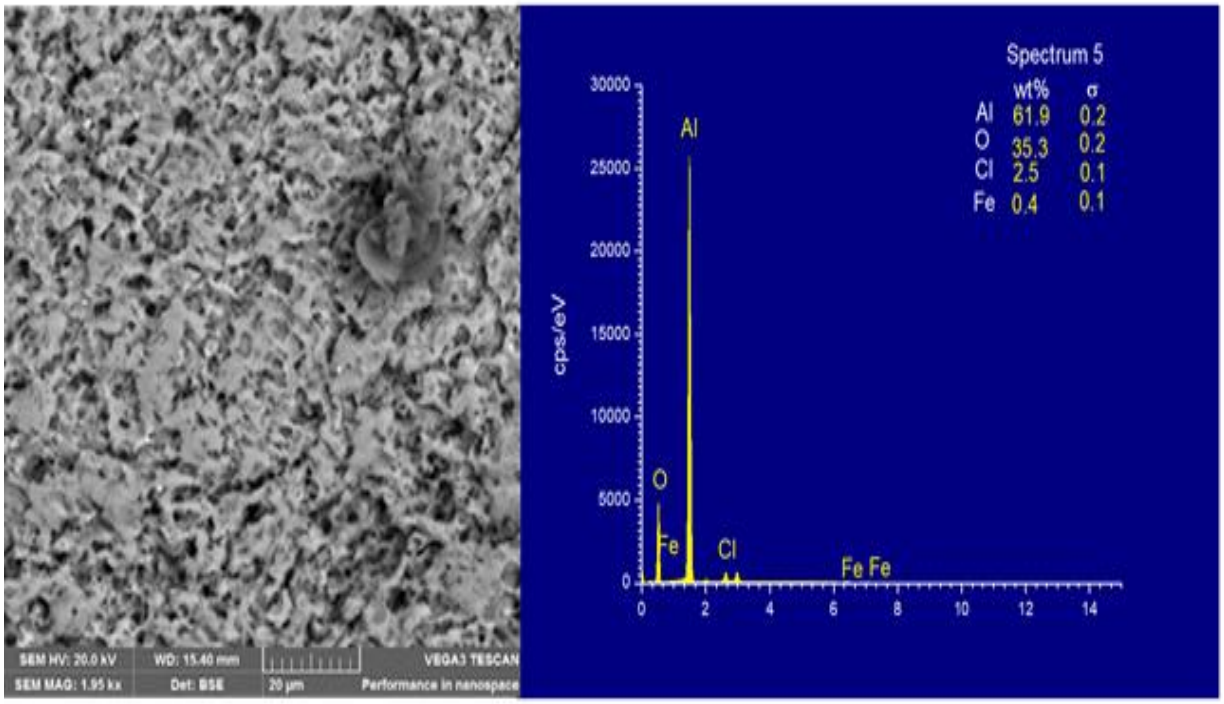

Figure 4. 35: SEM micrograph and aluminium EDS spectrum in 1.0 M HCl solution.

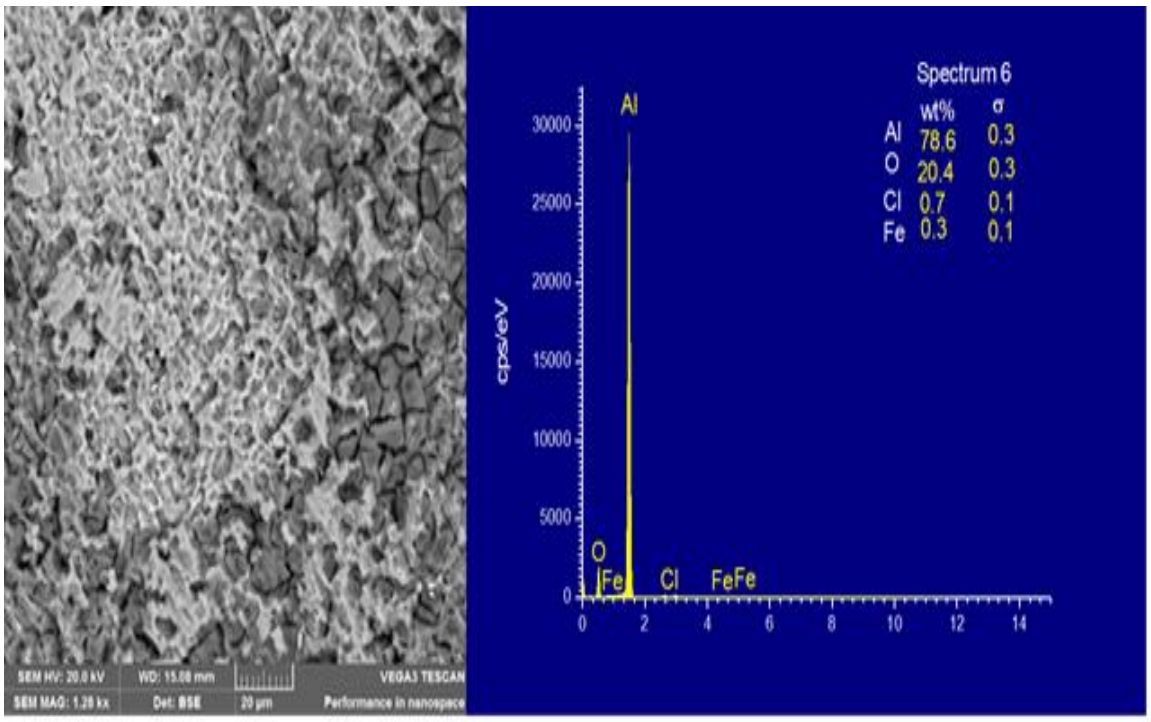

Figure 4. 36: SEM micrograph and EDS spectrum of aluminium in 1.0 M HCl and glycerol stearate inhibitor.

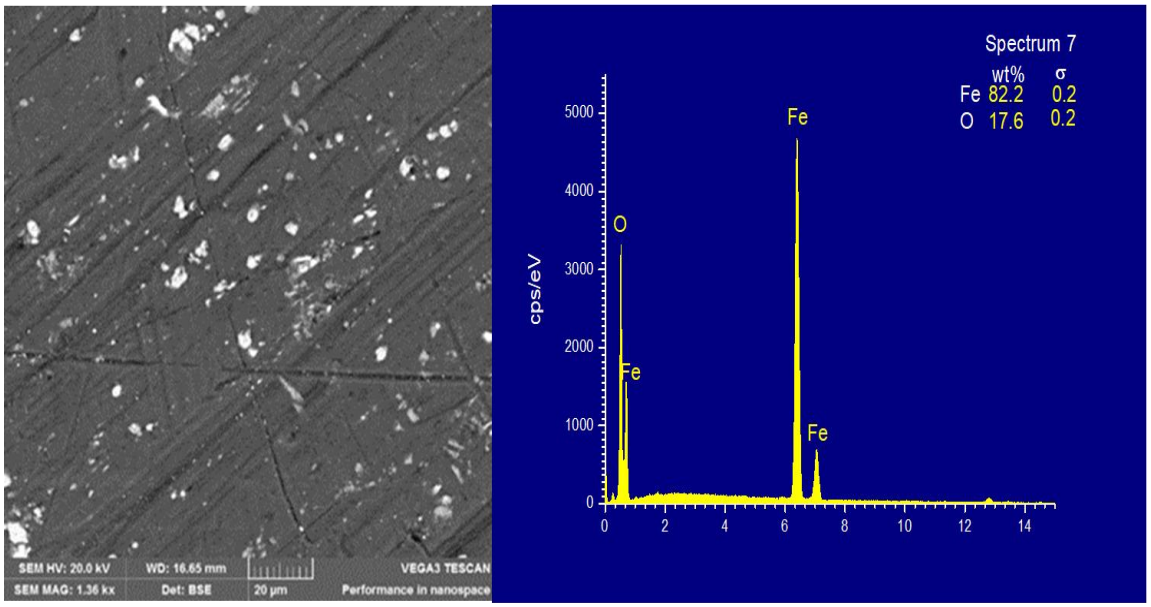

Figure 4. 37: SEM micrograph and EDS spectrum of pristine mild steel.

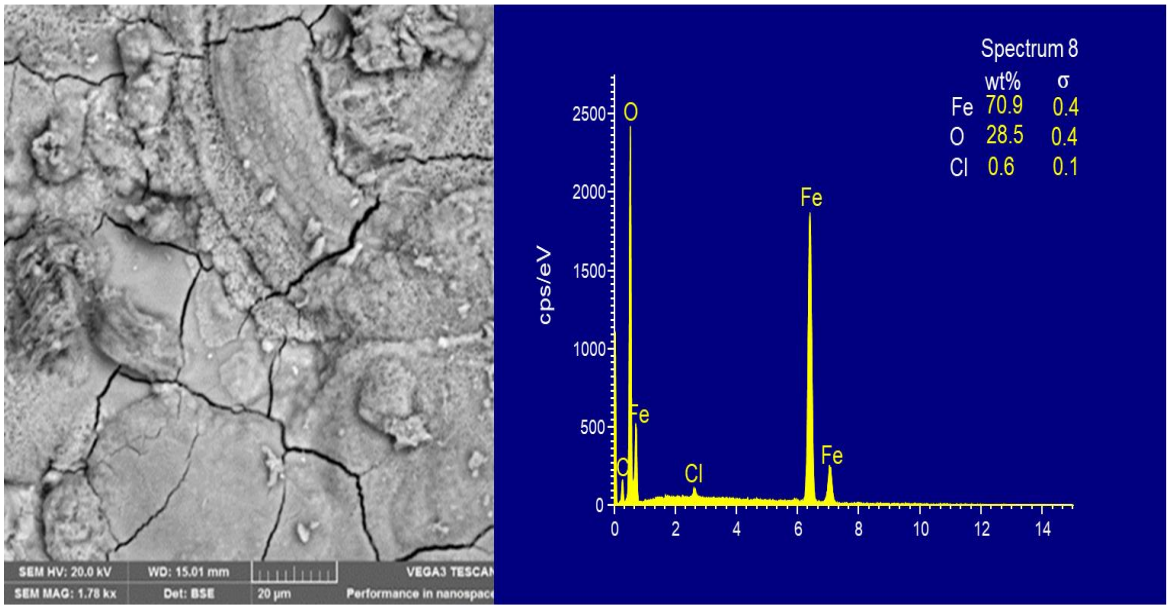

Figure 4. 38: SEM micrograph and mild steel EDS spectrum in 1.0 M HCl solution.

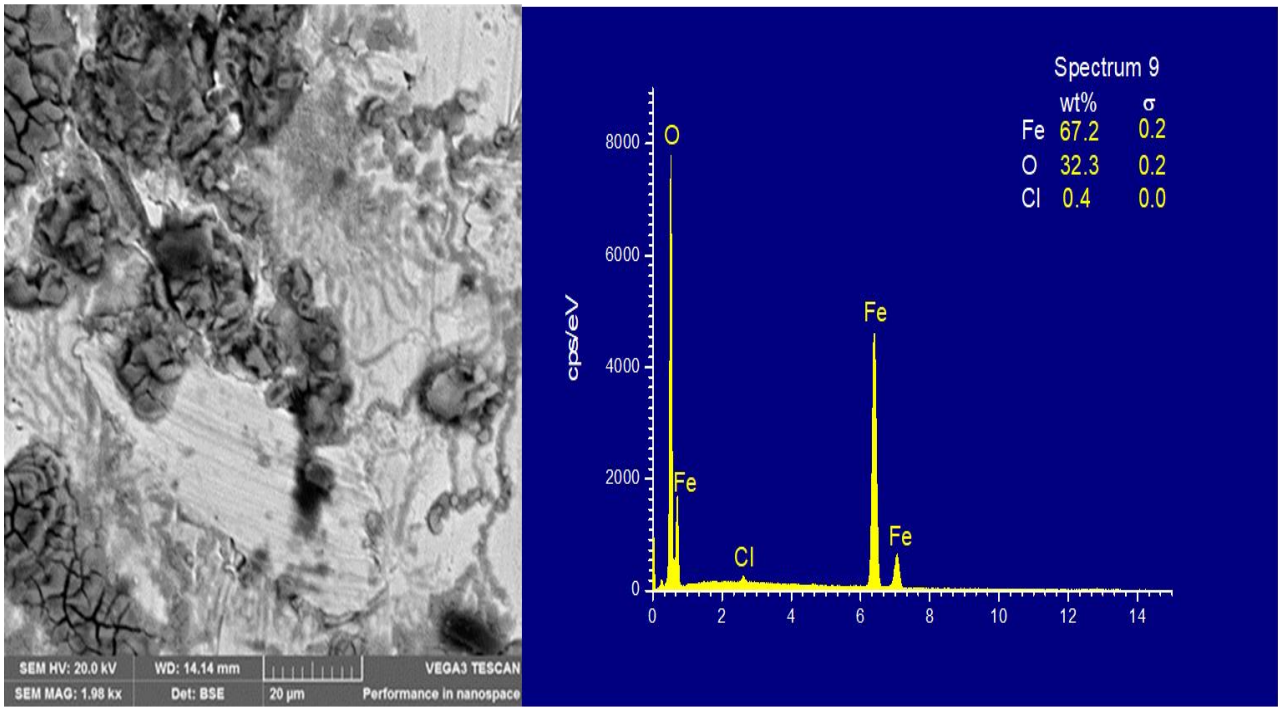

Figure 4. 39: SEM micrograph and EDS spectrum of mild steel in 1.0 M HCl and glycerol stearate inhibiton.

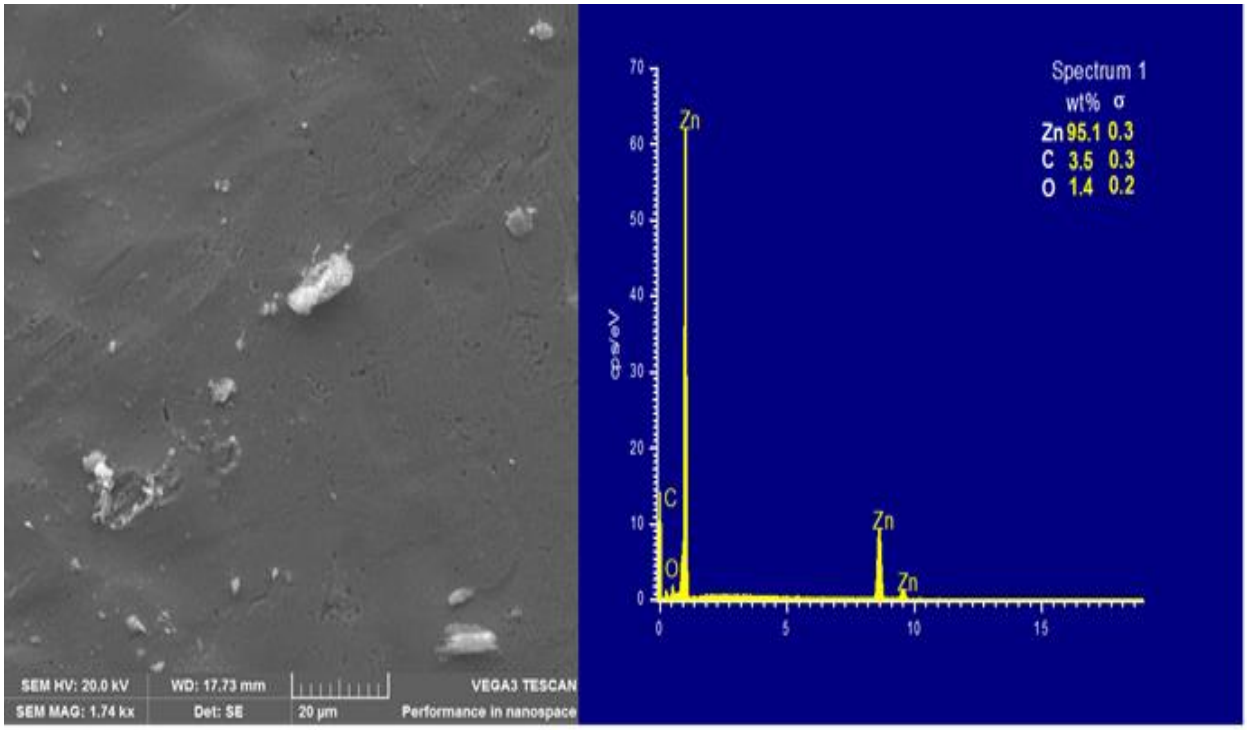

Figure 4. 40 **:** SEM micrograph and EDS spectrum of pristine zinc.

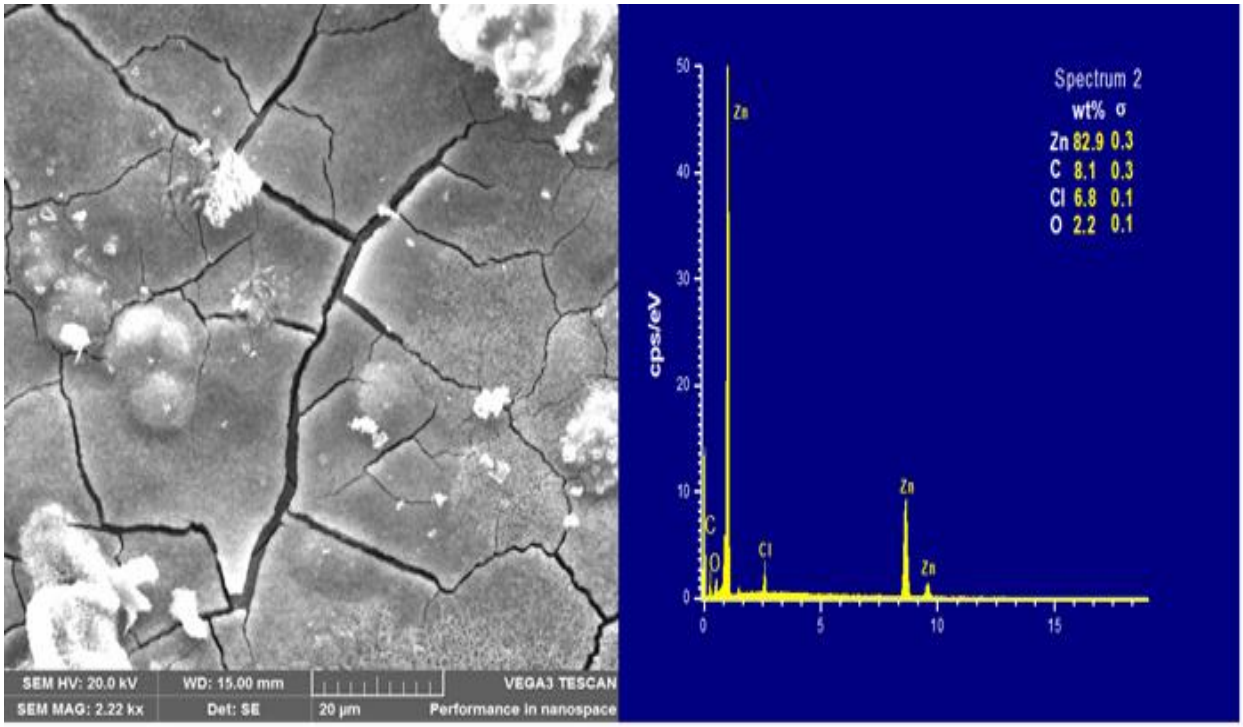

Figure 4. 41: SEM micrograph and EDS spectrum of zinc in 1.0 M HCl.

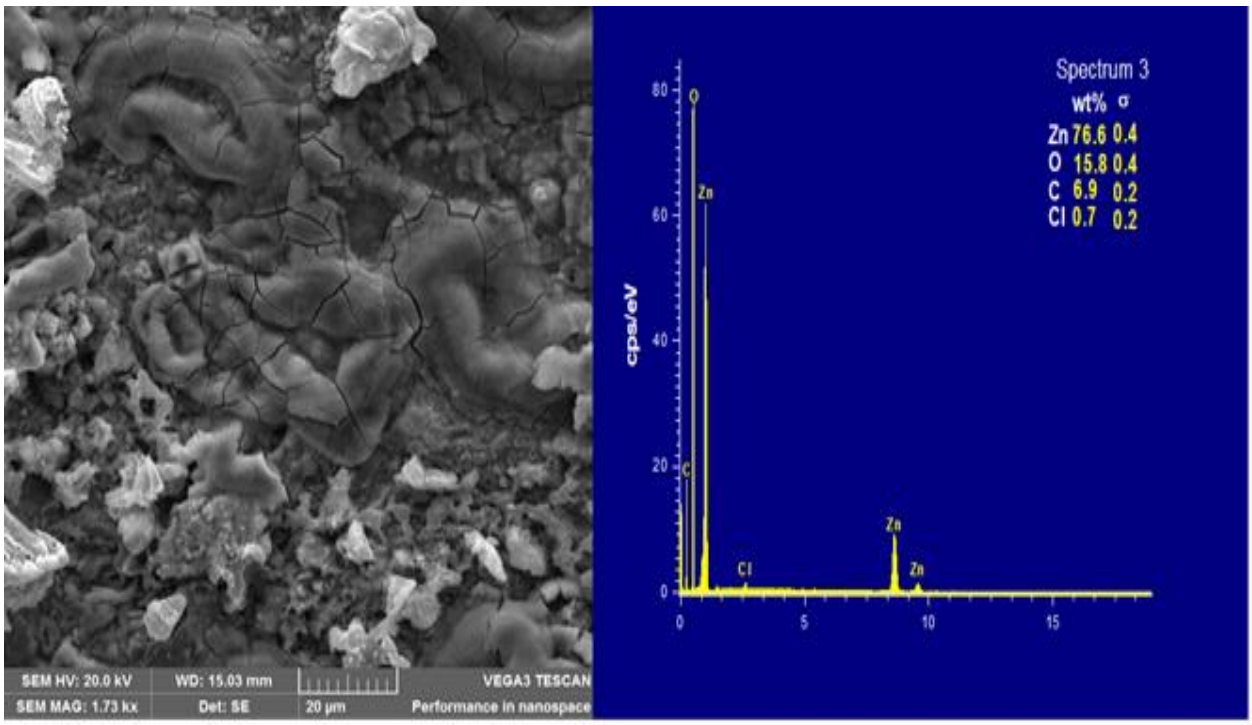

Figure 4. 42: SEM micrograph and EDS spectrum of zinc in 1.0 M HCl and glycerol stearate inhibiton.

4.5. DENSITY FUNCTIONAL THEORY (DFT)

The data collected from weight loss measurements and electrochemical techniques were further substantiated with chemical quantum calculations which played an essential role in studying the reactivity and selectivity parameters of glycerol stearate as the inhibitor molecule in this study [195]. There need to study the inhibitor's reactivity and selectivity emanate due to different regions within the inhibitor which interact with the metal surface. There are ample electronic properties on which the reactivity of the inhibitor depends, such as dipole moment, partial charges, and electronic density to mention few. In addition, the nature of functional groups within the inhibitor influences the electronic properties. In Figure 4.43, displayed is the schematic representation and optimised geometry of glycerol stearate with the atom numbering used in this study. Reason why the geometry of the inhibitor is of outmost importance is due to the dependence of the inhibition efficiency on the geometry of the

inhibitor molecule. Among many, inhibitor compounds with planar geometry are most preferred due to their inhibition efficiencies as compared to non-planar geometries [196]. This is due to high possibility of a planar inhibitor molecule to result in a larger surface coverage on the metal surface through the inhibitor's most reactive atomic sites.

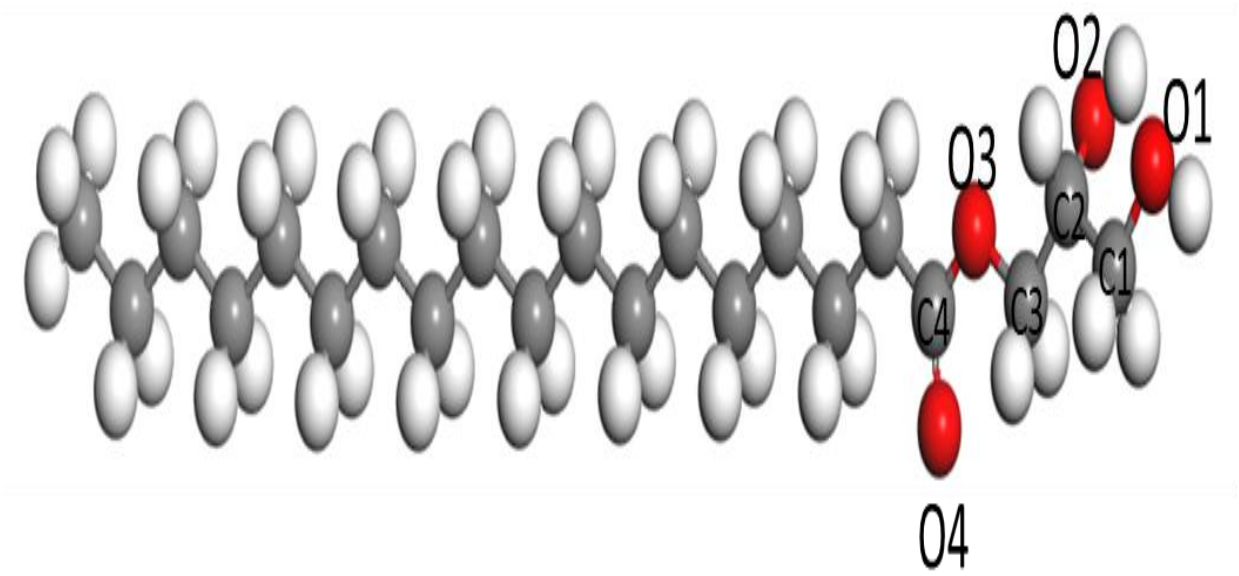

Figure 4. 43: The optimised geometry and the atom numbering of the studied glycerol stearate.

Through the analysis of the Highest Occupied Molecular Orbital (HOMO) and the Lowest Unoccupied Molecular Orbital (LUMO) the reactive sites of glycerol stearate can be studied. Furthermore, the study of reactivity parameters such as the HOMO energy (E_{HOMO}), the LUMO energy (E_{LUMO}), global softness (σ), global hardness (η), electron affinity (EA), ionisation potential (IP) and electronegativity (χ). The reactive sites of glycerol stearate can be studied using the Highest Occupied Molecular Orbital (HOMO) and the Lowest Unoccupied Molecular Orbital (LUMO). In addition, the investigation of reactivity parameters such as the HOMO energy (E_{HOMO}), the LUMO energy (E_{LUMO}), global softness (σ), global hardness (η), electron affinity (EA),

ionisation potential (IP), and electronegativity (χ) was done. In Figure 4.44 and Figure 4.45, shown are the HOMO and LUMO of the studied glycerol stearate respectively.

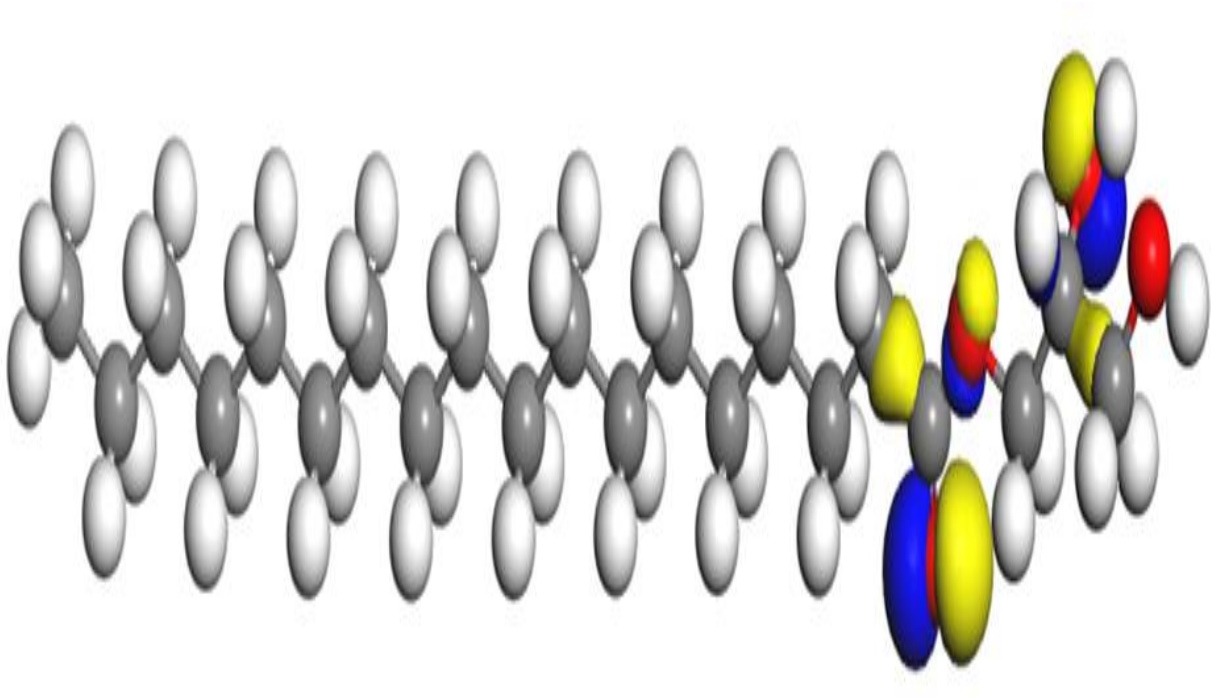

Figure 4. 44: Relaxed geometries and HOMO (isosurface generation isovalue = 0.05) of glycerol stearate.

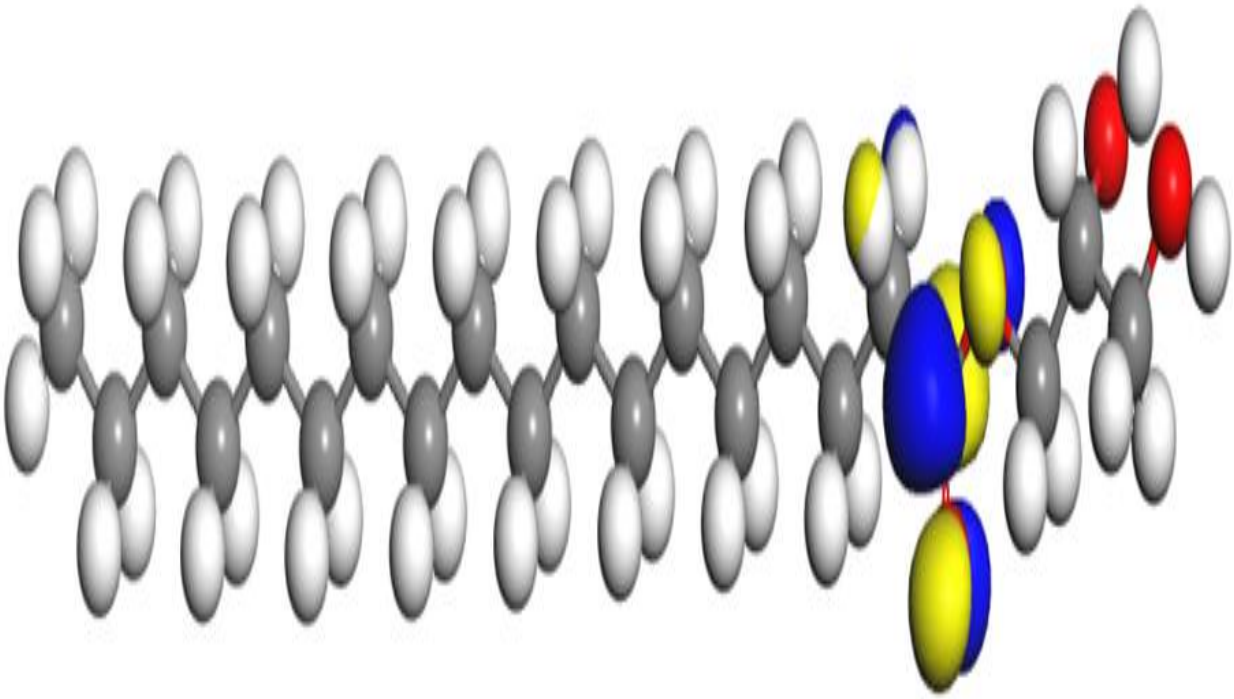

Figure 4. 45: Relaxed geometries and LUMO (isosurface generation isovalue = 0.05) isosurfaces of glycerol stearate.

The area where electrophilic attack is mostly emanating is at the HOMO while the area where the nucleophilic attack is likely to occur from the LUMO [197]. From this study, the highest HOMO densities of glycerol stearate occur at carbon atoms on C1, C2, C3, C4, on hydroxide oxygen atoms (O1 and O2), on the ether functional group O3 and lastly on the carbonyl O4. Since the LUMO densities entails information concerning the nucleophilic attack, however, this is mainly applicable provided the metal surface back donates electrons to glycerol stearate.

Table 4.16 shows the molecular quantum chemical parameters which relate with the reactivity of glycerol stearate used in this study. The parameters included are E_{HOMO}, E_{LUMO}, the energy gap (ΔE), among others. The interactions between the HOMO and LUMO of reacting glycerol stearate is responsible for electron transition between the metal-inhibitor interfaces and this was informed by Frontier Molecular Orbital Theory (FMO) [198]. In addition, at the E_{HOMO} glycerol stearate donate electrons to the empty d-orbital of the metal, thus higher E_{HOMO} values are appreciated since they cater for

the electron deficient species according to studies [199]. Furthermore, chemical compound possessing higher E_{HOMO} values show appreciable inhibition efficiencies and enhances an effective adsorption process at the metal-inhibitor interface [200].

Table 4. 16: Molecular quantum chemical parameters.

Molecular Property	**Inhibitor Compound**
	GS
EHOMO (eV)	-5.470
ELUMO (eV)	-0.067
ΔE (eV)	5.403
η	2.702
σ	0.370
I (eV)	5.470
A (eV)	0.067
ω	1.419
χ	2.769

The degree to which a chemical compound can receive electrons is shown by E_{LUMO} values. Lower E_{LUMO} values show a high probability to which a compound can accept electrons from some electron rich chemical species [201]. Further information with regards to glycerol stearate reactivity, it is through the study of the energy gap. From ΔE, the stability and reactivity of the inhibitor molecule can be studied. Thus, higher ΔE value is associated with high stability and less reactivity, meanwhile lower ΔE value associates with low stability and more reactive to other species [202]. Regarding the polarity of the molecule a dipole moment is studied. In addition, from other projects dipole moments were reported to increase with increasing inhibition efficiencies meanwhile in other reports a different trend was observed [203]. The other crucial reactivity parameter shown in Table 4.16 is the electronegativity (χ) which gives information regarding the electron density and the ability of an electron or atom to

attract more electrons to itself [204]. The complementing parameter to electronegativity is global electrophilicity index (ω), chemical inhibitor with higher ω value are named good electrophiles meanwhile those with lower ω value are named good nucleophiles [205]. Furthermore, information regarding the resistance of an atom to charge transfer is given by global hardness (η) and higher η values signify a higher resistance for the inhibitor to transfer charge to the metal surface. Thus, inhibitors with a lower η value are mostly appreciated as this will enhance a better adsorption process at the metal-inhibitor interface. Global softness is denoted by σ which relates to the softness of the inhibitor compound and at the highest σ inhibitor region an enhanced inhibitor-metal adsorption is observed [195]. Electron affinity (A) reveals an electron deficiency region hence it associates with the E_{LUMO}. Moreover, another crucial molecular reactivity parameter is ionisation potential (I) which reveals the amount of energy required to remove an electron from the molecule [187] and this is helpful in investigating the amount of energy it takes reactive atoms within glycerol stearate to transfer electrons to then metal's empty orbital.

CHAPTER FIVE

GENERAL DISCUSSION, CONCLUSIONS AND RECOMMENDATIONS

5.1. GENERAL DISCUSSION AND CONCLUSIONS

In this research, inhibition efficiencies of aluminium, mild steel, and zinc in 1. 0 M HCl by glycerol stearate was evaluated. This research was initiated in a quest to find an alternative method that is environmentally user friendly. This compound is nontoxic, biodegradable and it does not show signs of bioaccumulation. Its ecofriendly chemical nature elevates it to be evaluated as a corrosion inhibitor in line with all the aspects of green chemistry. It is readily available and well priced, and its application did not seem to react with the surrounding chemicals or ambient air to produce more toxic exudants. The efficiency of glycerol stearate as a corrosion inhibitor was researched by exploiting the following scientific techniques viz, gravimetric analysis, electrochemical techniques (potentiodynamic polarisation and electrochemical impedance), computational studies and visual comparison.

5.1.1. Visual comparison

i. From Figures 4.1-4.5 which displays the rate of corrosion of aluminium with passage of time it was clear that this was comparable throughout when either the inhibitor is used or not. There was no clear distinction of the one with the inhibitor or not. There was however a tinge of discolourisation after a year for one without the inhibitor.

ii. The results from mild steel evaluation as displayed from Figures 4.12-4.15 showed a clear level of deterioration of mild steel (without inhibitor) as compared to the one with the inhibitor. The rusting process showed its intensity with the progression of time. After a year the mild steel treated with the inhibitor was still intact with no visible signs of deterioration. In this case we will accept the hypothesis that glycerol stearate slows down or inhibits corrosion within a specified period. This

was further emphasised through Figure 4.15 (a) and Figure 4.15 (b) respectively.

iii. From Figures 4.22-4.25 there was a clear indication of rusting with progression of time mostly for zinc without inhibitor. At 6 months the one not treated with glycerol stearate had started showing signs of significant deterioration while the treated one remained intact and maintaining its original colour. After a year there was almost complete deterioration for the untreated one.

5.1.2. Gravimetric analysis

Gravimetric analysis is the easiest way to track the deterioration percentage versus time. The loss of some components of the material through corrosion can be computed to quantify the level of deterioration. The greater the mass loss the greater the deterioration.

i. In Table 4.2, Table 4.7 and Table 4.12 which are for aluminium, mild steel and zinc respectively, it was observed that $\Delta G°_{ads}$ values for GS inhibitor were less than -20 kJ.mol^{-1} for all metals in a negative direction, which indicated a physisorption mechanism of adsorption. The values of $\Delta G°_{ads}$ between -20 kJ.mol^{-1} and -40 kJ. mol^{-1} signify a mixed type of adsorption mechanism and $\Delta G°_{ads}$ of -40 kJ. mol^{-1} and more in a negative direction accounts for a chemisorption adsorption mechanism [163–165].

ii. In this study, positive values of $\Delta H°_{ads}$ were obtained for aluminium, mild steel and zinc which revealed that the corrosion of metals occurred via endothermic reaction as shown in Tables 4.3, 4.8 and 4.13. Figures 4.6 (d), 4.16 (d) and 4.26 (d) corroborate results for aluminium, mild steel and zinc as displayed in Tables 4.3, 4.8 and 4.13.

iii. The values of $\Delta S°$ for aluminium were observed to be positive and increasing as the inhibitor concentration increased which implies that there was an increase in disorder as inhibitor molecules were desorbing water molecules from the metal surface as shown in Table 4.3 and

Figure 4.6 (d). Furthermore, negative ΔS° values for both mild steel and zinc in the presence of the inhibitor concentrations were observed as shown from Table 4.8 and Table 4.13. This behavior is due to a decrease in disorderliness as a corrosion reaction proceeds from reactants into products upon the rate determining step which is associative instead of dissociative. Figures 4.16 (d) and 4.26 (d) are substantiating and confirming what has been given from Tables 4.8 and 4.13.

iv. The activation energy values for aluminium, mild steel and zinc were observed to be higher and increasing in the inhibited solutions than the uninhibited solutions which implies that indeed an activated complex which is akin to an adsorptive film has formed by the inhibitor molecules as shown in Tables 4.3, 4.8 and 4.13, this has been confirmed from Figures 4.6 (c), 4.16 (c) and 4.26 (c).

v. The percentage inhibition efficiencies for aluminium, zinc and mild steel were observed to increase by roughly +/- 2% as the inhibitor concentration increased with decreasing corrosion rates as shown in Tables 4.1, 4.6 and 4.11 and further confirmed from Figures 4.6 (a), 4.16 (a) and 4.26 (a).

vi. For all metals as derived from the Tables 4.2, 4.7 and 4.12 the isotherm followed is Langmuir. These Tables are constructed from Figures 4.6 (b), 4.16 (b) and 4.26 (b).

5.1.3. Electrochemical techniques

Tafel plots displayed as Figures 4.7, 4.17 and 4.27 showed that glycerol stearate behaved as mixed-type inhibitor due to the fact that corrosion potential difference of the uninhibited and inhibited systems was found to be less than 85 mV as shown in Tables 4.4, 4.9 and 4.14 [181]. From electrochemical impedance spectroscopy data displayed in Tables 4.5, 4.10 and 4.15 for aluminium, mild steel, and zinc respectively, double layer capacitances values decreased as compared to the blank solution when glycerol stearate was introduced. For example, as the inhibitor concentrations increased from 10×10^{-5} M, 30×10^{-5} M and 50×10^{-5} M the double layer capacitances

decreased from 60.24 x 10^{-6} F, 59.71 x 10^{-6} F and 45.05 x 10^{-6} F respectively for aluminium metal. This was the trend for mild steel and zinc as shown in Tables 4.10 and 4.15. This trend was explained based on the adsorption of glycerol stearate on aluminium, mild steel and zinc surfaces and was as a result of a decrease in water electric constant thus increasing the double layer capacitance.

5.1.4. Adsorption film studies (FTIR)

Fourier transform infrared (FTIR) spectra of glycerol stearate as compared to adsorption films formed on aluminium, mild steel and zinc surfaces there were disappearances of some functional groups such as the -OH stretching, -OH bending and -C-O at 3307 cm^{-1}, 3241 cm^{-1} and 1750 cm^{-1} respectively owing to successful adsorption of glycerol stearate on aluminium, mild steel and zinc with the emergence of new bands especially for aluminium such as Al-OH at 1250 cm^{-1} and Al-O at 1062.5 cm^{-1}.

5.1.5. Morphological studies

Figures 4.36, 4.39 and 4.42 are scanning electron microscopy results that show the adsorptive layer formed by glycerol stearate. The corrosion inhibition of aluminium, mild steel and zinc metal occurs through the pathway whereby metal acidic solution interface is deprived sufficient direct contact. This prevents oxidation of the metal by creating a barrier that prevents loss of electrons. This barrier prevents the flow of electrons from the metal to the oxidising agent.

5.1.6. Computational studies

Computational studies are employed to reveal the specific points at which the corrosion inhibitor will attach on the surface of the metal. As a result, this will give its selectivity and reactivity based on the ideal site of attachment. The reactivity is dictated upon by the site of attachment which is based on whether the reaction is endothermic or exothermic. This then leads to the rate at which corrosion will proceed with ease without external input of energy. The highest densities of HOMO for glycerol stearate occurred at carbon atoms on C1, C2, C3, C4, on hydroxide oxygen atoms (O1 and

O2), on the ether functional group O3 and lastly on the carbonyl O4 as shown in Figures 4.43 and 4.44.

OVERALL CONCLUSION

In view of all the data accumulated one can now reach a conclusion about the performance of glycerol stearate as a corrosion inhibitor. This is derived from the series of results such as gravimetric analysis, electrochemical techniques, computational studies, adsorption film studies, and morphological studies. From computation of the results, it was determined that the optimum corrosion inhibition efficiencies for aluminium metal from gravimetric analysis, potentiodynamic polarisation and electrochemical impedance spectroscopy were 98.51%, 81.06% and 86.18% respectively with the average 88.58%. In addition, for mild steel the optimum corrosion inhibition efficiencies were from gravimetric analysis, potentiodynamic polarisation and electrochemical impedance spectroscopy were 92.54%, 82.69% and 75.44% respectively with the average value of 83.56%. The optimum corrosion inhibition efficiency value obtained for zinc metal from gravimetric analysis, potentiodynamic polarisation and electrochemical impedance spectroscopy were 73.13%, 71.05% and 89.50% rescpectively with the average value of 77.89%. From the calculated percentages it is safe to conclude that the inhibition of corrosion by glycerol stearate on selected metals was succesful. The corrosion inhibition percentages and the fact that glycerol stearate is nontoxic, does not form new poisonous material as it associates with the metals, it is economical and abundantly available renders it an ideal corrosion inhibitor. The pathway and its effectiveness align it very well with green technology as a quest for environmental care and rehabilitation.

5.2. RECOMMENDATIONS FOR FUTURE WORK

Firstly, addition of nano material and electron donating functional groups to glycerol stearate can improve its inhibition efficiency in preventing corrosion of the aluminium, mild steel and zinc. In addition, introducing functional groups on glycerol stearate will improve its solubility. Secondly, a suitable solvent for the solubility of glycerol stearate

should be investigated. Furthermore, it will be worthy for other metals to be considered for corrosion testing other than aluminium, mild steel and zinc, in this way the optimum performance of glycerol stearate will be shown vividly. Quest for glycerol stearate derivatives is of paramount importance in order to run quantitative structure activity relationship with the aid of chemical quantum parameters such as dipole moment and many more.

REFERENCES

[1] Fayomi OS, Akande IG, Odigie S. Economic impact of corrosion in oil sectors and prevention: an overview. J Phys Conf Ser 2019;2:p. 022037. doi:10.1088/1742-6596/1378/2/022037

[2] Hakem M, Lebaili S, Mathieu S, Miroud D, Lebaili A, Cheniti B. Effect of microstructure and precipitation phenomena on the mechanical behavior of AA6061-T6 aluminum alloy weld. Int J Adv Manuf Technol 2019 1029 2019;102:2907–18. https://doi.org/10.1007/S00170-019-03401-1.

[3] Miao T. Nacre-like Aluminium Alloy Composite Plates for Ballistic Impact Applications 2019.

[4] Pesha T (Dissertation University of Limpopo 2018). Phthalocyanine compounds as corrosion inhibitors for metals in corrosive environment.

[5] Bueno AHS, Moreira ED, Gomes JACP. Evaluation of stress corrosion cracking and hydrogen embrittlement in an API grade steel. Eng Fail Anal 2014;36:423–31. https://doi.org/10.1016/J.ENGFAILANAL.2013.11.012.

[6] Muniandy MT, Rahim AA, Osman H, Shah AM, Yahya S, Raja PB. Investigation of some schiff bases as corrosion inhibitors for aluminium alloy in 0.5 m hydrochloric acid solutions. Http://DxDoiOrg/101142/S0218625X11014564 2012;18:127–33. https://doi.org/10.1142/S0218625X11014564.

[7] Tourabi M, Nohair K, Traisnel M, Jama C, Bentiss F. Electrochemical and XPS studies of the corrosion inhibition of carbon steel in hydrochloric acid pickling solutions by 3,5-bis(2-thienylmethyl)-4-amino-1,2,4-triazole. Corros Sci 2013;75:123–33. https://doi.org/10.1016/J.CORSCI.2013.05.023.

[8] Ansari KR, Quraishi MA, Singh A. Schiff's base of pyridyl substituted triazoles as new and effective corrosion inhibitors for mild steel in hydrochloric acid solution. Corros Sci 2014;79:5–15. https://doi.org/10.1016/j.corsci.2013.10.009.

[9] Raja PB, Ismail M, Ghoreishiamiri S, Mirza J, Ismail MC, Kakooei S, Rahim AA. Reviews on Corrosion Inhibitors: A Short View. Http://DxDoiOrg/101080/009864452016l172485 2016;203:1145–56. https://doi.org/10.1080/00986445.2016.1172485.

[10] Kuzmin SM, Filimonova YA, Chulovskaya SA, Parfenyuk VI. Morphology/potential-dependent electrochromic behaviour of

poly(Hydroxyphenyl porphyrin) films. Mater Chem Phys 2022;275:125214. https://doi.org/10.1016/J.MATCHEMPHYS.2021.125214.
[11] Usher KM, Kaksonen AH, Bouquet D, Cheng KY, Geste Y, Chapman PG, Johnston CD. The role of bacterial communities and carbon dioxide on the corrosion of steel. Corros Sci 2015;98:354–65. https://doi.org/10.1016/J.CORSCI.2015.05.043.
[12] Dorin T, Ramajayam M, Mester K, Rouxel B, Lamb J, Langan TJ. The effect of scandium and zirconium on the microstructure, mechanical properties and formability of a model Al–Cu alloy. Miner Met Mater Ser 2018;Part F4:1595–9. https://doi.org/10.1007/978-3-319-72284-9_208/COVER.
[13] Determination of the chemical mechanism of chromate conversion coating on magnesium alloys EV31A - ScienceDirect n.d. https://www.sciencedirect.com/science/article/pii/S0169433214002141?casa_token=6DKaoGFgCDQAAAAA:hpPHKWe494GK-fqF__bBt4aA8_Cudsacc1QM5bxZiyNeza7OHUdOuHtapTKyfdsabbaM4cOo1QU (accessed October 11, 2022).
[14] Delgado A, Briciu-Burghina C, Regan F. Antifouling Strategies for Sensors Used in Water Monitoring: Review and Future Perspectives. Sensors 2021, Vol 21, Page 389 2021;21:389. https://doi.org/10.3390/S21020389.
[15] Hu RG, Zhang S, Bu JF, Lin CJ, Song GL. Recent progress in corrosion protection of magnesium alloys by organic coatings. Prog Org Coatings 2012;73:129–41. https://doi.org/10.1016/J.PORGCOAT.2011.10.011.
[16] Muthukumar P, Kim HS, Jeong JW, Son YA. Synthesis and characterization of tetra phenoxy-substituted halogen-rich metallophthalocyanine derivatives: A study on their LCD color filter requirements. J Mol Struct 2016;1119:325–31. https://doi.org/10.1016/J.MOLSTRUC.2016.05.007.
[17] El-Shamy AM, Shehata MF, Ismail AIM. Effect of moisture contents of bentonitic clay on the corrosion behavior of steel pipelines. Appl Clay Sci 2015;114:461–6. https://doi.org/10.1016/J.CLAY.2015.06.041.
[18] Ağrtaş MS, Gümüş S. Synthesis, Characterization, and Theoretical Studies on Some Metallophthalocyanines With Octakis Phenoxyacetamide Substituents. Http://DxDoiOrg/101080/155331742012749897 2013;43:628–34. https://doi.org/10.1080/15533174.2012.749897.
[19] Ogunsipe AO, Ogoko EC, Abiola OK. Corrosion Inhibition of Aluminium in 1.0 M HCl by Zinc Phtalocyanine Sulfonate. J Chem Soc Niger 2020;45:533–9.
[20] Bammou L, Belkhaouda M, Salghi R, Benali O, Zarrouk A, Zarrok H, Hammouti B. Corrosion inhibition of steel in sulfuric acidic solution by the Chenopodium Ambrosioides Extracts. J Assoc Arab Univ Basic Appl Sci 2014;16:83–90. https://doi.org/10.1016/J.JAUBAS.2013.11.001.
[21] Sovizi MR, Abbasi R. Effect of carboxymethyl cellulose on the corrosion behavior of aluminum in H2SO4 solution and synergistic effect of potassium iodide. Https://DoiOrg/101080/0169424320201717803 2020;34:1664–78. https://doi.org/10.1080/01694243.2020.1717803.
[22] Aslam R, Mobin M, Aslam J, Aslam A, Zehra S, Masroor S. Application of surfactants as anticorrosive materials: A comprehensive review. Adv Colloid Interface Sci 2021;295:102481. https://doi.org/10.1016/J.CIS.2021.102481.

[23] Salunkhe PB, Jaya Krishna D. Investigations on latent heat storage materials for solar water and space heating applications. J Energy Storage 2017;12:243–60. https://doi.org/10.1016/J.EST.2017.05.008.
[24] Heydari M, Javidi M. Corrosion inhibition and adsorption behaviour of an amido-imidazoline derivative on API 5L X52 steel in CO2-saturated solution and synergistic effect of iodide ions. Corros Sci 2012;61:148–55. https://doi.org/10.1016/J.CORSCI.2012.04.034.
[25] Poomathi N, Perumal PT, Ramakrishna S. An efficient and eco-friendly synthesis of 2-pyridones and functionalized azaxanthone frameworks via indium triflate catalyzed domino reaction. Green Chem 2017;19:2524–9. https://doi.org/10.1039/C6GC03440C.
[26] Tian Y, Amal R, Wang DW. An aqueous metal-ion capacitor with oxidized carbon nanotubes and metallic zinc electrodes. Front Energy Res 2016;4:34. https://doi.org/10.3389/FENRG.2016.00034/BIBTEX.
[27] Eaves DR. A study of novel filiform corrosion phenomena on hot dip organically coated Zn-AI-M g steel n.d.
[28] Deyab MA. Electrochemical investigations on pitting corrosion inhibition of mild steel by provitamin B5 in circulating cooling water. Electrochim Acta 2016;202:262–8. https://doi.org/10.1016/J.ELECTACTA.2015.11.075.
[29] Abiola OK, James AO. The effects of Aloe vera extract on corrosion and kinetics of corrosion process of zinc in HCl solution. Corros Sci 2010;52:661–4. https://doi.org/10.1016/J.CORSCI.2009.10.026.
[30] Metallurgy and Corrosion Control in Oil and Gas Production - Robert Heidersbach - Google Books n.d. https://books.google.co.za/books?hl=en&lr=&id=IjpqDwAAQBAJ&oi=fnd&pg=PP13&dq=crevices+accelerate+corrosion+since+it+makes+chemical+environment+to+store+moisture,+this+type+of+corrosion+is+also+known+for+trapping+pollutants+and+concentrates+the+corrosion+products+with+the+exclusion+of+oxygen+&ots=c0d-6W59Ut&sig=WnydJb0hGVZRxohkHIenVNXDQBg&redir_esc=y#v=onepage&q&f=false (accessed October 12, 2022).
[31] Li K, Li X, Zhao Y, Wang K, Song S, Jin W, Xia D, Xu Y, Huang Y. Influence of Partial Rust Layer on the Passivation and Chloride-Induced Corrosion of Q235b Steel in the Carbonated Simulated Concrete Pore Solution. Met 2022, Vol 12, Page 1064 2022;12:1064. https://doi.org/10.3390/MET12071064.
[32] Alabbas FM, Bhola R, Spear JR, Olson DL, Mishra B. Electrochemical Characterization of Microbiologically Influenced Corrosion on Linepipe Steel Exposed to Facultative Anaerobic Desulfovibrio sp. Int J Electrochem Sci 2013;8:859–71.
[33] Abdolahi A, Hamzah E, Ibrahim Z, Hashim S. Microbially influenced corrosion of steels by Pseudomonas aeruginosa. Corros Rev 2014;32:129–41. https://doi.org/10.1515/CORRREV-2013-0047/MACHINEREADABLECITATION/RIS.
[34] Xu D, Li Y, Gu T. Mechanistic modeling of biocorrosion caused by biofilms of sulfate reducing bacteria and acid producing bacteria. Bioelectrochemistry 2016;110:52–8. https://doi.org/10.1016/J.BIOELECHEM.2016.03.003.

[35] Moore S, Burrows R, Kumar D, Kloucek MB, Warren AD, Flewitt PEJ, Picco L, Payton OD, Martin TL. Observation of stress corrosion cracking using real-time in situ high-speed atomic force microscopy and correlative techniques. Npj Mater Degrad 2021 51 2021;5:1–10. https://doi.org/10.1038/s41529-020-00149-y.
[36] Zhang X, Zhou X, Nilsson JO. Corrosion behaviour of AA6082 Al-Mg-Si alloy extrusion: The influence of quench cooling rate. Corros Sci 2019;150:100–9. https://doi.org/10.1016/J.CORSCI.2019.01.030.
[37] Guo MX, Du JQ, Zheng CH, Zhang JS, Zhuang LZ. Influence of Zn contents on precipitation and corrosion of Al-Mg-Si-Cu-Zn alloys for automotive applications. J Alloys Compd 2019;778:256–70. https://doi.org/10.1016/J.JALLCOM.2018.11.146.
[38] Singh SM. Corrosion Behavior of Calcium Containing 5xxx/6xxx Aluminum Alloys n.d.
[39] Pournazari S. Corrosion behavior of B206 aluminum-copper casting alloy in seawater environment : electrochemical and microstructural studies 2018. https://doi.org/10.14288/1.0365752.
[40] Wan S, Dong ZH, Guo X. Investigation on initial atmospheric corrosion of copper and inhibition performance of 2-phenyl imidazoline based on electrical resistance sensors. Mater Chem Phys 2021;262:124321. https://doi.org/10.1016/J.MATCHEMPHYS.2021.124321.
[41] Yang M, Kainuma S, Ishihara S, Kaneko A, Yamauchi T. Atmospheric corrosion protection method for corroded steel members using sacrificial anode of Al-based alloy. Constr Build Mater 2020;234:117405. https://doi.org/10.1016/J.CONBUILDMAT.2019.117405.
[42] George JS, Vijayan P P, Paduvilan JK, Salim N, Sunarso J, Kalarikkal N, Hameed N, Thomas S. Advances and future outlook in epoxy/graphene composites for anticorrosive applications. Prog Org Coatings 2022;162:106571. https://doi.org/10.1016/J.PORGCOAT.2021.106571.
[43] Lamani AR, Jayanna HS, Prasanna GD, Naveen CS. Characterization and Electrical Conductivity of Electron Beam Irradiated Metal Phthalocyanine Complexes 2015;1:1–7. https://doi.org/10.12723/mjs.32.1.
[44] Höche D. Simulation of Corrosion Product Deposit Layer Growth on Bare Magnesium Galvanically Coupled to Aluminum. J Electrochem Soc 2015;162:C1–11. https://doi.org/10.1149/2.0071501JES/XML.
[45] Wei L, Liu Y, Li Q, Cheng YF. Effect of roughness on general corrosion and pitting of (FeCoCrNi)0.89(WC)0.11 high-entropy alloy composite in 3.5 wt.% NaCl solution. Corros Sci 2019;146:44–57. https://doi.org/10.1016/J.CORSCI.2018.10.025.
[46] Zhang R, Castel A, François R. Concrete cover cracking with reinforcement corrosion of RC beam during chloride-induced corrosion process. Cem Concr Res 2010;40:415–25. https://doi.org/10.1016/J.CEMCONRES.2009.09.026.
[47] RAO ACU, VASU V, GOVINDARAJU M, SRINADH KVS. Stress corrosion cracking behaviour of 7xxx aluminum alloys: A literature review. Trans Nonferrous Met Soc China 2016;26:1447–71. https://doi.org/10.1016/S1003-6326(16)64220-6.

[48] Xu Y, Jing H, Xu L, Han Y, Zhao L. Stress corrosion cracking characteristics of CF8A austenitic stainless steels and interactions between multiple cracks in a simulated PWR environment. Constr Build Mater 2019;203:642–54. https://doi.org/10.1016/J.CONBUILDMAT.2019.01.090.
[49] Wu S, Chen H, Craig P, Ramandi HL, Timms W, Hagan PC, Crosky A, Hebblewhite B, Saydam S. An experimental framework for simulating stress corrosion cracking in cable bolts. Tunn Undergr Sp Technol 2018;76:121–32. https://doi.org/10.1016/J.TUST.2018.03.004.
[50] Na K-H, Yun E, Park YS. Selective Leaching of Gray Cast Iron-Electrochemical Aspects. Trans Korean Nucl Soc Autumn Meet Jeju n.d.
[51] Reboul MC, Baroux B. Metallurgical aspects of corrosion resistance of aluminium alloys. Mater Corros 2011;62:215–33. https://doi.org/10.1002/MACO.201005650.
[52] Rieth AJ, Wright AM, Dincă M. Kinetic stability of metal–organic frameworks for corrosive and coordinating gas capture. Nat Rev Mater 2019 411 2019;4:708–25. https://doi.org/10.1038/s41578-019-0140-1.
[53] Challenges in Corrosion: Costs, Causes, Consequences, and Control - V. S. Sastri - Google Books n.d. https://books.google.co.za/books?hl=en&lr=&id=FMuOCQAAQBAJ&oi=fnd&pg=PA6&dq=Consequences+of+corrosion&ots=M4GF4Z28cZ&sig=2Cuh8BZJx1r4uYEPJzaKqWPdxvo&redir_esc=y#v=onepage&q=Consequences of corrosion&f=false (accessed October 12, 2022).
[54] Arthur DE, Jonathan A, Ameh PO, Anya C. A review on the assessment of polymeric materials used as corrosion inhibitor of metals and alloys. Int J Ind Chem 2013 41 2013;4:1–9. https://doi.org/10.1186/2228-5547-4-2.
[55] Xhanari K, Finšgar M, Knez Hrnčič M, Maver U, Knez Ž, Seiti B. Green corrosion inhibitors for aluminium and its alloys: A review. RSC Adv 2017;7:27299–330. https://doi.org/10.1039/c7ra03944a.
[56] Hossain N, Chowdhury MA, Kchaou M. An overview of green corrosion inhibitors for sustainable and environment friendly industrial development. Https://DoiOrg/101080/0169424320201816793 2020. https://doi.org/10.1080/01694243.2020.1816793.
[57] Tezdogan T, Demirel YK. An overview of marine corrosion protection with a focus on cathodic protection and coatings. Brodogr Teor i Praksa Brodogr i Pomor Teh 2014;65:49–59.
[58] Karimi Azar MM, Shooshtari Gugtapeh H, Rezaei M. Evaluation of corrosion protection performance of electroplated zinc and zinc-graphene oxide nanocomposite coatings in air saturated 3.5 wt. % NaCl solution. Colloids Surfaces A Physicochem Eng Asp 2020;601:125051. https://doi.org/10.1016/J.COLSURFA.2020.125051.
[59] Obot IB, Obi-Egbedi NO. Adsorption properties and inhibition of mild steel corrosion in sulphuric acid solution by ketoconazole: Experimental and theoretical investigation. Corros Sci 2010;52:198–204. https://doi.org/10.1016/J.CORSCI.2009.09.002.
[60] Prosek T, Le Bozec N, Thierry D. Application of automated corrosion sensors for monitoring the rate of corrosion during accelerated corrosion tests. Mater

Corros 2014;65:448–56. https://doi.org/10.1002/MACO.201206655.
[61] Hu E, Xu Y, Hu X, Pan L, Jiang S. Corrosion behaviors of metals in biodiesel from rapeseed oil and methanol. Renew Energy 2012;37:371–8. https://doi.org/10.1016/J.RENENE.2011.07.010.
[62] Wang Z, Liu J, Wu L, Han R, Sun Y. Study of the corrosion behavior of weathering steels in atmospheric environments. Corros Sci 2013;67:1–10. https://doi.org/10.1016/J.CORSCI.2012.09.020.
[63] Hwang B, Lee CG, Lee TH. Correlation of microstructure and mechanical properties of thermomechanically processed low-carbon steels containing boron and copper. Metall Mater Trans A Phys Metall Mater Sci 2010;41:85–96. https://doi.org/10.1007/S11661-009-0070-4/FIGURES/11.
[64] Deng J, Wang RZ, Han GY. A review of thermally activated cooling technologies for combined cooling, heating and power systems. Prog Energy Combust Sci 2011;37:172–203. https://doi.org/10.1016/J.PECS.2010.05.003.
[65] Oguzie EE. Evaluation Of The Inhibitive Effect Of Some Plant Extracts On The Acid Corrosion Of Mild Steel 2010.
[66] Qin H, Zhao Y, An Z, Cheng M, Wang Q, Cheng T, Wang Q, Wang J, Jiang Y, Zhang X, Yuan G. Enhanced antibacterial properties, biocompatibility, and corrosion resistance of degradable Mg-Nd-Zn-Zr alloy. Biomaterials 2015;53:211–20. https://doi.org/10.1016/J.BIOMATERIALS.2015.02.096.
[67] Han D, Wu S, Zhang S, Deng Y, Cui C, Zhang L, Long Y, Li H, Tao Y, Weng Z, Yang QH. A Corrosion-Resistant and Dendrite-Free Zinc Metal Anode in Aqueous Systems. Small 2020;16:2001736. https://doi.org/10.1002/SMLL.202001736.
[68] Li Q, Han L, Luo Q, Liu X, Yi J. Towards Understanding the Corrosion Behavior of Zinc-Metal Anode in Aqueous Systems: From Fundamentals to Strategies. Batteries Supercaps 2022 Apr;4:e202100417. https://doi.org/10.1002/batt.202100417
[69] Cheng F, Chen J. Metal–air batteries: from oxygen reduction electrochemistry to cathode catalysts. Chem Soc Rev 2012;41:2172–92. https://doi.org/10.1039/C1CS15228A.
[70] Friedrich K, Almajid AA. Manufacturing aspects of advanced polymer composites for automotive applications. Appl Compos Mater 2013;20:107–28. https://doi.org/10.1007/S10443-012-9258-7/FIGURES/32.
[71] Dursun T, Soutis C. Recent developments in advanced aircraft aluminium alloys. Mater Des 2014;56:862–71. https://doi.org/10.1016/J.MATDES.2013.12.002.
[72] Aboulkhair NT, Simonelli M, Parry L, Ashcroft I, Tuck C, Hague R. 3D printing of Aluminium alloys: Additive Manufacturing of Aluminium alloys using selective laser melting. Prog Mater Sci 2019;106:100578. https://doi.org/10.1016/J.PMATSCI.2019.100578.
[73] Wang S-S, Yang F, Frankel GS. Effect of Altered Surface Layer on Localized Corrosion of Aluminum Alloy 2024. J Electrochem Soc 2017;164:C317–23. https://doi.org/10.1149/2.1541706JES/XML.
[74] Krogstad HN, Johnsen R. Corrosion properties of nickel-aluminium bronze in natural seawater—Effect of galvanic coupling to UNS S31603. Corros Sci 2017;121:43–56. https://doi.org/10.1016/J.CORSCI.2017.03.016.

[75] Donatus U, Thompson GE, Omotoyinbo JA, Alaneme KK, Aribo S, Agbabiaka OG. Corrosion pathways in aluminium alloys. Trans Nonferrous Met Soc China 2017;27:55–62. https://doi.org/10.1016/S1003-6326(17)60006-2.
[76] Yang Y, Yan B, Li J, Wang J. The effect of large heat input on the microstructure and corrosion behaviour of simulated heat affected zone in 2205 duplex stainless steel. Corros Sci 2011;53:3756–63. https://doi.org/10.1016/J.CORSCI.2011.07.022.
[77] Huang H, Guo X, Zhang G, Dong Z. The effects of temperature and electric field on atmospheric corrosion behaviour of PCB-Cu under absorbed thin electrolyte layer. Corros Sci 2011;53:1700–7. https://doi.org/10.1016/J.CORSCI.2011.01.031.
[78] Li X, Deng S, Fu H. Adsorption and inhibition effect of vanillin on cold rolled steel in 3.0 M H3PO4. Prog Org Coatings 2010;67:420–6. https://doi.org/10.1016/J.PORGCOAT.2009.12.006.
[79] Beniken M, Driouch M, Sfaira M, Hammouti B, Ebn Touhami M, Mohsin M. Kinetic–Thermodynamic Properties of a Polyacrylamide on Corrosion Inhibition for C-Steel in 1.0 M HCl Medium: Part 2. J Bio- Tribo-Corrosion 2018;4:1–13. https://doi.org/10.1007/S40735-018-0152-1/TABLES/7.
[80] Gao Y, Yue Q, Gao B, Sun Y, Wang W, Li Q, Wang Y. Preparation of high surface area-activated carbon from lignin of papermaking black liquor by KOH activation for Ni(II) adsorption. Chem Eng J 2013;217:345–53. https://doi.org/10.1016/J.CEJ.2012.09.038.
[81] Zarrouk A, Warad I, Hammouti B, Dafali A, Al-Deyab SS, Benchat N. The Effect of Temperature on the Corrosion of Cu/HNO 3 in the Presence of Organic Inhibitor: Part-2. Int J Electrochem Sci 2010;5:1516–26.
[82] Piumetti M, Illanes A. Introduction to Molecular Catalysis. Mol Dyn Complex Catal Biocatal 2022:55–83. https://doi.org/10.1007/978-3-030-88500-7_3.
[83] Barth S, Hernandez-Ramirez F, Holmes JD, Romano-Rodriguez A. Synthesis and applications of one-dimensional semiconductors. Prog Mater Sci 2010;55:563–627. https://doi.org/10.1016/J.PMATSCI.2010.02.001.
[84] Hosseini S, Farnoush H. Characterization and in vitro bioactivity of electrophoretically deposited Mn-modified bioglass-alginate nanostructured composite coatings. Mater Res Express 2018;6:025404. https://doi.org/10.1088/2053-1591/AAEDFE.
[85] Hisatomi T, Kubota J, Domen K. Recent advances in semiconductors for photocatalytic and photoelectrochemical water splitting. Chem Soc Rev 2014;43:7520–35. https://doi.org/10.1039/C3CS60378D.
[86] Butti SK, Velvizhi G, Sulonen MLK, Haavisto JM, Oguz Koroglu E, Yusuf Cetinkaya A, Singh S, Arya D, Modestra JA, Krishna KV, Verma A. Microbial electrochemical technologies with the perspective of harnessing bioenergy: Maneuvering towards upscaling. Renew Sustain Energy Rev 2016;53:462–76. https://doi.org/10.1016/J.RSER.2015.08.058.
[87] Ricky EX, Mpelwa M, Xu X. The study of m-pentadecylphenol on the inhibition of mild steel corrosion in 1 M HCl solution. J Ind Eng Chem 2021;101:359–71. https://doi.org/10.1016/J.JIEC.2021.05.047.
[88] Hussin MH, Kassim MJ. The corrosion inhibition and adsorption behavior of

Uncaria gambir extract on mild steel in 1 M HCl. Mater Chem Phys 2011;125:461–8. https://doi.org/10.1016/J.MATCHEMPHYS.2010.10.032.
[89] Gao Y, Yang W, Zheng C, Hou X, Wu L. On-line preconcentration and in situ photochemical vapor generation in coiled reactor for speciation analysis of mercury and methylmercury by atomic fluorescence spectrometry. J Anal At Spectrom 2010;26:126–32. https://doi.org/10.1039/C0JA00137F.
[90] Škerget M, Knez Ž, Knez-Hrnčič M. Solubility of Solids in Sub- and Supercritical Fluids: a Review. J Chem Eng Data 2011;56:694–719. https://doi.org/10.1021/JE1011373.
[91] Xhanari K, Finšgar M, Knez Hrnčič M, Maver U, Knez Ž, Seiti B. Green corrosion inhibitors for aluminium and its alloys: a review. RSC Adv 2017;7:27299–330. https://doi.org/10.1039/C7RA03944A.
[92] Cirimbei MR, Dinică R, Gitin L, Vizireanu C. Study on herbal actions of horseradish (Armoracia rusticana) 2013;19:111–5.
[93] Liu L, Chen Y, Dang F, Liu Y, Tian X, Chen X. Synergistic effect of supercritical CO 2 and organic solvent on exfoliation of graphene: experiment and atomistic simulation studies. Phys Chem Chem Phys 2019;21:22149–57. https://doi.org/10.1039/C9CP03654G.
[94] Dai Y, Rozema E, Verpoorte R, Choi YH. Application of natural deep eutectic solvents to the extraction of anthocyanins from Catharanthus roseus with high extractability and stability replacing conventional organic solvents. J Chromatogr A 2016;1434:50–6. https://doi.org/10.1016/J.CHROMA.2016.01.037.
[95] Hammouda H, Chérif JK, Trabelsi-Ayadi M, Baron A, Guyot S. Detailed Polyphenol and Tannin Composition and Its Variability in Tunisian Dates (Phoenix dactylifera L.) at Different Maturity Stages 2013. https://doi.org/10.1021/JF304614J.
[96] Ćurko N, Kovačević Ganić K, Gracin L, Dapić M, Jourdes M, Teissedre PL. Characterization of seed and skin polyphenolic extracts of two red grape cultivars grown in Croatia and their sensory perception in a wine model medium. Food Chem 2014;145:15–22. https://doi.org/10.1016/J.FOODCHEM.2013.07.131.
[97] Pirvu L. Obtaining and chemical characterization of some vegetal extracts with corrosion-scaling inhibition properties. Part II. Juglandis folium and Agrimoniae herba extracts. Rom Biotechnol Lett 2011;16.
[98] Pirvu L, Armatu A, Bubueanu C, Pintilie G, Nita S. Obtaining and chemical characterization of some vegetal extracts with corrosion-scaling inhibition properties. Part I. Fagus sylvatica and Alii cepae bulbus extracts. Rom Biotechnol Lett 2010;15.
[99] Gece G. Drugs: A review of promising novel corrosion inhibitors. Corros Sci 2011;53:3873–98. https://doi.org/10.1016/J.CORSCI.2011.08.006.
[100] Negm NA, Kandile NG, Badr EA, Mohammed MA. Gravimetric and electrochemical evaluation of environmentally friendly nonionic corrosion inhibitors for carbon steel in 1 M HCl. Corros Sci 2012;65:94–103. https://doi.org/10.1016/J.CORSCI.2012.08.002.
[101] Abdallah M, Jahdaly BA Al. Gentamicin, Kanamycin and Amikacin Drugs as Non-Toxic Inhibitors for Corrosion of Aluminum in 1.0M Hydrochloric Acid. Int J

Electrochem Sci 2015;10:9808–23.
[102] Obi-Egbedi NO, Obot IB. Inhibitive properties, thermodynamic and quantum chemical studies of alloxazine on mild steel corrosion in H2SO4. Corros Sci 2011;53:263–75. https://doi.org/10.1016/J.CORSCI.2010.09.020.
[103] Obot IB, Obi-Egbedi NO, Umoren SA, Ebenso EE. Adsorption and kinetic studies on the inhibition potential of fluconazole for the corrosion of Al in HCl solution. Http://DxDoiOrg/101080/009864452011532746 2011;198:711–25. https://doi.org/10.1080/00986445.2011.532746.
[104] Bangera S, Alva VDP. Corrosion Inhibitive Property of Environmentally Benign Syzygium jambos Leaf Extract on Mild Steel in 1 M HCl. J Fail Anal Prev 2020;20:734–43. https://doi.org/10.1007/S11668-020-00869-Y/FIGURES/8.
[105] Abdallah M, Zaafarany I, Al-Karanee SO, Abd El-Fattah AA. Antihypertensive drugs as an inhibitors for corrosion of aluminum and aluminum silicon alloys in aqueous solutions. Arab J Chem 2012;5:225–34. https://doi.org/10.1016/J.ARABJC.2010.08.017.
[106] Miralrio A, Vázquez AE. Plant Extracts as Green Corrosion Inhibitors for Different Metal Surfaces and Corrosive Media: A Review. Process 2020, Vol 8, Page 942 2020;8:942. https://doi.org/10.3390/PR8080942.
[107] Goswami S, Naik S. Natural gums and its pharmaceutical application. J Sci Innov Res 2014;3:112–21.
[108] Peter A, Obot IB, Sharma SK. Use of natural gums as green corrosion inhibitors: an overview. Int J Ind Chem 2015;6:153–64. https://doi.org/10.1007/S40090-015-0040-1/FIGURES/2.
[109] Prajapati VD, Jani GK, Moradiya NG, Randeria NP. Pharmaceutical applications of various natural gums, mucilages and their modified forms. Carbohydr Polym 2013;92:1685–99. https://doi.org/10.1016/J.CARBPOL.2012.11.021.
[110] Deshmukh AS, Chauhan PN, Noolvi MN, Chaturvedi K, Ganguly K, Shukla SS, Nadagouda MN, Aminabhavi TM. Polymeric micelles: Basic research to clinical practice. Int J Pharm 2017;532:249–68. https://doi.org/10.1016/J.IJPHARM.2017.09.005.
[111] Vaclavik VA, Christian EW. Food Packaging 2014:367–90. https://doi.org/10.1007/978-1-4614-9138-5_18.
[112] Fruits, Vegetables, Corn and Oilseeds Processing Handbook: Fruits ... - H. Panda - Google Books n.d. https://books.google.co.za/books?hl=en&lr=&id=WdJMAQAAQBAJ&oi=fnd&pg=PA1&dq=H.+Panda,+The+complete+book+on+gums+and+stabilizers+for+food+industry,+Asia+Paci□c+Business+Press+Inc.,+2010&ots=9ADD9WGBWk&sig=X5b0vptbZmi6PmMgKvNm8d7iBCs&redir_esc=y#v=onepage&q&f=false (accessed October 13, 2022).
[113] Umoren SA, Ekanem UF. Inhibition of mild steel corrosion in H2SO4 using exudate gum from pachylobus edulis and synergistic potassium halide additives. Http://DxDoiOrg/101080/00986441003626086 2010. https://doi.org/10.1080/00986441003626086.
[114] Ebenso EE, Obot IB, Murulana LC. Quinoline and its Derivatives as Effective Corrosion Inhibitors for Mild Steel in Acidic Medium. Int J Electrochem Sci 2010;5:1574–86.

[115] Husaini M, Bashir Ibrahim M. Engineering and Manufacturing 2019;6:53–64. https://doi.org/10.5815/ijem.2019.06.05.
[116] Obi-Egbedi NO, Obot IB, Umoren SA. Spondias mombin L. as a green corrosion inhibitor for aluminium in sulphuric acid: Correlation between inhibitive effect and electronic properties of extracts major constituents using density functional theory. Arab J Chem 2012;5:361–73. https://doi.org/10.1016/J.ARABJC.2010.09.002.
[117] Ameh PO, Eddy NO. Commiphora pedunculata gum as a green inhibitor for the corrosion of aluminium alloy in 0.1 M HCl. Res Chem Intermed 2014;40:2641–9. https://doi.org/10.1007/S11164-013-1117-0/FIGURES/3.
[118] Eddy N, Ameh P, Gwarzo M, Okop I, Dodo S. PORTUGALIAE ELECTROCHIMICA ACTA Physicochemical Study and Corrosion Inhibition Potential of Ficus tricopoda for Aluminium in Acidic Medium. Port Electrochim Acta 2013;31:79–93. https://doi.org/10.4152/pea.201302079.
[119] Okon Eddy N, Ocheje Ameh P, Victor E, Odiongenyi AO. International journal of chemical, material and environmental research Chemical Information from GCMS and FTIR Studies on Ficus thonningii Gum and its Potential as a Corrosion Inhibitor for Aluminium in Acidic Medium. Int J Chem Mater Environ Res 2014;2014:3–15.
[120] Deepa P, Petchiammal A, Pirammarajeswari M, Rajeswari C, Selvaraj S. Eugenia Jambolana Used as Corrosion Inhibitor on Mild Steel in 1N Hydrochloric Acid Medium n.d.
[121] Solomon MM, Gerengi H, Umoren SA. Carboxymethyl Cellulose/Silver Nanoparticles Composite: Synthesis, Characterization and Application as a Benign Corrosion Inhibitor for St37 Steel in 15% H2SO4 Medium. ACS Appl Mater Interfaces 2017;9:6376–89. https://doi.org/10.1021/ACSAMI.6B14153/ASSET/IMAGES/LARGE/AM-2016-14153U_0016.JPEG.
[122] Eddy NO, Ibok UJ, Ameh PO, Alobi NO, Sambo MM. Adsorption and quantum chemical studies on the inhibition of the corrosion of aluminum in HCl by gloriosa superba (gs) gum. Http://DxDoiOrg/101080/009864452013809000 2014;201:1360–83. https://doi.org/10.1080/00986445.2013.809000.
[123] Uma K, Rekha S. Investigation and inhibition of aluminium corrosion in methane sulphonic acid solution by organic compound. Available Online WwwJocprCom J Chem Pharm Res 2015;7:165–9. https://doi.org/10.13140/RG.2.2.35376.79367.
[124] Umoren SA, Solomon MM. Synergistic corrosion inhibition effect of metal cations and mixtures of organic compounds: A Review. J Environ Chem Eng 2017;5:246–73. https://doi.org/10.1016/J.JECE.2016.12.001.
[125] Arukalam IO, Ijomah NT, Nwanonenyi SC, Obasi HC, Aharanwa BC, Anyanwu PI. Studies on acid corrosion of aluminium by a naturally occurring polymer (Xanthan gum). Int J Sci Eng Res 2014;5.
[126] Strehblow HH, Marcus P. Mechanisms of pitting corrosion. Corros Mech Theory Pract Third Ed 2011:349–94. https://doi.org/10.1201/B11020-11/mechanisms-pitting-corrosion-hans-henning-strehblow-philippe-marcus.
[127] Umoren SA, Solomon MM. Effect of halide ions on the corrosion inhibition

efficiency of different organic species – A review. J Ind Eng Chem 2015;21:81–100. https://doi.org/10.1016/J.JIEC.2014.09.033.
[128] Capuzzo A, Maffei ME, Occhipinti A. Supercritical Fluid Extraction of Plant Flavors and Fragrances. Mol 2013, Vol 18, Pages 7194-7238 2013;18:7194–238. https://doi.org/10.3390/MOLECULES18067194.
[129] Alam M, Akram D, Sharmin E, Zafar F, Ahmad S. Vegetable oil based eco-friendly coating materials: A review article. Arab J Chem 2014;7:469–79. https://doi.org/10.1016/J.ARABJC.2013.12.023.
[130] Abdallah M, Zaafarany I, Khairou KS, Emad Y. Natural oils as corrosion inhibitors for stainless steel in sodium hydroxide solutions. Chem Technol Fuels Oils 2012;48:234–45. https://doi.org/10.1007/S10553-012-0364-X/TABLES/4.
[131] Hassan U. Inhibition of Copper Corrosion in 2 M HNO3 by the Essential Oil of Thyme Morocco Biological activity of essential oils View project Corrosion Inhibition of Aluminium in Acidic Media View project Houbairi Sara 2013. https://doi.org/10.4152/pea.201304221.
[132] Popoola API, Fayomi OSI, Abdulwahab M. Degradation Behaviour of Aluminium in 2M HCl/HNO 3 in the Presence of Arachis hypogeae Natural Oil. Int J Electrochem Sci 2012;7:5817–27.
[133] Halambek J, Bubalo MC, Redovniković IR, Berković K. Corrosion Behaviour of Aluminium and AA5754 Alloy in 1% Acetic Acid Solution in Presence of Laurel Oil. Int J Electrochem Sci 2014;9:5496–506.
[134] Fayomi OSI, Popoola API. The Inhibitory Effect and Adsorption Mechanism of Roasted Elaeis guineensis as Green Inhibitor on the Corrosion Processof Extruded AA6063 Al-Mg-Si Alloy in Simulated Solution. Silicon 2014 62 2014;6:137–43. https://doi.org/10.1007/S12633-014-9177-3.
[135] Halambek J, Berković K. Inhibitive Action of Anethum graveolens L. oil on Aluminium Corrosion in Acidic Media. Artic Int J Electrochem Sci 2012;7:8356–68.
[136] Danlami JM, Zaini MAA, Arsad A, Yunus MAC. A parametric investigation of castor oil (Ricinus comminis L) extraction using supercritical carbon dioxide via response surface optimization. J Taiwan Inst Chem Eng 2015;53:32–9. https://doi.org/10.1016/J.JTICE.2015.02.033.
[137] Al-Abdul Wahhab HI, Hussein IA, Parvez MA, Shawabkeh RA. Use of modified oil fly ash to enhance asphalt concrete performance. Mater Struct Constr 2015;48:3231–40. https://doi.org/10.1617/S11527-014-0393-5/FIGURES/7.
[138] Abdallah M, Altass HM, AL Jahdaly BA, Salem MM. Some natural aqueous extracts of plants as green inhibitor for carbon steel corrosion in 0.5 M sulfuric acid. Green Chem Lett Rev 2018;11:189–96. https://doi.org/10.1080/17518253.2018.1458161.
[139] Xhanari K, Finšgar M, Knez Hrnčič M, Maver U, Knez Ž, Seiti B. Green corrosion inhibitors for aluminium and its alloys: a review. RSC Adv 2017;7:27299–330. https://doi.org/10.1039/C7RA03944A.
[140] Vorobyova V, Chygyrynets´, O, Skiba M, Kurmakova I, Bondar O. Self-assembled monoterpenoid phenol as vapor phase atmospheric corrosion inhibitor of carbon steel. Int J Corros Scale Inhib 2017;6:485–503. https://doi.org/10.17675/2305-6894-2017-6-4-8.

[141] Shen J, Huang G, An C, Xin X, Huang C, Rosendahl S. Removal of Tetrabromobisphenol A by adsorption on pinecone-derived activated charcoals: Synchrotron FTIR, kinetics and surface functionality analyses. Bioresour Technol 2018;247:812–20. https://doi.org/10.1016/J.BIORTECH.2017.09.177.
[142] Saha SK, Banerjee P. A theoretical approach to understand the inhibition mechanism of steel corrosion with two aminobenzonitrile inhibitors. RSC Adv. 2015;5(87):71120-30. https://doi.org/10.1039/C5RA15173B
[143] Navizet I, Liu YJ, Ferré N, Roca-Sanjuán D, Lindh R. The Chemistry of Bioluminescence: An Analysis of Chemical Functionalities. ChemPhysChem 2011;12:3064–76. https://doi.org/10.1002/CPHC.201100504.
[144] Archodoulaki V-M, Koch T, Jones MP. Thermo(oxidative) Stability of Polymeric Materials. Therm Anal Polym Mater 2022:353–79. https://doi.org/10.1002/9783527828692.CH9.
[145] Schindler A, Doedt M, Gezgin Ş, Menzel J, Schmölzer S. Identification of polymers by means of DSC, TG, STA and computer-assisted database search. J Therm Anal Calorim 2017;129:833–42. https://doi.org/10.1007/S10973-017-6208-5/FIGURES/7.
[146] Ts'epo T, Luong J, Rodriguez MC, Ts'epo Supervisor TR, Hailemachiel A. Voltametric Behaviour of Dichlofenac at Single-Walled Carbon Nanotube Modified GCE Carbon nanot ubes for elect rochemical biosensing Voltametric Behaviour of Dichlofenac at Single-Walled Carbon Nanotube Modified GCE a project report submitted in partial fulfillment of the requirements for the award of bachelor of science in chemical technology 2014.
[147] Basic overview of the working principle of a potentiostat/galvanostat (PGSTAT)-Electrochemical cell setup n.d.
[148] Dissertation TP. Phthalocyanine compounds as corrosion inhibitors for metals in corrosive environment 2018.
[149] Şafak S, Duran B, Yurt A, Türkoğlu G. Schiff bases as corrosion inhibitor for aluminium in HCl solution. Corros Sci 2012;54:251–9. https://doi.org/10.1016/J.CORSCI.2011.09.026.
[150] Han L, Wang T. Preparation of glycerol monostearate from glycerol carbonate and stearic acid. RSC Adv 2016;6:34137–45. https://doi.org/10.1039/C6RA02912D.
[151] Liu S, Yu B, Zhang W, Zhu J, Zhai Y, Chen J. A New Generation Density Functional XYG3. Prog Chem 2012;24:1023. https://doi.org/10.7536/PC140420.
[152] Jansen Van Vuuren DB, Krieg HM, Van Sittert CGCE. Computational chemistry study of zirconium monomers in low acid concentration aqueous solutions. IOP Conf Ser Mater Sci Eng 2018;430:012017. https://doi.org/10.1088/1757-899X/430/1/012017.
[153] Perdew JP, Ruzsinszky A, Sun J, Burke K. Gedanken densities and exact constraints in density functional theory. J Chem Phys 2014;140:18A533. https://doi.org/10.1063/1.4870763.
[154] Timrov I, Marzari N, Cococcioni M. Self-consistent Hubbard parameters from density-functional perturbation theory in the ultrasoft and projector-augmented wave formulations. Phys Rev B 2021;103:045141.

https://doi.org/10.1103/PHYSREVB.103.045141/FIGURES/3/MEDIUM.
[155] Zhang GX, Tkatchenko A, Paier J, Appel H, Scheffler M. Van der Waals interactions in ionic and semiconductor solids. Phys Rev Lett 2011;107:245501. https://doi.org/10.1103/PHYSREVLETT.107.245501/FIGURES/3/MEDIUM.
[156] Obot IB, Kaya S, Kaya C, Tüzün B. Theoretical evaluation of triazine derivatives as steel corrosion inhibitors: DFT and Monte Carlo simulation approaches. Res Chem Intermed 2016;42:4963–83. https://doi.org/10.1007/S11164-015-2339-0/TABLES/6.
[157] Nazir U, Akhter Z, Ali NZ, Shah FU. Experimental and theoretical insights into the corrosion inhibition activity of novel Schiff bases for aluminum alloy in acidic medium. RSC Adv 2019;9:36455–70. https://doi.org/10.1039/C9RA07105A.
[158] Shi R, Liu L, Lu Y, Wang C, Li Y, Li L, Yan Z, Chen J. Nitrogen-rich covalent organic frameworks with multiple carbonyls for high-performance sodium batteries. Nat Commun 2020 111 2020;11:1–10. https://doi.org/10.1038/s41467-019-13739-5.
[159] Arjomandi J, Moghanni-Bavil-Olyaei H, Parvin MH, Lee JY, Chul Ko K, Joshaghani M, Hamidian K. Inhibition of corrosion of aluminum in alkaline solution by a novel azo-schiff base: Experiment and theory. J Alloys Compd 2018;746:185–93. https://doi.org/10.1016/J.JALLCOM.2018.02.288.
[160] Negm NA, Elkholy YM, Zahran MK, Tawfik SM. Corrosion inhibition efficiency and surface activity of benzothiazol-3-ium cationic Schiff base derivatives in hydrochloric acid. Corros Sci 2010;52:3523–36. https://doi.org/10.1016/J.CORSCI.2010.07.001.
[161] Nnanna LA, Onwuagba BN, Mejeha IM, Okeoma KB. Inhibition effects of some plant extracts on the acid corrosion of aluminium alloy. African J Pure Appl Chem 2010;4:11–016.
[162] Shukla SK, Shukla SK, Ebenso EE. Corrosion Inhibition, Adsorption Behavior and Thermodynamic Properties of Streptomycin on Mild Steel in Hydrochloric Acid Medium Electrocatalysis of Lindane Using Antimony Oxide Nanoparticles Based-SWCNT/PANI Nanocomposites View project Corrosion Inhibition, Adsorption Behavior and Thermodynamic Properties of Streptomycin on Mild Steel in Hydrochloric Acid Medium. Artic Int J Electrochem Sci 2011;6:3277–91.
[163] Mourya P, Banerjee S, Singh MM. Corrosion inhibition of mild steel in acidic solution by Tagetes erecta (Marigold flower) extract as a green inhibitor. Corros Sci 2014;85:352–63. https://doi.org/10.1016/J.CORSCI.2014.04.036.
[164] Patel NS, Jauhariand S, Mehta GN, Al-Deyab SS, Warad I, Hammouti B. Mild Steel Corrosion Inhibition by Various Plant Extracts in 0.5 M Sulphuric acid. Int J Electrochem Sci 2013;8:2635–55.
[165] Gopiraman M, Selvakumaran N, Kesavan D, Karvembu R. Adsorption and corrosion inhibition behaviour of N-(phenylcarbamothioyl)benzamide on mild steel in acidic medium. Prog Org Coatings 2012;73:104–11. https://doi.org/10.1016/J.PORGCOAT.2011.09.006.
[166] Ouali I El, Hammouti B, Aouniti A, Ramli Y, Azougagh M, Essassi EM, Bouachrine M. Thermodynamic characterisation of steel corrosion in HCl in the presence of 2-phenylthieno (3, 2-b) quinoxaline. J Mater Envir Sci 2010;1:1–8.
[167] Tran HN, You SJ, Chao HP. Thermodynamic parameters of cadmium adsorption

onto orange peel calculated from various methods: A comparison study. J Environ Chem Eng 2016;4:2671–82. https://doi.org/10.1016/J.JECE.2016.05.009.
[168] Husaini M. Organic compound as inhibitor for corrosion of aluminum in sulphuric acid solution. Alger J Chem Eng AJCE 2021;1:22–30.
[169] Ameh PO. Electrochemical and computational study of gum exudates from Canarium schweinfurthii as green corrosion inhibitor for mild steel in HCl solution. Https://DoiOrg/101080/1658365520181514147 2018;12:783–95. https://doi.org/10.1080/16583655.2018.1514147.
[170] Green Inhibitors for Corrosion Protection of Metals and Alloys: An Overview n.d. https://www.hindawi.com/journals/ijc/2012/380217/ (accessed October 13, 2022).
[171] Sedik A, Lerari D, Salci A, Athmani S, Bachari K, Gecibesler H, Solmaz R. Dardagan Fruit extract as eco-friendly corrosion inhibitor for mild steel in 1 M HCl: Electrochemical and surface morphological studies. J Taiwan Inst Chem Eng 2020;107:189–200. https://doi.org/10.1016/J.JTICE.2019.12.006.
[172] Lačnjevac Č, Miskovic-Stankovic V, Rajendran S. ZAŠTITA MATERIJALA 2021.
[173] Ansari KR, Quraishi MA, Singh A. Schiff's base of pyridyl substituted triazoles as new and effective corrosion inhibitors for mild steel in hydrochloric acid solution. Corros Sci 2014;79:5–15. https://doi.org/10.1016/J.CORSCI.2013.10.009.
[174] Xiong S, Si J, Sun J, Wu H, Dong H, Zhang C. Experimental and computational studies on heterocyclic organic compounds as corrosion inhibitors for copper immersed in O/W emulsion medium. Anti-Corrosion Methods Mater 2020;67:214–27. https://doi.org/10.1108/ACMM-10-2019-2200/FULL/PDF.
[175] Obot IB, Obi-Egbedi NO. Indeno-1-one [2,3-b]quinoxaline as an effective inhibitor for the corrosion of mild steel in 0.5 M H2SO4 solution. Mater Chem Phys 2010;122:325–8. https://doi.org/10.1016/J.MATCHEMPHYS.2010.03.037.
[176] Akinbulumo OA, Odejobi OJ, Odekanle EL. Thermodynamics and adsorption study of the corrosion inhibition of mild steel by Euphorbia heterophylla L. extract in 1.5 M HCl. Results Mater 2020;5:100074. https://doi.org/10.1016/J.RINMA.2020.100074.
[177] Abdel-Gaber AM, Rahal HT, Beqai FT. Eucalyptus leaf extract as a eco-friendly corrosion inhibitor for mild steel in sulfuric and phosphoric acid solutions. Int J Ind Chem 2020;11:123–32. https://doi.org/10.1007/S40090-020-00207-Z/TABLES/4.
[178] Dhaundiyal P, Bashir S, Sharma V, Kumar A. An investigation on mitigation of corrosion of mildsteel by Origanum vulgare in acidic medium. Bull Chem Soc Ethiop 2019;33:159–68. https://doi.org/10.4314/bcse.v33i1.
[179] Oguzie EE, Li Y, Wang FH. Corrosion inhibition and adsorption behavior of methionine on mild steel in sulfuric acid and synergistic effect of iodide ion. J Colloid Interface Sci 2007;310:90–8. https://doi.org/10.1016/J.JCIS.2007.01.038.
[180] Bashir S, Thakur A, Lgaz H, Chung IM, Kumar A. Corrosion inhibition efficiency

of bronopol on aluminium in 0.5 M HCl solution: Insights from experimental and quantum chemical studies. Surfaces and Interfaces 2020;20:100542. https://doi.org/10.1016/J.SURFIN.2020.100542.
[181] Pesha T, Monama GR, Hato MJ, Maponya TC, Makhatha ME, Ramohlola KE, Molapo KM, Modibane KD, Thomas MS. Inhibition Effect of Phthalocyaninatocopper(II) and 4-Tetranitro(phthalocyaninato)copper(II) Inhibitors for Protection of Aluminium in Acidic Media. Int J Electrochem Sci 2019;14:137–49. https://doi.org/10.20964/2019.01.17.
[182] Asadi N, Ramezanzadeh M, Bahlakeh G, Ramezanzadeh B. Utilizing Lemon Balm extract as an effective green corrosion inhibitor for mild steel in 1M HCl solution: A detailed experimental, molecular dynamics, Monte Carlo and quantum mechanics study. J Taiwan Inst Chem Eng 2019;95:252–72. https://doi.org/10.1016/J.JTICE.2018.07.011.
[183] Noyel Victoria S, Prasad R, Manivannan R. Psidium Guajava Leaf Extract as Green Corrosion Inhibitor for Mild steel in Phosphoric Acid. Int J Electrochem Sci 2015;10:2220–38.
[184] Hong S, Chen W, Luo HQ, Li NB. Inhibition effect of 4-amino-antipyrine on the corrosion of copper in 3 wt.% NaCl solution. Corros Sci 2012;57:270–8. https://doi.org/10.1016/J.CORSCI.2011.12.009.
[185] Cherrak K, Benhiba F, Sebbar NK, Essassi EM, Taleb M, Zarrouk A, Dafali A. Corrosion inhibition of mild steel by new Benzothiazine derivative in a hydrochloric acid solution: Experimental evaluation and theoretical calculations. Chem Data Collect 2019;22:100252. https://doi.org/10.1016/J.CDC.2019.100252.
[186] Shukla SK, Shukla SK, Ebenso EE. Corrosion Inhibition, Adsorption Behavior and Thermodynamic Properties of Streptomycin on Mild Steel in Hydrochloric Acid Medium Electrocatalysis of Lindane Using Antimony Oxide Nanoparticles Based-SWCNT/PANI Nanocomposites View project Corrosion Inhibition, Adsorption Behavior and Thermodynamic Properties of Streptomycin on Mild Steel in Hydrochloric Acid Medium. Artic Int J Electrochem Sci 2011;6:3277–91.
[187] Org WE, Zarrouk A, Zarrok H, Salghi R, Hammouti B, Al-Deyab SS, Touzani R, Bouachrine M, Warad I, Hadda TB. ELECTROCHEMICAL SCIENCE A Theoretical Investigation on the Corrosion Inhibition of Copper by Quinoxaline Derivatives in Nitric Acid Solution. Int J Int J Electrochem Sci 2012;7:6353–64.
[188] Kouache A, Khelifa A, Boutoumi H, Moulay S, Feghoul A, Idir B, Aoudj S. Experimental and theoretical studies of *Inula viscosa* extract as a novel eco-friendly corrosion inhibitor for carbon steel in 1 M HCl. J Adhes Sci Technol 2022;36:988–1016. https://doi.org/10.1080/01694243.2021.1956215.
[189] Behpour M, Ghoreishi SM, Soltani N, Salavati-Niasari M. The inhibitive effect of some bis-N,S-bidentate Schiff bases on corrosion behaviour of 304 stainless steel in hydrochloric acid solution. Corros Sci 2009;51:1073–82. https://doi.org/10.1016/j.corsci.2009.02.011.
[190] Murulana LC. {Adsorption}, {Thermodynamic} {and} {Density} {Functional} {Theory} {Investigation} {of} {Some} {Sulphonamides} {As} {Corrosion} {Inhibitors} {for} {Some} {Selected} {Metals} {in} {Acidic} {Medium} 2015.
[191] Hamdy A, El-Gendy NS. Thermodynamic, adsorption and electrochemical

studies for corrosion inhibition of carbon steel by henna extract in acid medium. Egypt J Pet 2013;22:17–25. https://doi.org/10.1016/J.EJPE.2012.06.002.
[192] Lupi FR, Shakeel A, Greco V, Baldino N, Calabrò V, Gabriele D. Organogelation of extra virgin olive oil with fatty alcohols, glyceryl stearate and their mixture. LWT 2017;77:422–9. https://doi.org/10.1016/J.LWT.2016.11.082.
[193] Lopez-Martínez A, Charó-Alonso MA, Marangoni AG, Toro-Vazquez JF. Monoglyceride organogels developed in vegetable oil with and without ethylcellulose. Food Res Int 2015;72:37–46. https://doi.org/10.1016/J.FOODRES.2015.03.019.
[194] Murulana LC, Kabanda MM, Ebenso EE. Experimental and theoretical studies on the corrosion inhibition of mild steel by some sulphonamides in aqueous HCl. RSC Adv 2015;5:28743–61. https://doi.org/10.1039/C4RA11414K.
[195] Suhasaria A, Murmu M, Satpati S, Banerjee P, Sukul D. Bis-benzothiazoles as efficient corrosion inhibitors for mild steel in aqueous HCl: Molecular structure-reactivity correlation study. J Mol Liq 2020;313:113537. https://doi.org/10.1016/J.MOLLIQ.2020.113537.
[196] Hassan AT, Hussein RK, Abou-Krisha M, Attia MI. Density Functional Theory Investigation of Some Pyridine Dicarboxylic Acids Derivatives as Corrosion Inhibitors. Int J Electrochem Sci 2020;15:4274–86. https://doi.org/10.20964/2020.05.11.
[197] Rizk SA, Abdelwahab SS, El-Badawy AA. Design, Regiospecific Green Synthesis, Chemical Computational Analysis, and Antimicrobial Evaluation of Novel Phthalazine Heterocycles. J Heterocycl Chem 2019;56:2347–57. https://doi.org/10.1002/JHET.3622.
[198] Mourad AK, Makhlouf AA, Soliman AY, Mohamed SA. Phthalazines and phthalazine hybrids as antimicrobial agents: Synthesis and biological evaluation. J Chem Res 2020;44:31–41. https://doi.org/10.1177/1747519819883840/ASSET/IMAGES/LARGE/10.1177_1747519819883840-FIG1.JPEG.
[199] Singh A, Ansari KR, Quraishi MA, Lgaz H. Effect of Electron Donating Functional Groups on Corrosion Inhibition of J55 Steel in a Sweet Corrosive Environment: Experimental, Density Functional Theory, and Molecular Dynamic Simulation. Mater 2019, Vol 12, Page 17 2018;12:17. https://doi.org/10.3390/MA12010017.
[200] Ehsani A, Mahjani MG, Hosseini M, Safari R, Moshrefi R, Mohammad Shiri H. Evaluation of Thymus vulgaris plant extract as an eco-friendly corrosion inhibitor for stainless steel 304 in acidic solution by means of electrochemical impedance spectroscopy, electrochemical noise analysis and density functional theory. J Colloid Interface Sci 2017;490:444–51. https://doi.org/10.1016/J.JCIS.2016.11.048.
[201] Abdullahi A, Ameenullah A. Corrosion inhibition potentials of Strichnos spinosa L. on Aluminium in 0.9 M HCl medium: experimental and theoretical investigations. AJET. 2020;3:028-37.
[202] Beronio ER, Hipolito AN, Ocon JD, Nakanishi H, Kasai H, Padama AA. Cluster size effects on the adsorption of CO, O, and CO2 and the dissociation of CO2 on two-dimensional Cux (x= 1, 3, and 7) clusters supported on Cu (111) surface: a density functional theory study. J Phys Condens Matter 2020;32:405201.

https://doi.org/10.1088/1361-648X/AB945D.
[203] Qiang Y, Zhang S, Guo L, Zheng X, Xiang B, Chen S. Experimental and theoretical studies of four allyl imidazolium-based ionic liquids as green inhibitors for copper corrosion in sulfuric acid. Corros Sci 2017;119:68–78. https://doi.org/10.1016/J.CORSCI.2017.02.021.
[204] Ogede RO, Abdulrahman NA, Apata DA, Ogede RO, Abdulrahman NA, Apata DA. DFT computational study of pyridazine derivatives as corrosion inhibitors for mild steel in acidic media. Https://WwwGsconlinepressCom/Journals/Gscarr/Sites/Default/Files/GSCARR-2022-0151Pdf 2022;11:106–14. https://doi.org/10.30574/GSCARR.2022.11.3.0151.
[205] Madkour LH, Kaya S, Guo L, Kaya C. Quantum chemical calculations, molecular dynamic (MD) simulations and experimental studies of using some azo dyes as corrosion inhibitors for iron. Part 2: Bis–azo dye derivatives. J Mol Struct 2018;1163:397–417. https://doi.org/10.1016/J.MOLSTRUC.2018.03.013.

APPENDIX 1

Date: Mar 08, 2023
To: "Thabo Pesha" thabopesha@yahoo.co.uk
From: "Arabian Journal of Chemistry" support@elsevier.com
Subject: Your Submission

Ms. Ref. No.: ARABJC-D-23-00029R1
Title: Evaluation of corrosion inhibition effect of glycerol stearate on aluminium metal by electrochemical techniques
Arabian Journal of Chemistry

Dear Mr Thabo Pesha,

I am pleased to inform you that your paper "Evaluation of corrosion inhibition effect of glycerol stearate on aluminium metal by electrochemical techniques" has been accepted for publication in Arabian Journal of Chemistry.

Below are comments from the editor and reviewers.

Thank you for submitting your work to Arabian Journal of Chemistry.

Yours sincerely,

Abdulrahman A. Alwarthan, Ph.D.
Editor-in-Chief
Arabian Journal of Chemistry

Comments from the editors and reviewers:

****
For further assistance, please visit our customer support site at http://help.elsevier.com/app/answers/list/p/7923. Here you can search for solutions on a range of topics, find answers to frequently asked questions and learn more about EM via interactive tutorials. You will also find our 24/7 support contact details should you need any further assistance from one of our customer support representatives.

#AU_ARABJC#

To ensure this email reaches the intended recipient, please do not delete the above code